國 立 交 通 大 學

機械工程學系
碩士論文

新延遲 Ikeda-Mackey-Glass 系統的渾沌、渾沌同步、
渾沌控制、參數估測,與應用 GYC 部分區域穩定理論
實現新 Ikeda-Lorenz 系統之渾沌廣義同步及渾沌控制

Chaos, Chaos Synchronization, Chaos Control,

Estimation of Parameters of a New

Ikeda-Mackey-Glass Time-delayed System, and

Generalized Synchronization and Chaos Control of a

New Ikeda-Lorenz System by GYC Partial Region

Stability Theory
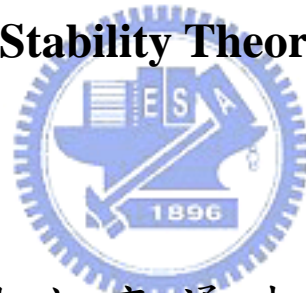
研 究 生: 何俊諺

指導教授: 戈正銘 教授

中華民國九十七年六月

新延遲 Ikeda-Mackey-Glass 系統的渾沌、渾沌同步、

渾沌控制、參數估測,與應用 GYC 部分區域穩定理論

實現新 Ikeda-Lorenz 系統之渾沌廣義同步及渾沌控制

Chaos, Chaos Synchronization, Chaos Control,

Estimation of Parameters of a New

Ikeda-Mackey-Glass Time-delayed System, and

Generalized Synchronization and Chaos Control of a

New Ikeda-Lorenz System by GYC Partial Region

Stability Theory

研究生: 何俊諺   Student: Chun-Yen Ho

指導教授: 戈正銘   Advisor: Zheng-Ming Ge

國 立 交 通 大 學

機 械 工 程 研 究 所

碩 士 論 文

國 立 交 通 大 學

論 文 口 試 委 員 會 審 定 書

本校＿＿＿機 械 工 程＿＿＿學系碩士班＿＿＿＿何俊諺＿＿＿＿＿君

所提論文：

（中文）新延遲 Ikeda-Mackey-Glass 系統的渾沌、渾沌同步、渾沌化控制，與應用 GYC 部

分區域穩定理論實現新 Ikeda-Lorenz 系統之渾沌廣義同步及渾沌控制

（英文）Chaos, Chaos Synchronization, Chaos Control, Estimation of Parameters of a New

Ikeda-Mackey-Glass Time-delayed System, and Generalized Synchronization and

Chaos Control of a New Ikeda-Lorenz System by GYC Partial Region Stability Theory

合於碩士資格水準、業經本委員會評審認可。

口試委員：＿＿＿＿＿＿＿＿＿＿＿＿＿＿＿＿＿＿＿＿＿＿＿＿

李青一

陳軾庭　　　古富能

指導教授：＿戈正銘＿＿＿＿＿＿＿＿＿＿＿＿＿＿

系 主 任：＿＿＿＿＿＿＿＿＿＿＿＿＿＿　教授

中 華 民 國　97　年　6　月　12　日

新延遲 Ikeda-Mackey-Glass 系統的渾沌、渾沌同步、渾沌控制、參數估測,與應用 GYC 部分區域穩定理論實現新 Ikeda-Lorenz 系統之渾沌廣義同步及渾沌控制

學生: 何俊諺　　　　　　　　　　指導教授: 戈正銘

摘要

本篇論文以相圖、分歧圖等之數值方法來研究新延遲 Ikeda-Mackey-Glass 系統及新 Ikeda-Lorenz 系統的渾沌行為。 發現新延遲 Ikeda-Mackey-Glass 系統不需加入控制器,只需調整延遲項, 即可讓系統達到渾沌廣義同步、渾沌反同步及渾沌廣義延遲同步。 接著利用此新延遲 Ikeda-Mackey-Glass 系統之渾沌訊號, 使新延遲 Ikeda-Mackey-Glass 系統實現渾沌化控制。 此外本篇論文以相圖、李亞普諾夫指數等數值方法來研究新 Ikeda-Lorenz 系統之渾沌行為。 並應用 GYC 部分區域穩定理論, 可以設計出較簡單的控制器使誤差較小。 以新 Ikeda-Lorenz 系統得出渾沌廣義同步及渾沌控制, 以驗證此方法之有效。最後, 利用渾沌同步使新延遲 Ikeda-Mackey-Glass 系統達到參數估測之效果。根據最小平方法則, 得出系統參數之微分方程式。模擬 12 個微分方程式, 當系統達渾沌同步時, 使所估測的兩個參數達目標值,模擬的結果非常成功。

Chaos, Chaos Synchronization, Chaos Control, Estimation of Parameters of a New Ikeda-Mackey-Glass Time-delayed System, and Generalized Synchronization and Chaos Control of a New Ikeda-Lorenz System by GYC Partial Region Stability Theory

Student: Chun-Yen Ho **Advisor: Zheng-Ming Ge**

Abstract

In this thesis, a new Ikeda-Mackey-Glass (IMG) time-delayed system and a new Ikeda-Lorenz (IL) system are studied. Their chaotic behaviors are presented by phase portraits, bifurcation diagrams, and Lyapunov exponent. When one of delay times is zero, two identical IMG systems cannot be synchronized with slightly different initial conditions. It is found that when one of delay time is positive, different types of synchronization can be obtained with slightly different initial conditions, such as generalized synchronization, anti-synchronization, and generalized lag-synchronization. One chaotization method is presented by using different types of chaos signals as parameters, it can be obtained the chaotic behaviors of a new Ikeda-Mackey-Glass time-delayed system. A new strategy to achieve chaos

generalized synchronization and chaos control by GYC partial region stability theory is proposed. The control design method is simple and a less simulation error because they are in lower degree than that of traditional controllers. A new IL system is used to show the effectiveness of the scheme. Finally, estimation of parameters of a new IMG system through synchronization is studied. By a minimization problem, a system of differential equations governing the evolution of parameters is constructed. Two time delay IMG systems are synchronized and their corresponding two parameters converge to same values by solving twelve differential equations. The simulation results are very satisfactory.

誌謝

本篇碩士論文得以完成，最先要感謝的人，就是我的指導教授戈正銘老師，戈老師在我的碩士生涯中，扮演了很重要的角色。在研究上，戈老師給我許多意見及指引我正確的研究方向，在研究過程中，也讓我學習到如何發現問題、解決問題。戈老師也不厭其煩的修訂論文，得以讓論文更加完整。還有戈老師的文學素養，讓我在跟老師交談中，感染到老師詩詞的涵養，增進我對文學上更深的了解。最後，感謝老師兩年來的教導，讓我對未來的人生有了新的啟發。

在兩年的碩士生涯裡，感謝博士班楊振雄、張晉銘、李仕宇學長，碩士班李乾豪、吳宗訓、李式中、林森生學長及翁郁婷學姊，在我研究遇到瓶頸時，給予我寶貴的意見及傳授經驗；也感謝我的同學李彥賢、許凱銘、陳聰文…等，大家彼此互相扶持成長，共同度過這兩年研究的時光，留下許多快樂的回憶；另外要感謝學弟陳志銘、徐瑜韓、張育銘，幫忙處理繁瑣雜事，得以讓我們專心致力於研究。

最後，感謝我的家人，您們全力支持我攻讀碩士學位，使我無後顧之憂地專致於研究。雖然您們在南，我在北，但是久久返家一次，一通關心的電話，都讓我感到非常的溫暖。感謝您們的教養，得以讓我順利拿到碩士學位。也謝謝女友盈琇，妳對我的關心、體諒及支持，讓我於疲累時能繼續支撐下去，妳是我支撐下去的動力。最後，僅以此論文獻給你們。

CONTENTS

LIST OF FIGURES

Chapter 1

Introduction

Chaos, as an interesting nonlinear phenomenon, has been intensively investigated. It is well known that chaotic system has sensitive dependence on initial conditions. A chaotic system is a nonlinear deterministic system that displays complex dynamical behaviors [1].

Due to finite signal transmission times, switching speeds, and memory effects, time-delayed systems exist in everywhere, such as nature, technology, and society[2]. Mackey-Glass time-delayed system has been introduced as a model of blood generation for patients with leukemia. Nowadays this model is very popular in chaos theory[3]. The Ikeda time-delayed system has been introduced to describe the dynamics of an optical bistable resonator, plays an important role in electronics and physiological studies and is well-known for delay-induced chaotic behavior[4-6]. In 1963, Lorenz proposed a simple model for the unpredictable behavior of the weather. He used fluid convection theory to model the motion of a two-dimensional cell of fluid cooled from above and warmed from below [7].A new Ikeda-Mackey-Glass (IMG) time-delayed system and a new Ikeda-Lorenz system are studied in this thesis.

There are different types of synchronization for interacting chaotic systems, such as complete synchronization [8,9], generalized synchronization [10], phase synchronization [11,12], lag synchronization[9,13,14], anticipating synchronization [15,16] and so on.

To achieve synchronization, different schemes, such as the Pecora and Carroll (PC) method [8], unidirectional coupling [9], bidirectional coupling [15], adaptive control [17,18] and impulsive control [19-21] are proposed.

In this thesis, it is found that when one of delay time of a new time-delayed system is positive, different types of synchronization can be obtained with slightly different initial conditions, such as generalized synchronization, anti-synchronization, and generalized lag- synchronization.

The theory of chaos control has developed since 1990[22-24] and today is at the forefront of research in the field of nonlinear dynamics. Techniques have been experimentally implemented in mechanical [25], chemical [26], electronic[27], laser[28], communication[29], and biological[30] systems.

There are many chaos control have been proposed such as different geometric method[31], feedback and non-feedback control[32-35], inverse optimal control[36], adaptive control[37,38], and backstepping control[39].

In this thesis, one chaos control method is presented by using different types of chaos signal as parameter, it can be obtained the chaotic behaviors of a New Ikeda-Mackey-Glass time-delayed system.

By using the GYC partial region stability theory[40,41], generalized chaos synchronization and chaos control can be obtained. A new Ikeda-Lorenz system is used as a simulation example.

Parameters estimation of chaotic system is an important issue[42-44]. Because chaotic system is very sensitive to initial conditions, parameters cannot be exactly known a priori. Parameter estimation through chaos synchronization is being further investigated.[45-47] .

In this thesis, estimation of parameters of a new Ikeda-Mackey-Glass system through synchronization is studied. By a minimization problem, a system of differential equations governing the evolution of parameters is constructed. Two time delay Ikeda-Mackey- Glass systems are synchronized and their corresponding two parameters converge to same values by solving twelve differential equations. The

simulation results are very satisfactory.

This thesis is organized as follows. In Chapter 2, the dynamic equation of a new Ikeda-Mackey-Glass(IMG) system is given. The phase portraits, bifurcation diagram of a new IMG system are presented. It is verified that the IMG system presents chaotic behaviors by numerical simulation.

In Chapter 3, synchronization scheme is given. It is found that no synchronization of the two identical IMG systems can be obtained with slightly different initial conditions when one of delay time τ_2 is zero and without any control scheme or coupling terms. It is also found that generalized synchronization, anti-synchronization and generalized lag-synchronization of the two identical IMG systems with slightly different conditions when two of delay time are positive and without any control scheme or coupling terms. Only by adjusting delay time τ_2, chaos synchronization of the two identical IMG systems can be obtained.

In Chapter 4, one chaos control method is presented by using different types of chaos signal as parameter, it can be obtained the chaotic behaviors of a new Ikeda-Mackey-Glass time-delayed system.

In Chapter 5, a new Ikeda-Lorenz(IL) system is studied. The phase portraits, Lyapunov exponent of a new IL system are presented. It is verified that the IL system presents the chaotic behaviors by numerical simulation.

In Chapter 6, a new strategy to achieve chaos generalized synchronization by GYC partial region stability theory is proposed. Simulation results show that for the new IL system chaos generalized synchronization can be achieved by GYC partial region stability theory.

In Chapter 7, simulation results show that for the new IL system chaos control can be achieved by GYC partial region stability theory.

In Chapter 8, conclusions are drawn.

Chapter 2

Chaos of a New Ikeda-Mackey-Glass System

2.1 Preliminaries

In this chapter, the chaotic behaviors in IMG system with different parameters are studied numerically by phase portraits, Poincare maps and bifurcation diagrams.

2.2 A New Ikeda-Mackey-Glass System

A new IMG system is described by the following differential equations:

$$\dot{x}_1(t) = -\alpha_1 x_1(t) - \beta \sin x_1(t - \tau_1) + K_1 x_2(t - \tau_2)$$

$$\dot{x}_2(t) = -\alpha_2 x_2(t) + b \frac{x_2(t - \tau_1)}{1 + \{x_2(t - \tau_1)\}^c} + K_2 x_1(t - \tau_2)$$

(2.1)

where the Ikeda model x_1 is the phase lag of the electric field across the resonator; α_1 is the relaxation coefficient for the driving x_1 dynamical variable; β is the laser intensity injected into the driving system. τ_1, τ_2 are the delay time in the new IMG system, and the dynamical variable x_2 in the Mackey-Glass model is the concentration of the mature cells in blood at time t and the delay time is the time between the initiation of cellular production in the bone marrow and release of mature cells into the blood[10]. α_2 is the relaxation coefficient for the driven x_2 dynamical variable, b is the feedback rate for the driven system, and K_1, K_2 is the coupling rate between the driver system x_1 and the response system x_2.

This system has a chaotic attractor shown in Fig.2.1. Fig.2.2 shows the bifurcation diagram, where $\alpha_1 = 25$, $\beta = 24.8$, $K_1 = 14.1$, $\alpha_2 = 4.7$, $b = 1.2348$, c=10, $K_2 = 8$, τ_1

=5 and $\tau_2=1$.

If the delay time τ_2 is zero, also it is found that there is also a chaotic behavior for IMG system. Fig.2.3 show the chaotic attractor of this system. Fig.2.4 shows the bifurcation diagram, where $\alpha_1=25$, $\beta=24.8$, $k_1=14.1$, $\alpha_2=4.7$, $b=1.2348$, c=10, $K_2=8$, $\tau_1=5$ and $\tau_2=0$.
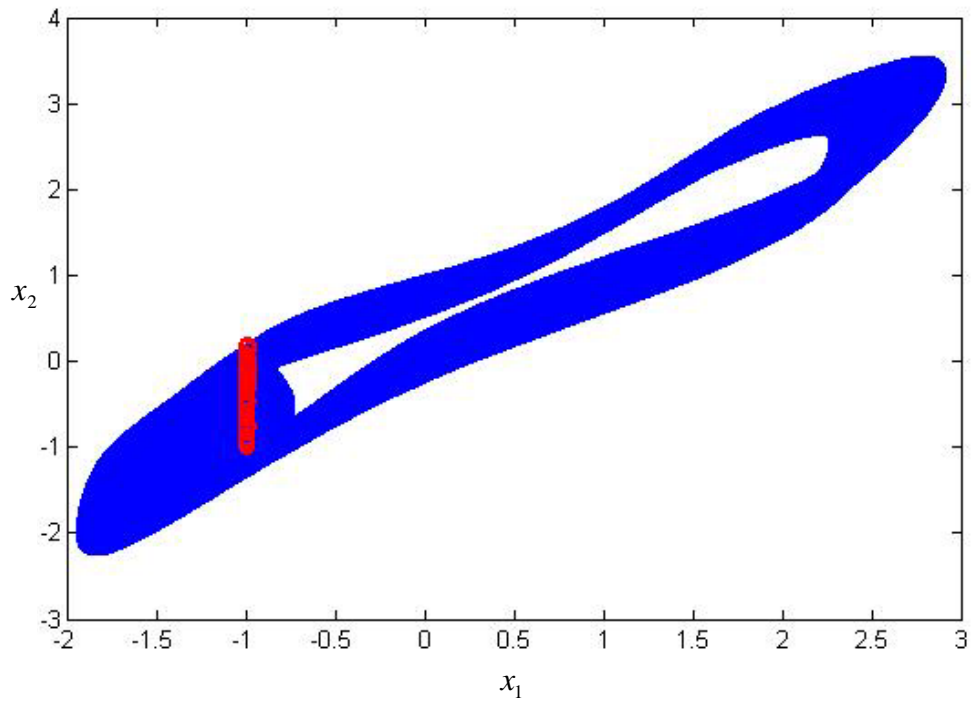
Fig. 2.1. An IMG chaotic attractor when the delay times $\tau_1=5, \tau_2=1$.
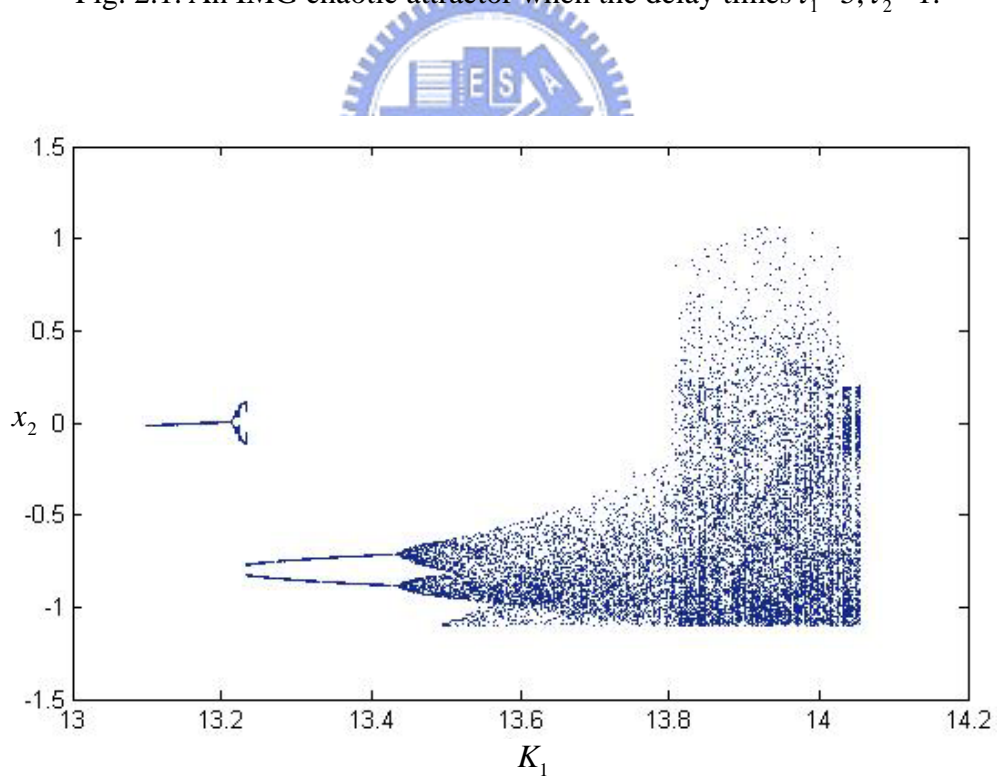
Fig.2.2. The bifurcation diagram of the IMG system when the delay times $\tau_1=5, \tau_2=1$.
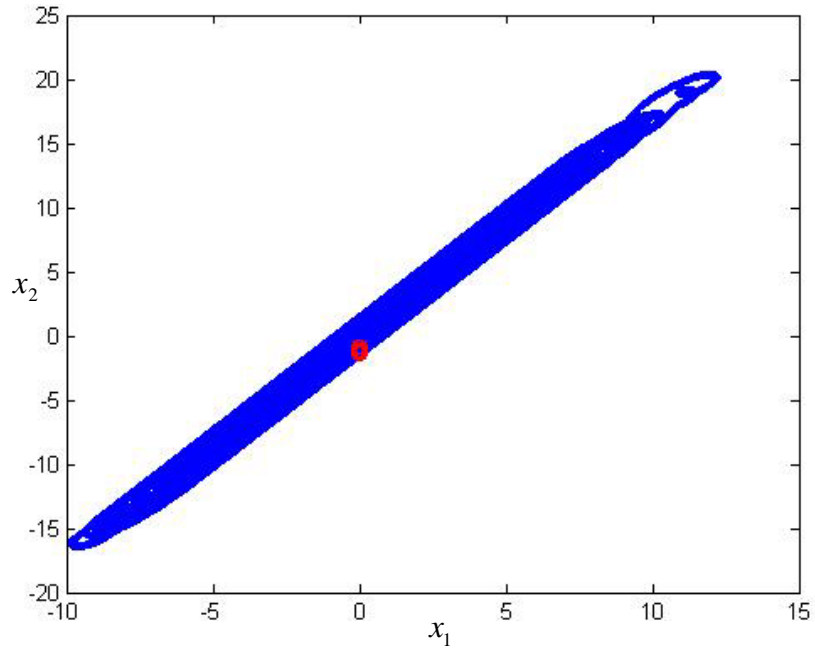
Fig.2.3. An IMG chaotic attractor when the delay times $\tau_1 = 5, \tau_2 = 0$.
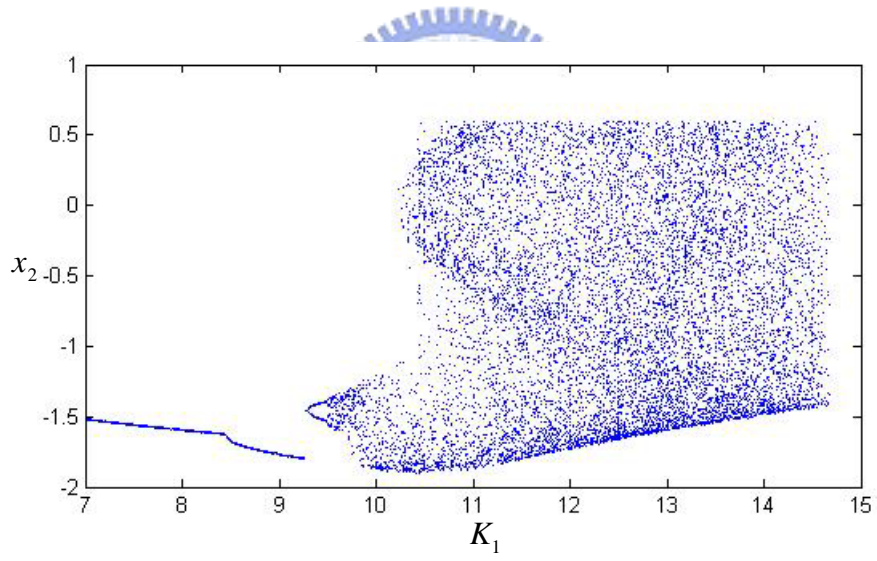
Fig.2.4. The bifurcation diagram of the IMG system when the delay times $\tau_1 = 5, \tau_2 = 0$.

Chapter 3

Chaos Synchronization of the Two Identical Ikeda-Mackey-Glass Systems

3.1 Preliminaries

In this Chapter, synchronization of the two identical new Ikeda-Mackey-Glass (IMG) systems without any control is studied. Two identical IMG system cannot be synchronized with slightly different conditions if one of delay time is zero and different types of synchronization can be obtained with slightly different initial conditions, such as generalized synchronization, anti-synchronization, and generalized lag-synchronization when two of delay time are positive. It is shown that we only adjust delay time τ_2, chaos synchronization of the two identical IMG systems can be obtained.
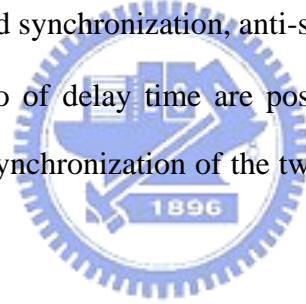
3.2 Synchronization Scheme

Consider the time-delayed system:

$$\dot{x}(t) = f(x(t), x(t - \tau)) \tag{3.1}$$

where $x \in R$ represents the state of the system, and $\dot{x}(t) = \dfrac{dx}{dt}$.

To synchronize system (3.1), the form of the other system is

$$\dot{y}(t) = f(y(t), y(t - \tau)) + u \tag{3.2}$$

where u is the controlling term.

In this Chapter, we find that these two Ikeda-Mackey-Glass system can be synchronized without any controller, only by changing the delay time τ_1 and τ_2.

Consider synchronization between two Ikeda-Mackey-Glass systems:

$$\begin{cases} \dot{x}_1(t) = -\alpha_1 x_1(t) - \beta \sin x_1(t-\tau_1) + K_1 x_2(t-\tau_2) \\ \dot{x}_2(t) = -\alpha_2 x_2(t) + b\dfrac{x_2(t-\tau_1)}{1+\{x_2(t-\tau_1)\}^c} + K_2 x_1(t-\tau_2) \end{cases} \tag{3.3}$$

$$\begin{cases} \dot{y}_1(t) = -\alpha_1 y_1(t) - \beta \sin y_1(t-\tau_1) + K_1 y_2(t-\tau_2) + u_1 \\ \dot{y}_2(t) = -\alpha_2 y_2(t) + b\dfrac{y_2(t-\tau_1)}{1+\{y_2(t-\tau_1)\}^c} + K_2 y_1(t-\tau_2) + u_2 \end{cases} \tag{3.4}$$

where the controlling term $u_1 = u_2 = 0$.

3.2.1 Case1: If the delay time $\tau_2 = 0$

In this Section it is shown that if the delay time τ_2 is zero, no synchronization can be obtained. Simulation results are shown in Fig.3.1 and Fig.3.2.

3.2.2 Case2: If the delay time $\tau_2 = 1$

In this Section it is shown that if the delay time τ_2 is not zero, different types of synchronization can be obtained.

Fig.3.3 and Fig.3.4 show that the generalized synchronization of the two identical IMG systems can be obtained. Define

$$\begin{cases} e_1 = x_1 - y_1 \\ e_2 = x_2 - y_2 \\ e_1 = R_1(t) \\ e_2 = R_2(t) \end{cases} \tag{3.5}$$

$R_1(t), R_2(t)$ are two periodic functions of time.

9

Fig.3.5 and Fig.3.6 show that the time responses of two identical IMG systems. It is verified that the anti-synchronization can be obtained by Fig.3.7 and Fig.3.8, where error

$$
\begin{cases}
e_1 = x_1 + y_1 \\
e_2 = x_2 + y_2
\end{cases}
\tag{3.6}
$$

Fig.3.9 and Fig.3.10 show that the time responses of two identical IMG systems. It is verified that the generalized lag-synchronization can be obtained by Fig.3.11 and Fig.3.12, where error

$$
e_1(t) = x_1(t - \mu_1) - y_1(t) + F(t)
\tag{3.7}
$$

$$
e_2(t) = x_2(t) - y_2(t - \mu_2) + F'(t)
\tag{3.8}
$$

$\mu_1 = 1.2427 \sec, \mu_2 = 1.08 \sec,$ $F(t)$ and $F'(t)$ are periodic functions of time.
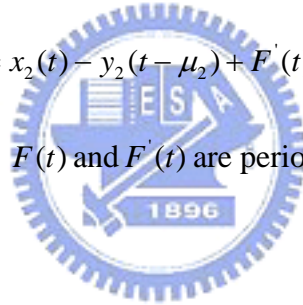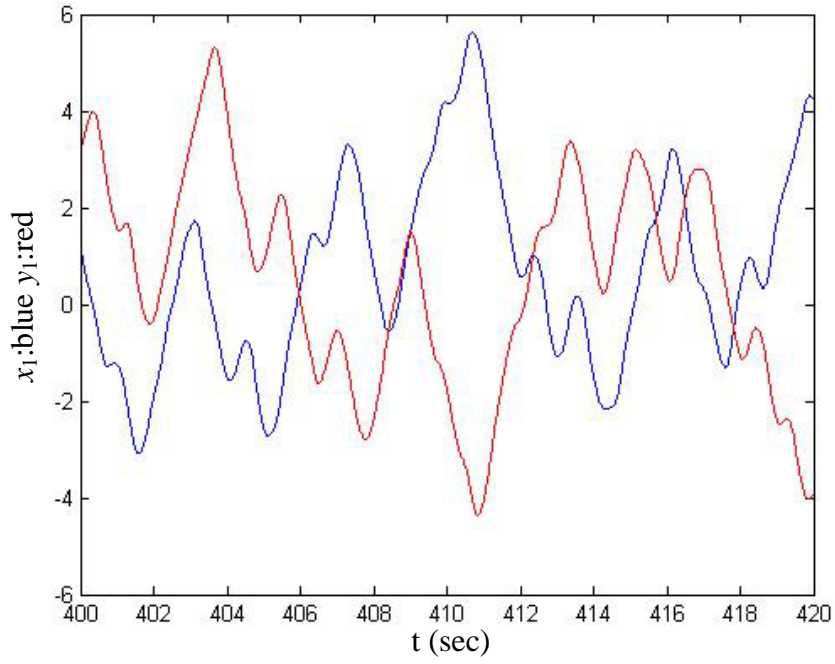
Fig.3.1.Time responses of two identical IMG systems with
$x_1(0)=1$, $x_2(0)=0$, $y_1(0)=-1$ and $y_2(0)=0.5$, when $\tau_2 =0$.
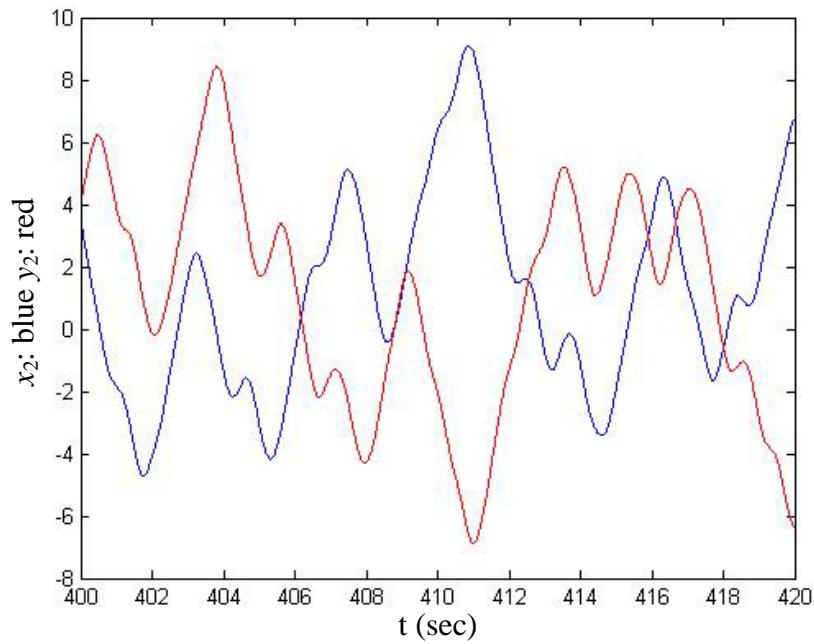
Fig.3.2.Time responses of two identical IMG systems with
$x_1(0)=1$, $x_2(0)=0$, $y_1(0)=-1$ and $y_2(0)=0.5$, when $\tau_2 =0$.

11
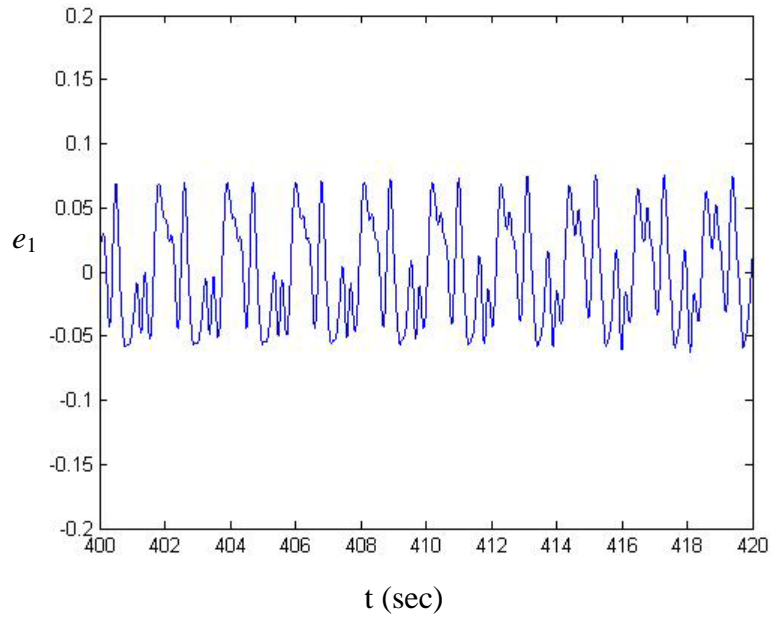
Fig.3.3. Error of two identical IMG systems with
$x_1(0)=100$, $x_2(0)=10$, $y_1(0)=101$ and $y_2(0)=10.001$, when $\tau_2 = 1$.
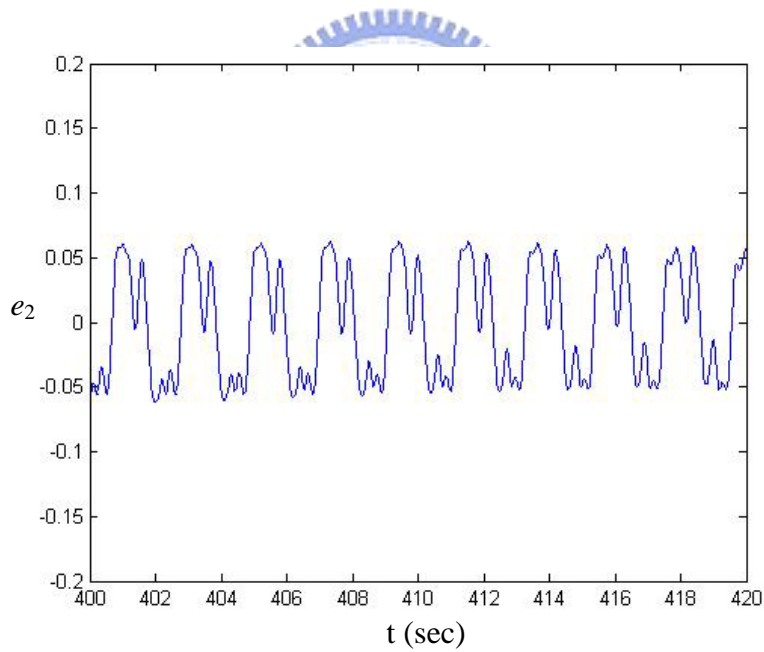
Fig.3.4. Error of two identical IMG systems with
$x_1(0)=100$, $x_2(0)=10$, $y_1(0)=101$ and $y_2(0)=10.001$, when $\tau_2 = 1$.

12
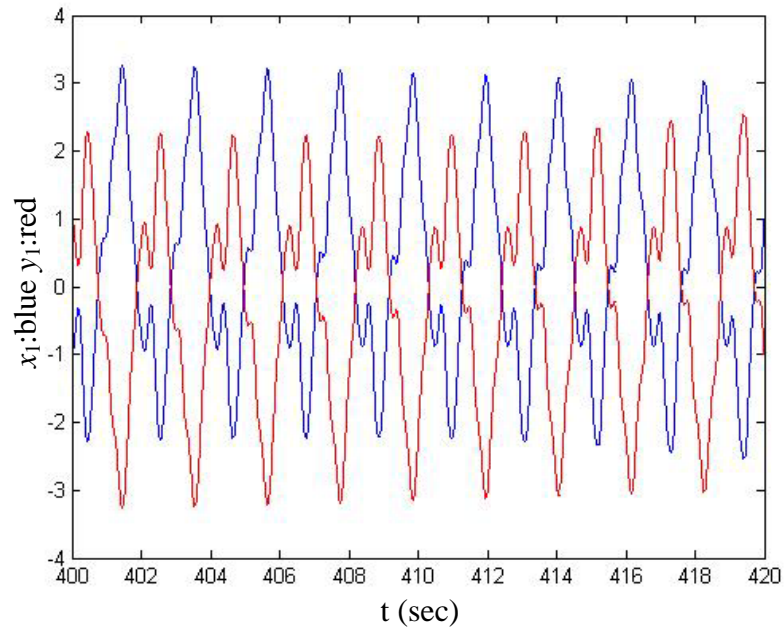
Fig.3.5. Time responses of two identical IMG systems with
$x_1(0)=1$, $x_2(0)=0$, $y_1(0)=-1$ and $y_2(0)=0$, when $\tau_2 = 1$.
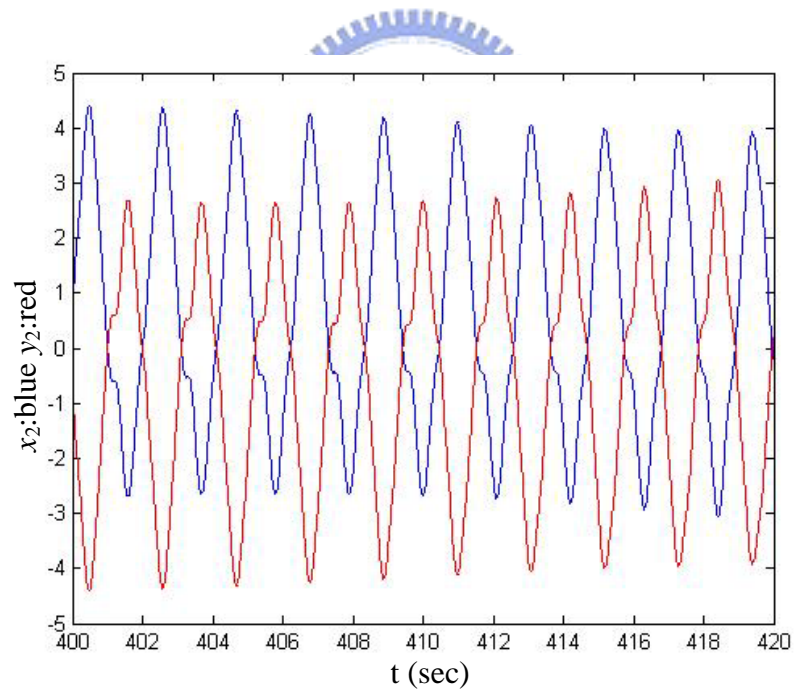
Fig.3.6. Time responses of two identical IMG systems with
$x_1(0)=1$, $x_2(0)=0$, $y_1(0)=-1$ and $y_2(0)=0$, when $\tau_2 = 1$.

13
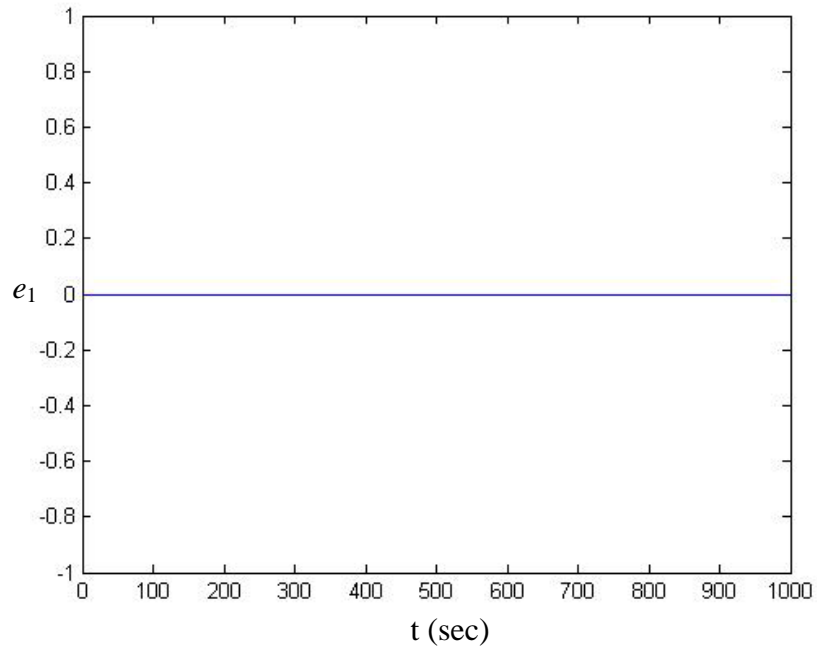
Fig.3.7. Error of two identical IMG systems with
$x_1(0)=1$, $x_2(0)=0$, $y_1(0)=-1$ and $y_2(0)=0$, when $\tau_2 = 1$.
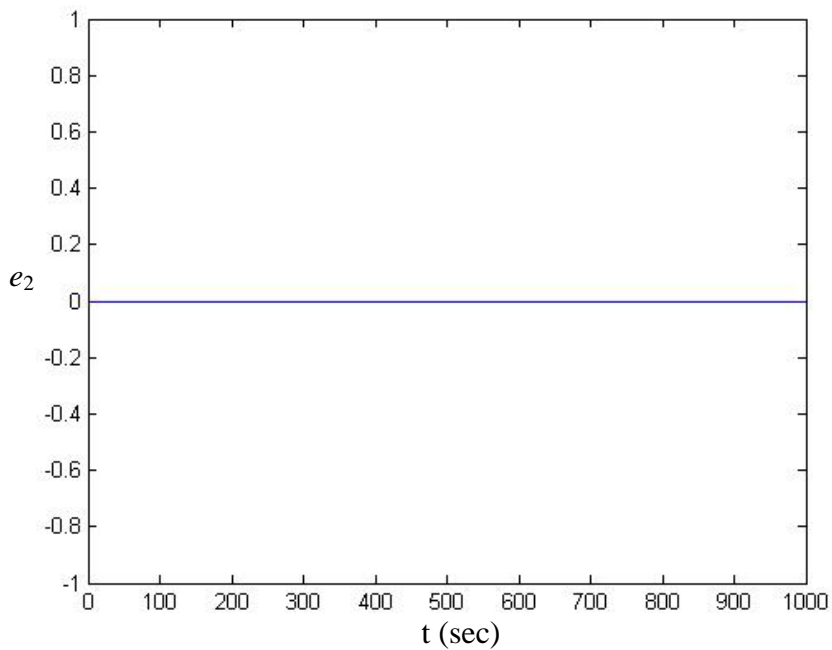
Fig.3.8. Error of two identical IMG systems with
$x_1(0)=1$, $x_2(0)=0$, $y_1(0)=-1$ and $y_2(0)=0$, when $\tau_2 = 1$.
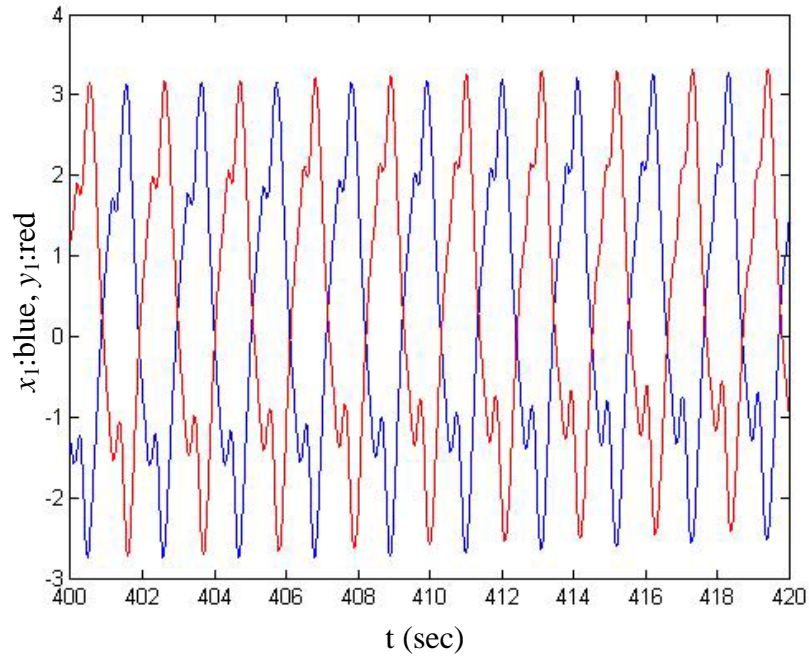
Fig.3.9. Time responses of two identical IMG systems with
$x_1(0)=1$, $x_2(0)=0.1$, $y_1(0)=-1$ and $y_2(0)=0.5$, when $\tau_2 = 1$, $\mu_1 = 1.2427$ sec.
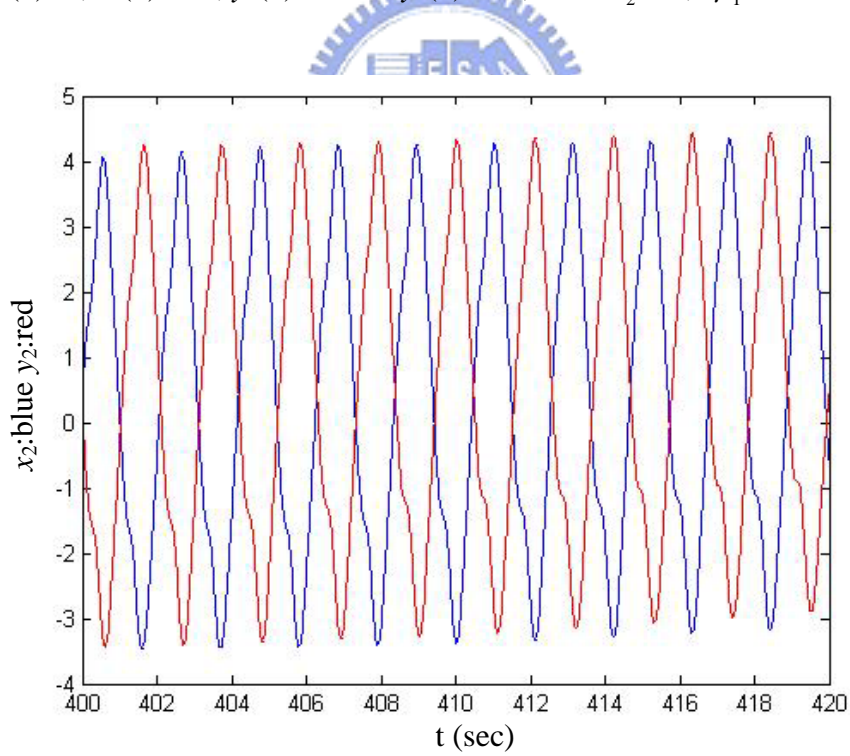
Fig.3.10. Time responses of two identical IMG systems with
$x_1(0)=1$, $x_2(0)=0.1$, $y_1(0)=-1$ and $y_2(0)=0.5$, when $\tau_2 = 1$, $\mu_2 = 1.08$ sec.
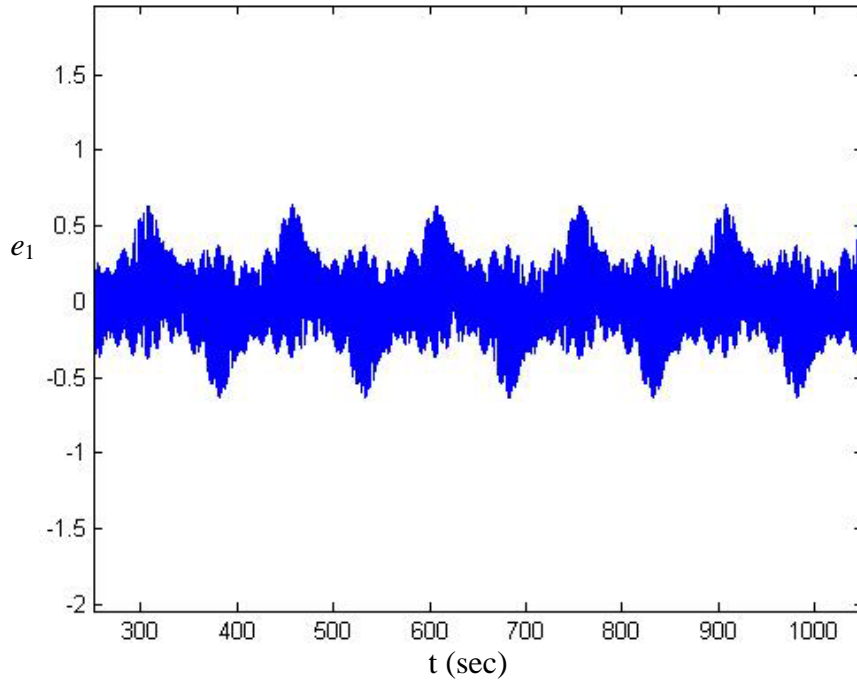
Fig.3.11. Error of two identical IMG systems with
$x_1(0)$=1, $x_2(0)$=0.1, $y_1(0)$=-1 and $y_2(0)$=0.5, when $\tau_2 = 1$.
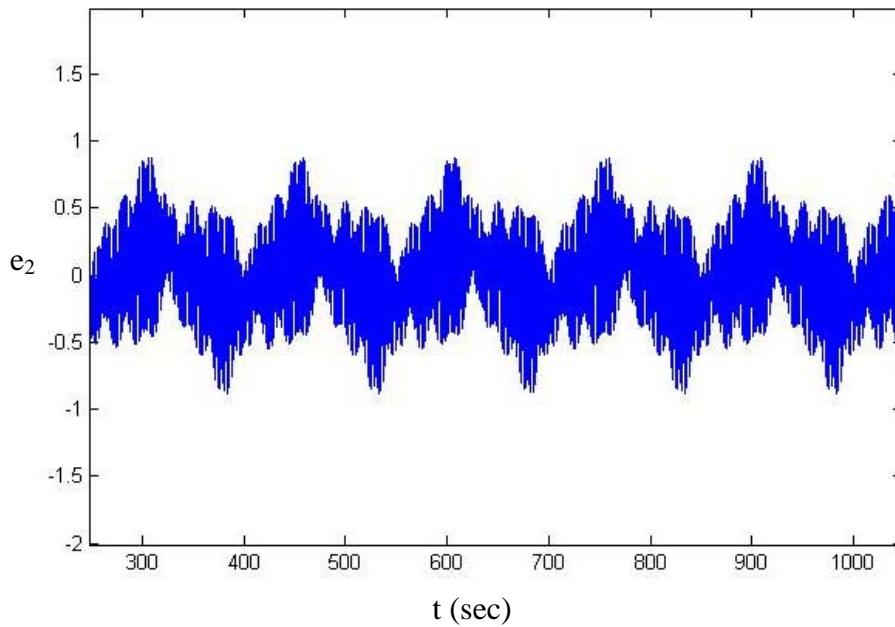
Fig.3.12. Error of two identical IMG systems with
$x_1(0)$=1, $x_2(0)$=0.1, $y_1(0)$=-1 and $y_2(0)$=0.5, when $\tau_2 = 1$.

16

Chapter 4

Chaotization of a New Ikeda-Mackey-Glass System

by Chaos Signals as Parameters

4.1 Preliminaries

In this Chapter, another chaotization method is presented by using different types of chaos signal as parameter. A new Ikeda-Mackey-Glass system is described in Chapter 2.2. By using different types of chaos signals as parameters, a regular motion new IMG system becomes chaotic system.

4.2 Chaotization Scheme

Differential equations of two general delay systems are described as follows:

$$\dot{x} = f(x(t), x(t-\tau), K) \tag{4.1}$$

$$\dot{y} = f(y(t), y(t-\tau), G) \tag{4.2}$$

where $x, y \in R^n$ are the state vector, $K = [k_1\ k_2...k_n], G = [g_1\ g_2...g_n] \in R^n$ are the parameter vectors. The dynamics of system (4.1) is periodic motion, while the dynamics of system (4.2) is chaotic motion. Replacing one of the parameters of system (4.1) by chaotic states of system (4.2), system (4.1) becomes:

$$\dot{z} = f(z(t), z(t-\tau), P) \tag{4.3}$$

where z is the state vector, P is the same as K, except that one of parameters of

K is replaced by chaotic states of system (4.2). Simulations show that system (4.3)

becomes a chaotic system. In other worlds, a delay system (4.3) becomes chaotic

system by parameter replacement method.

4.3 Simulation Results

By using Eq.(4.1), the periodic motion of a new Ikeda-Mackey-Glass system is

described as follows:

$$\dot{x}_1(t) = -\alpha_1 x_1(t) - \beta \sin x_1(t-\tau_1) + k_1 x_2(t-\tau_2)$$

(4.4)

$$\dot{x}_2(t) = -\alpha_2 x_2(t) + b\frac{x_2(t-\tau_1)}{1+\{x_2(t-\tau_1)\}^c} + k_2 x_1(t-\tau_2)$$
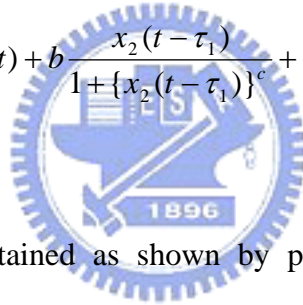
A periodic motion is obtained as shown by phase portraits in Fig.4.1, time

histories in Fig.4.2 and Fig.4.3, and bifurcation diagram in Fig.4.4, where α_1=25, β

=24.8, k_1= 13.4, α_2=4.7, b=1.2348, c=10, k_2=8, τ_1=5 and τ_2=1.

By using Eq.(4.2), the chaotic motion of a new Ikeda-Mackey-Glass system is

described as follows:

$$\dot{y}_1(t) = -\alpha_1 y_1(t) - \beta \sin y_1(t-\tau_1) + g_1 y_2(t-\tau_2)$$

(4.5)

$$\dot{y}_2(t) = -\alpha_2 y_2(t) + b\frac{y_2(t-\tau_1)}{1+\{y_2(t-\tau_1)\}^c} + g_2 y_1(t-\tau_2)$$

A chaotic motion is obtained as shown by phase portrait in Fig.4.5 and bifurcation

diagram in Fig.4.4, where $\alpha_1 = 25$, $\beta = 24.8$, $g_1 = 14.1$, $\alpha_2 = 4.7$, $b = 1.2348$, $c = 10$,

$g_2 = 8$, $\tau_1 = 5$ and $\tau_2 = 1$.

Replacing k_1 by p_1, Eq.(4.4) becomes:

$$\dot{z}_1(t) = -\alpha_1 z_1(t) - \beta \sin z_1(t - \tau_1) + p_1 z_2(t - \tau_2)$$

(4.6)

$$\dot{z}_2(t) = -\alpha_2 z_2(t) + b \frac{z_2(t - \tau_1)}{1 + \{z_2(t - \tau_1)\}^c} + k_2 z_1(t - \tau_2)$$

where $k_2 = 8$. A new Ikeda-Mackey-Glass system(4.6) is a chaotic system by parameter replacement method.

CASE I: p₁=y₁

The chaotic simulation results obtained is achieved in phase portrait in Fig.4.6 and time histories in Fig.4.7 and Fig.4.8.

CASE II: p₁=y₂

The chaotic simulation results obtained is achieved in phase portrait in Fig.4.9 and time histories in Fig.4.10 and Fig.4.11.

CASE III: $p_1 = y_1^2$

The chaotic simulation results obtained is achieved in phase portrait in Fig.4.12 and time histories in Fig.4.13 and Fig.4.14.

CASE IV: $p_1 = y_2^2$

The chaotic simulation results obtained is achieved in phase portrait in Fig.4.15 and time histories in Fig.4.16 and Fig.4.17.

CASE V: $p_1 = y_1 y_2$

The chaotic simulation results obtained is achieved in phase portrait in Fig.4.18 and time histories in Fig.4.19 and Fig.4.20.

CASE VI: $\quad p_1 = y_2 y_2(t - \tau)$*, where* $\tau = 30$ *sec.*

The chaotic simulation results obtained is achieved in phase portrait in Fig.4.21 and time histories in Fig.4.22 and Fig.4.23.

CASE VII: $\quad p_1 = \cos y_1 \cos y_2$

The chaotic simulation results obtained is achieved in phase portrait in Fig.4.24 and time histories in Fig.4.25 and Fig.4.26.

CASE VIII: $\quad p_1 = R + y_2$*, where R is the Rayleigh noise.*

The chaotic simulation results obtained is achieved in phase portrait in Fig.4.27 and time histories in Fig.4.28 and Fig.4.29

CASE IX: $\quad p_1 = Ry_2$*, where R is the Rayleigh noise.*

The chaotic simulation results obtained is achieved in phase portrait in Fig.4.30 and time histories in Fig.4.31 and Fig.4.32.
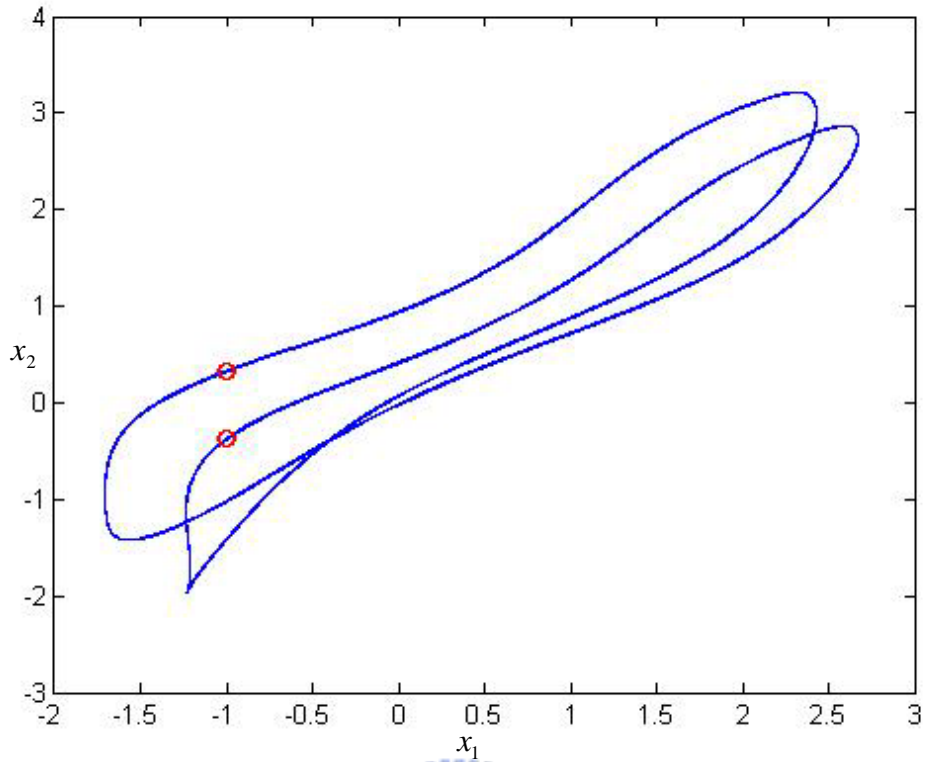
Fig.4.1. Phase portrait of an IMG system in period 2 when $\alpha_1 = 25$, $\beta = 24.8$, $K_1 = 13.4$, $\alpha_2 = 4.7$, $b = 1.2348$, c=10, $K_2 = 8$, $\tau_1 = 5$ and $\tau_2 = 1$.
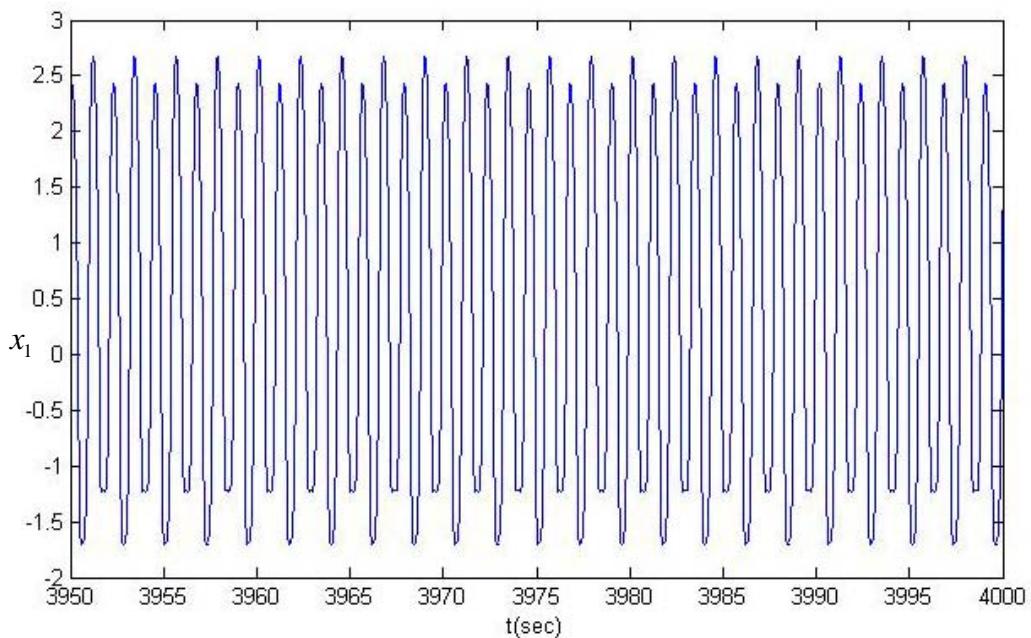
Fig.4.2. The time history of x_1 of an IMG system in period 2 when $\alpha_1 = 25$, $\beta = 24.8$, $K_1 = 13.4$, $\alpha_2 = 4.7$, $b = 1.2348$, c=10, $K_2 = 8$, $\tau_1 = 5$ and $\tau_2 = 1$.
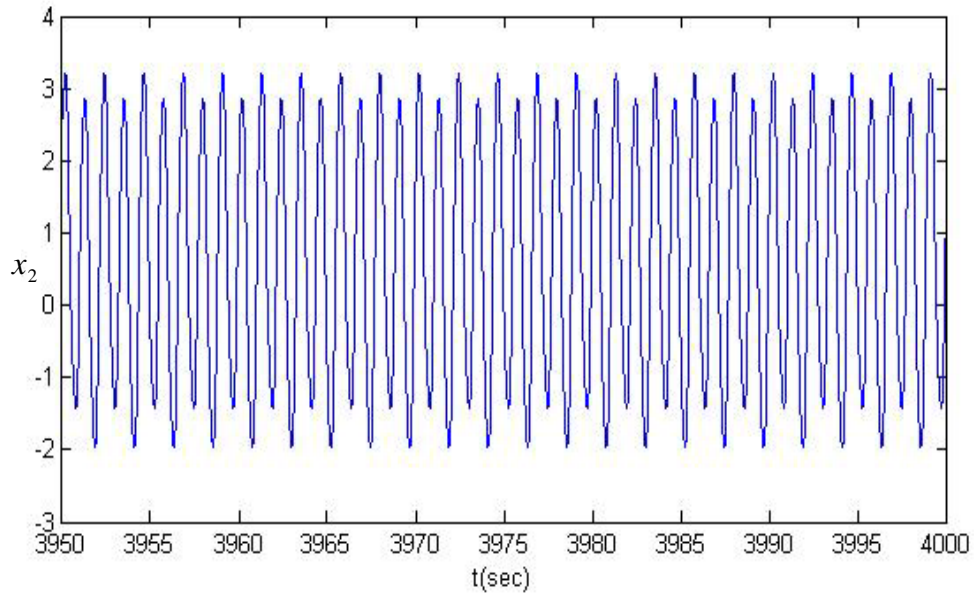
Fig.4.3. The time history of x_2 of an IMG system in period 2 when $\alpha_1 = 25$, $\beta = 24.8$,

$K_1 = 13.4$, $\alpha_2 = 4.7$, $b = 1.2348$, $c = 10$, $K_2 = 8$, $\tau_1 = 5$ and $\tau_2 = 1$.
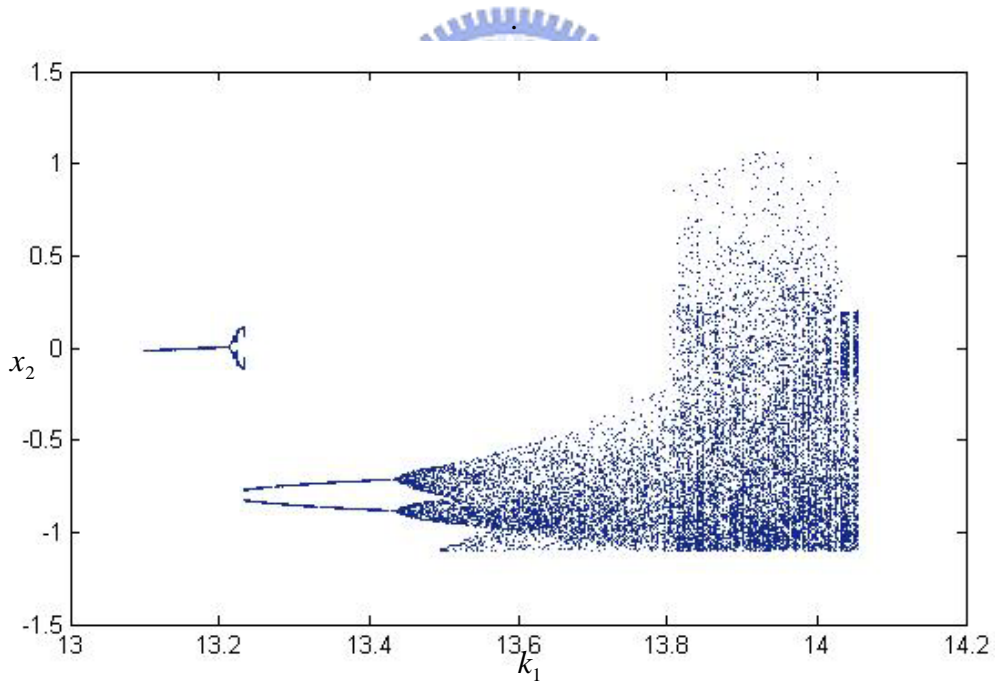
Fig.4.4. The bifurcation diagram of an IMG system when $\alpha_1 = 25$, $\beta = 24.8$, α_2

$= 4.7$, $b = 1.2348$, $c = 10$, $K_2 = 8$, $\tau_1 = 5$ and $\tau_2 = 1$.

22
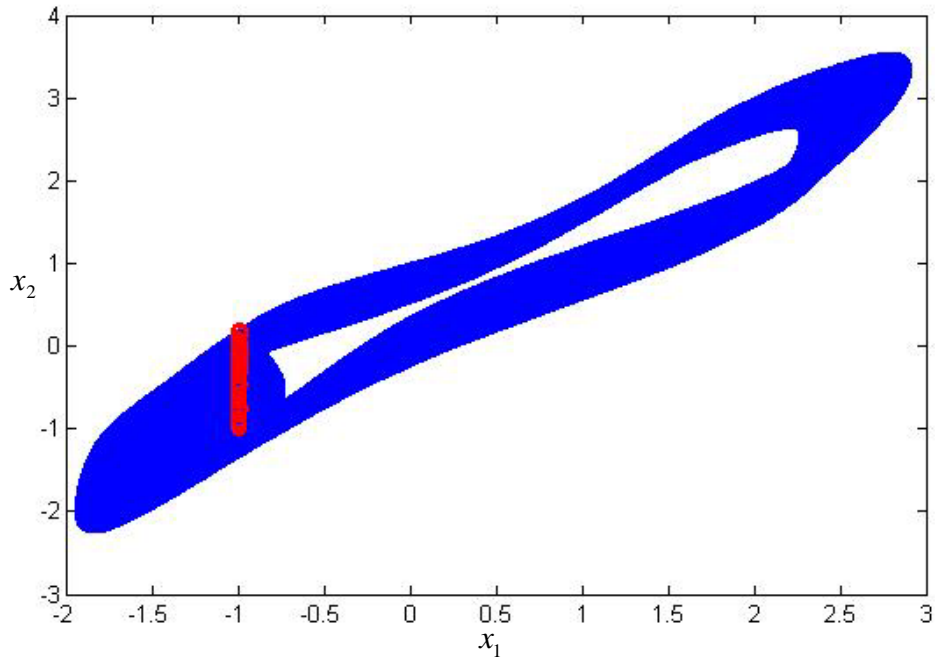
Fig4.5. An IMG chaotic attractor when $\alpha_1 = 25$, $\beta = 24.8$, $K_1 = 14.1$, $\alpha_2 = 4.7$, b

$= 1.2348$, c=10, $K_2 = 8$, $\tau_1 = 5$ and $\tau_2 = 1$.
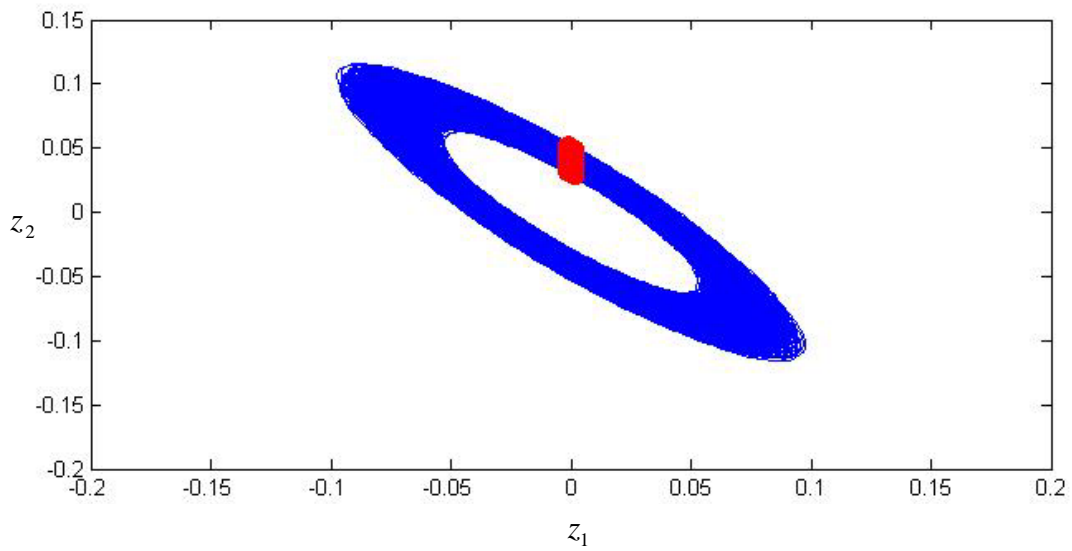
Fig4.6. An IMG chaotic attractor when parameter is a chaos signal
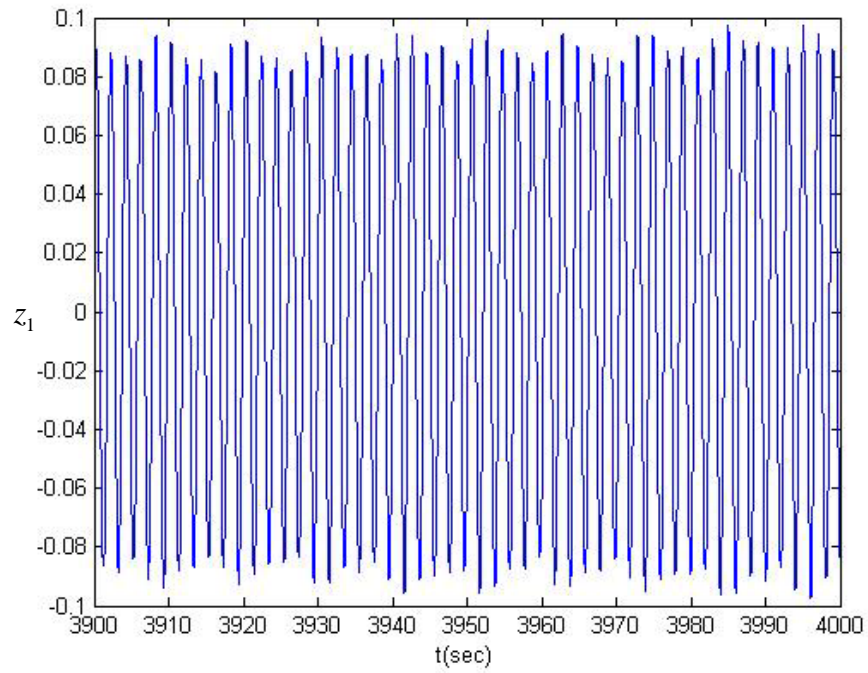
for *CASE I.*

Fig4.7. The time history of z_1 of an IMG system in chaotic behavior when parameter is a chaos signal for *CASE I*.
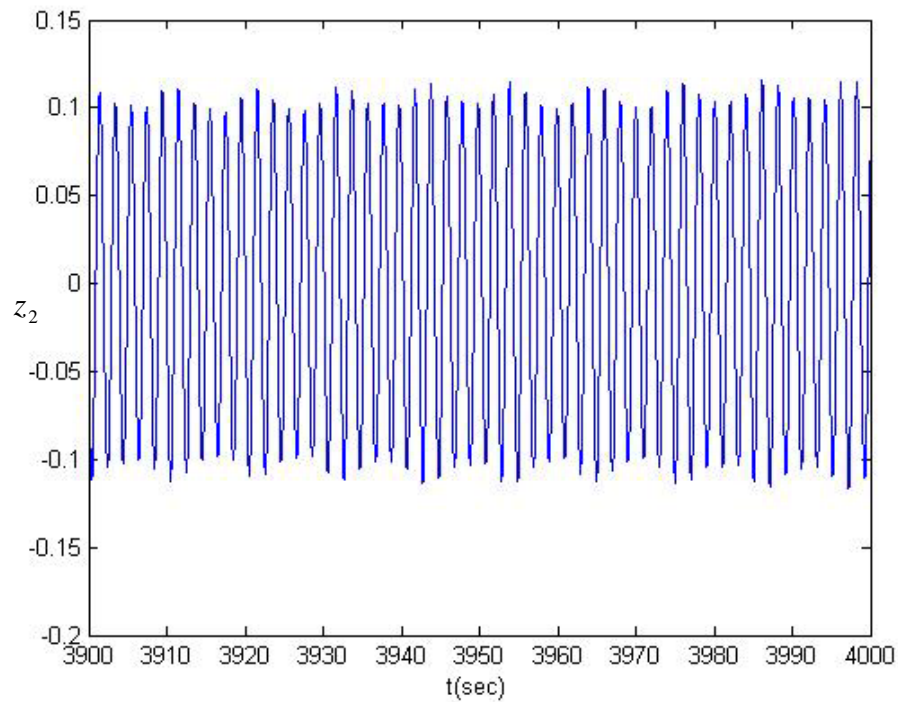
Fig.4.8. The time history of z_2 of an IMG system in chaotic behavior when parameter is a chaos signal for *CASE I*.

.
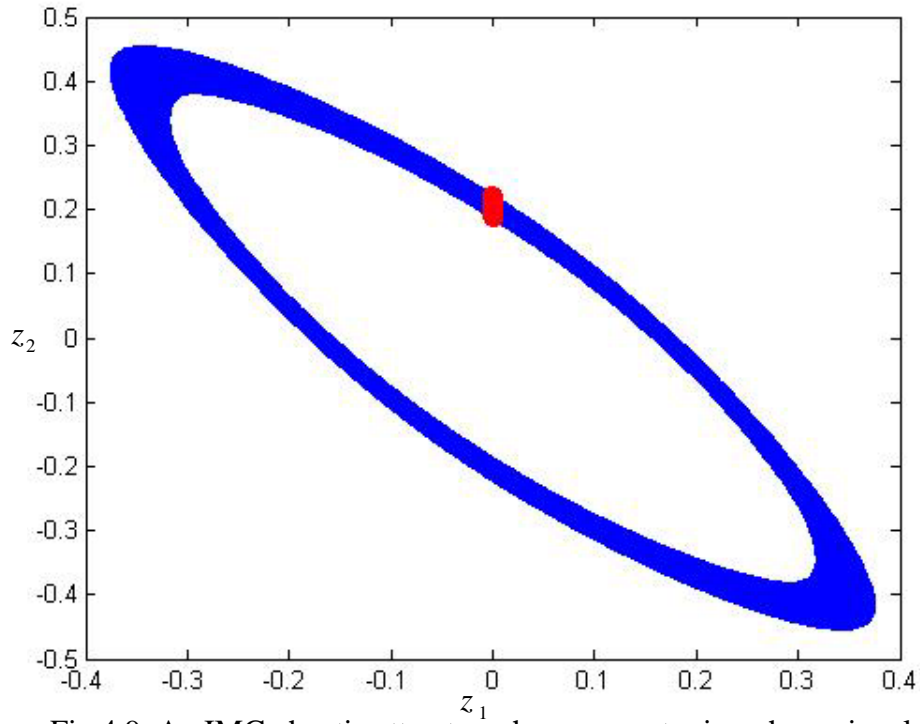
Fig.4.9. An IMG chaotic attractor when parameter is a chaos signal
for *CASE II*.
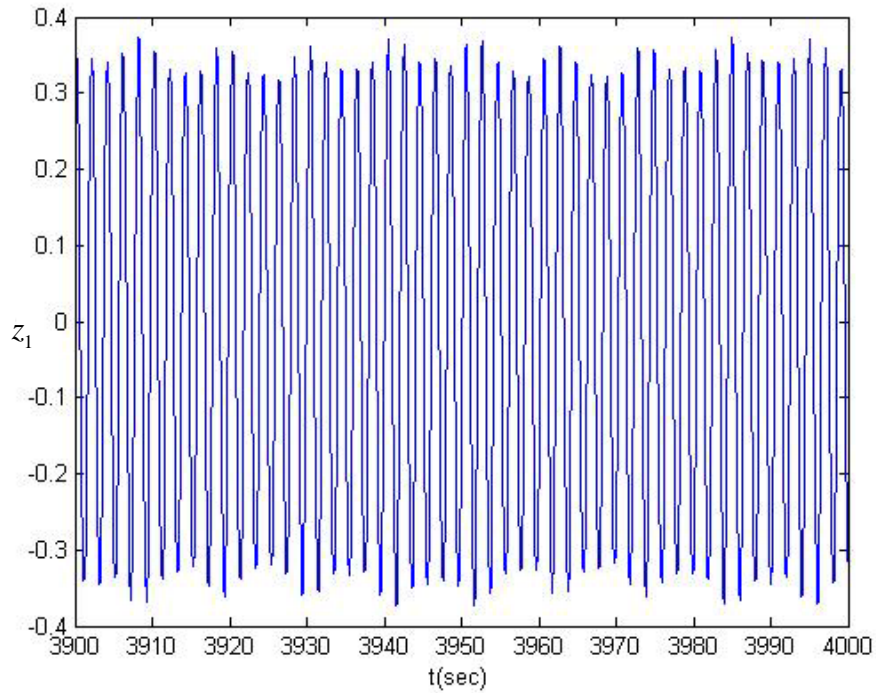
Fig.4.10. The time history of z_1 of an IMG system in chaotic behavior
when parameter is a chaos signal for *CASE II*.

.

25
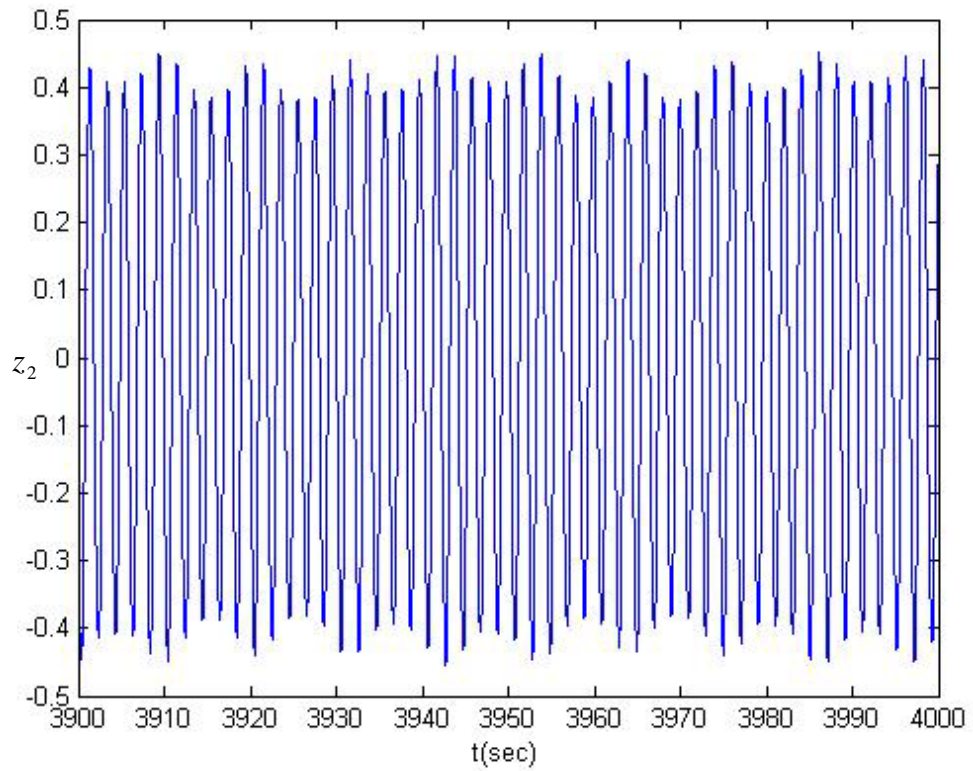
Fig.4.11. The time history of z_2 of an IMG system in chaotic behavior when parameter is a chaos signal for *CASE II*.
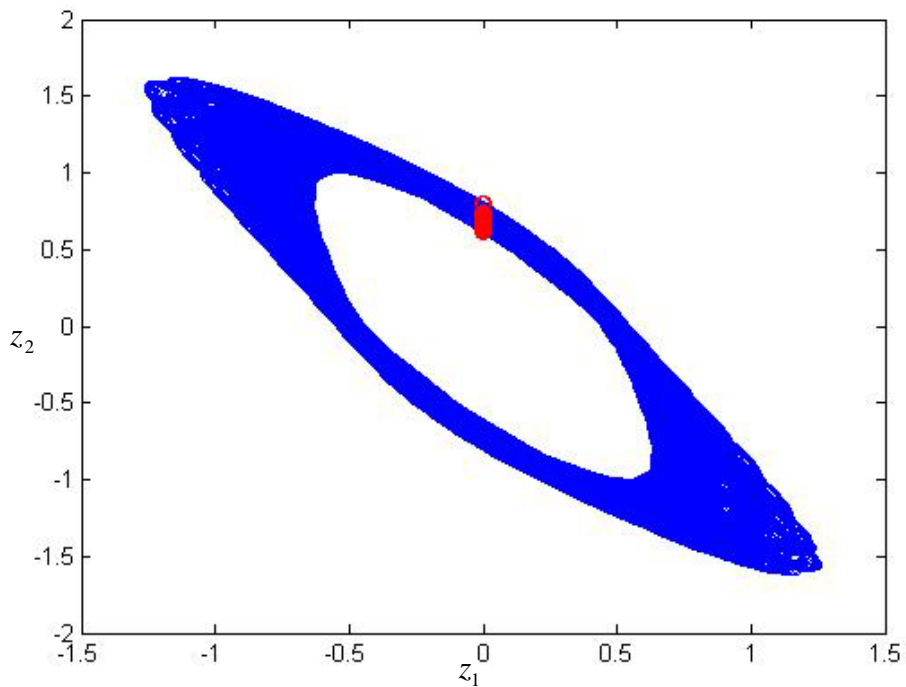
Fig.4.12. An IMG chaotic attractor when parameter is a chaos signal for *CASE III*.
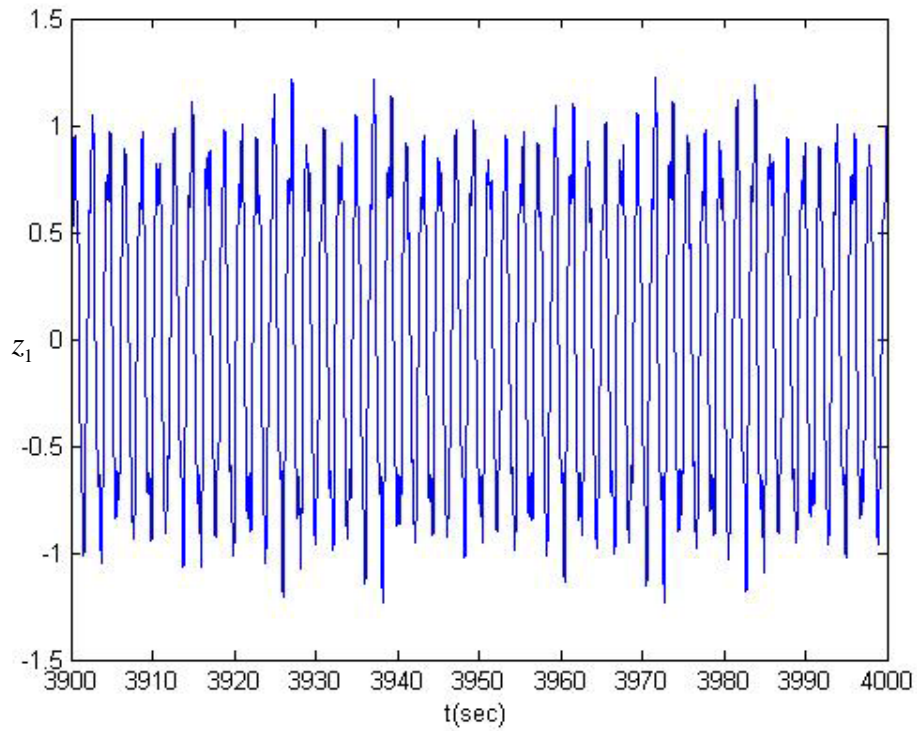
Fig.4.13. The time history of z_1 of an IMG system in chaotic behavior when parameter is a chaos signal for *CASE III*.
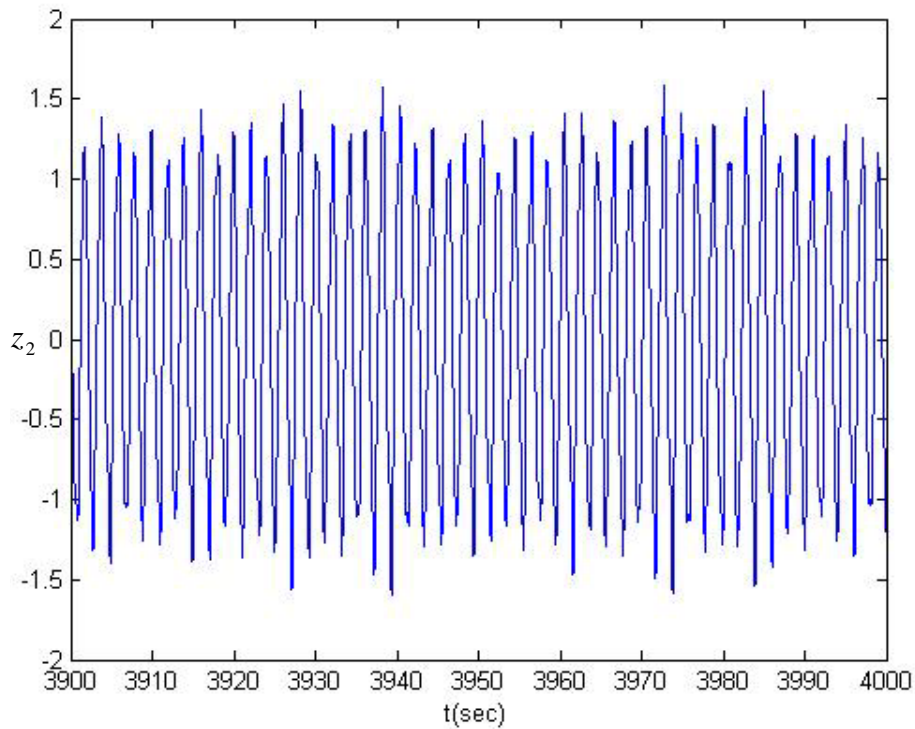
Fig.4.14. The time history of z_2 of an IMG system in chaotic behavior when parameter is a chaos signal for *CASE III*.
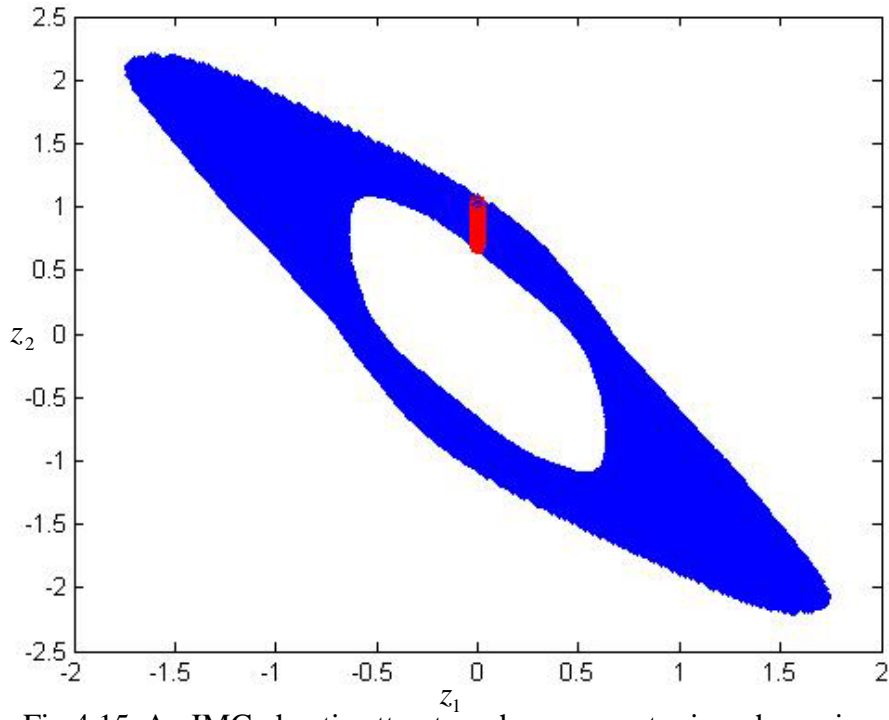
Fig.4.15. An IMG chaotic attractor when parameter is a chaos signal
for *CASE IV*.
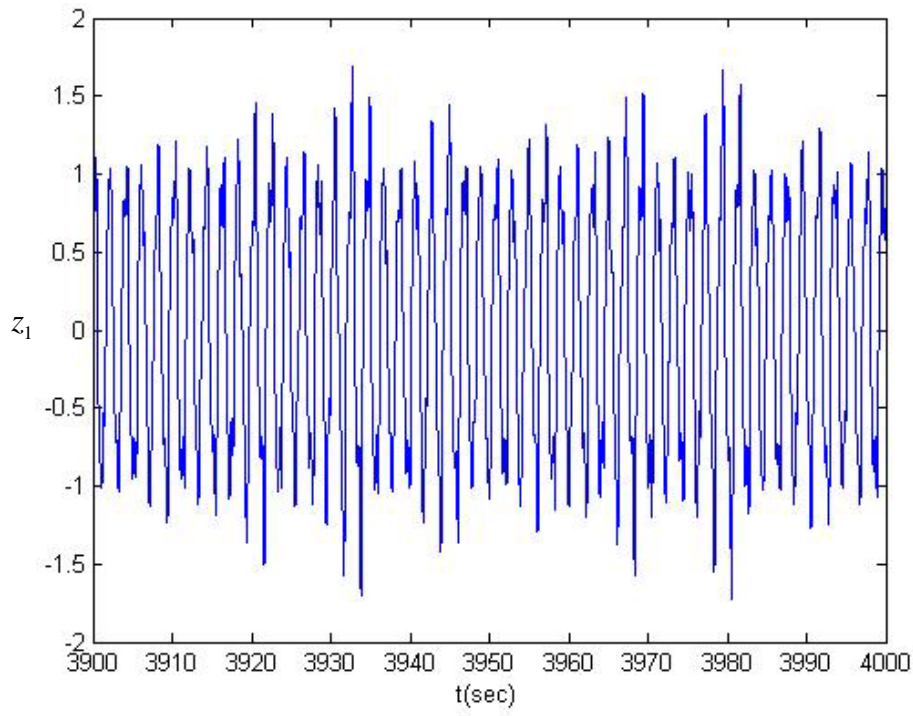
Fig.4.16. The time history of z_1 of an IMG system in chaotic behavior when parameter
is a chaos signal for *CASE IV*.
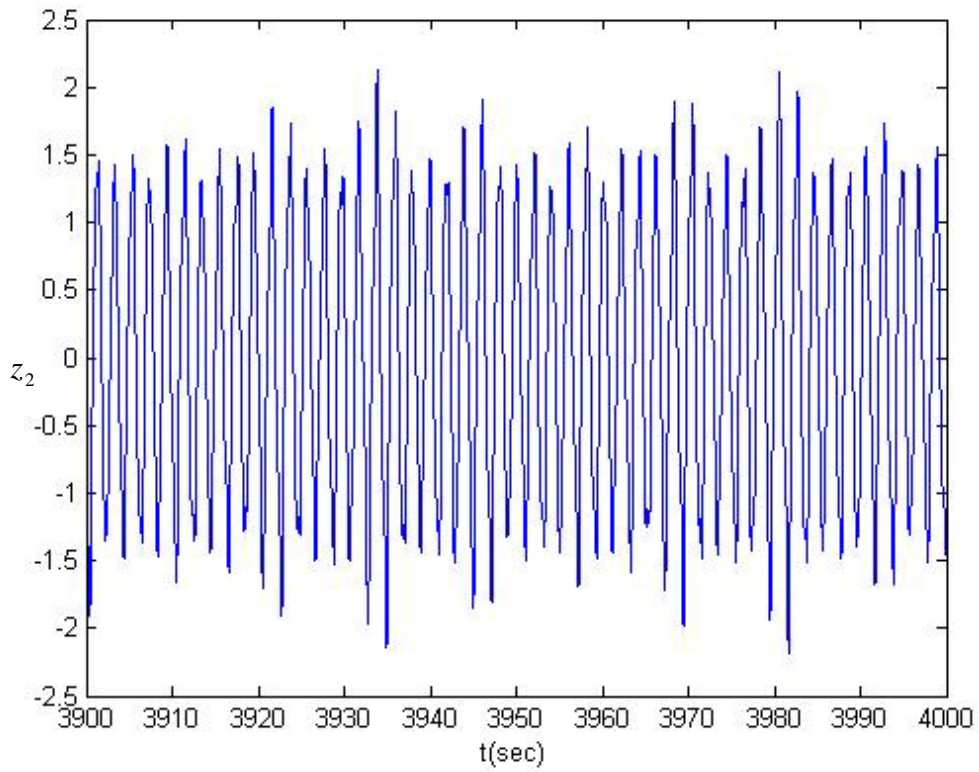
Fig.4.17. The time history of z_2 of an IMG system in chaotic behavior when parameter is a chaos signal for *CASE IV*.
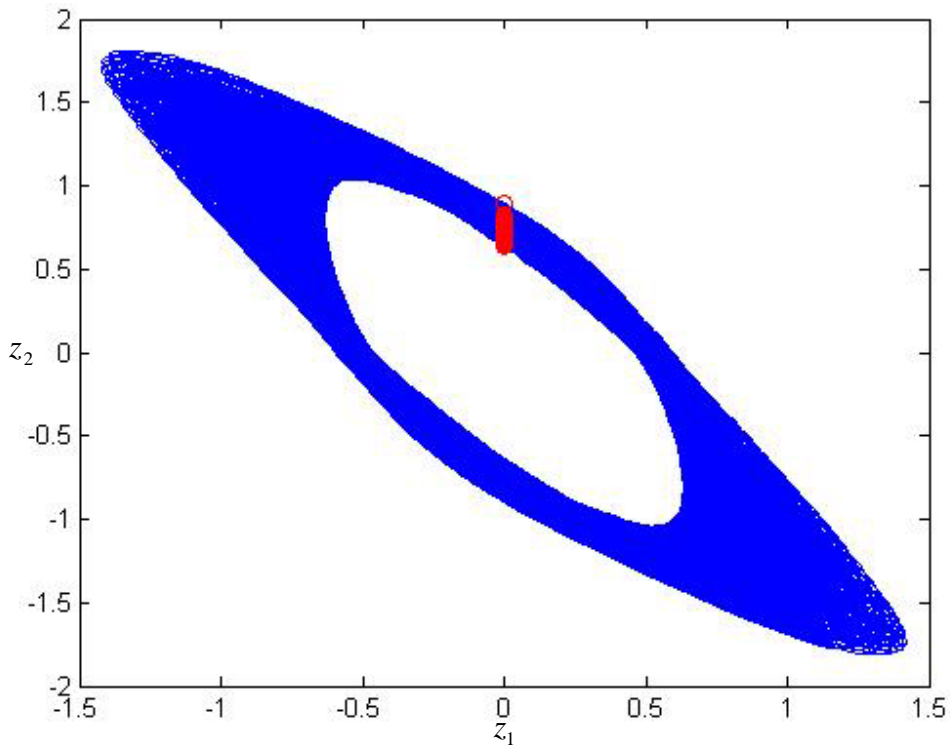
Fig.4.18. An IMG chaotic attractor when parameter is a chaos signal for *CASE V*.

29
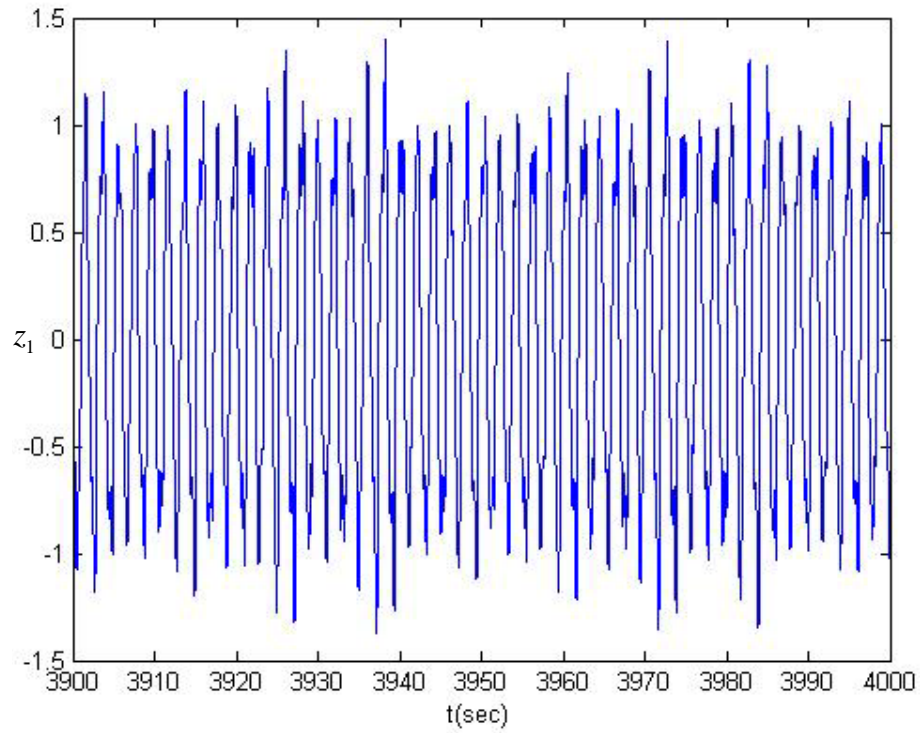
Fig.4.19. The time history of z_1 of an IMG system in chaotic behavior when parameter is a chaos signal for *CASE V*.
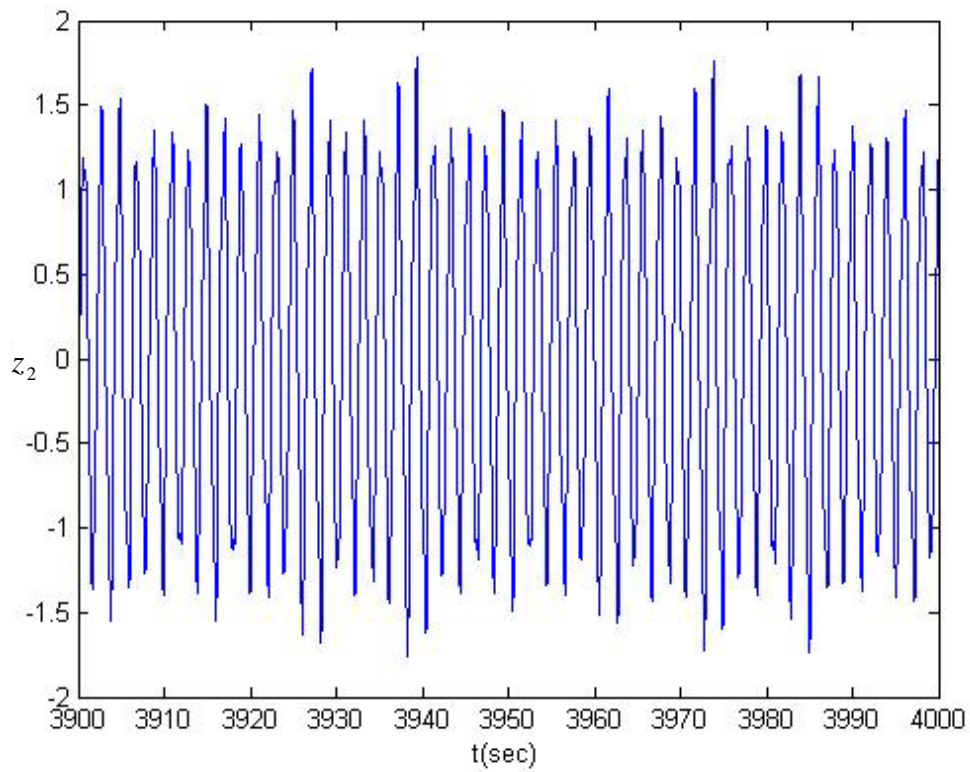
Fig.4.20. The time history of z_2 of an IMG system in chaotic behavior when parameter is a chaos signal for *CASE V*.
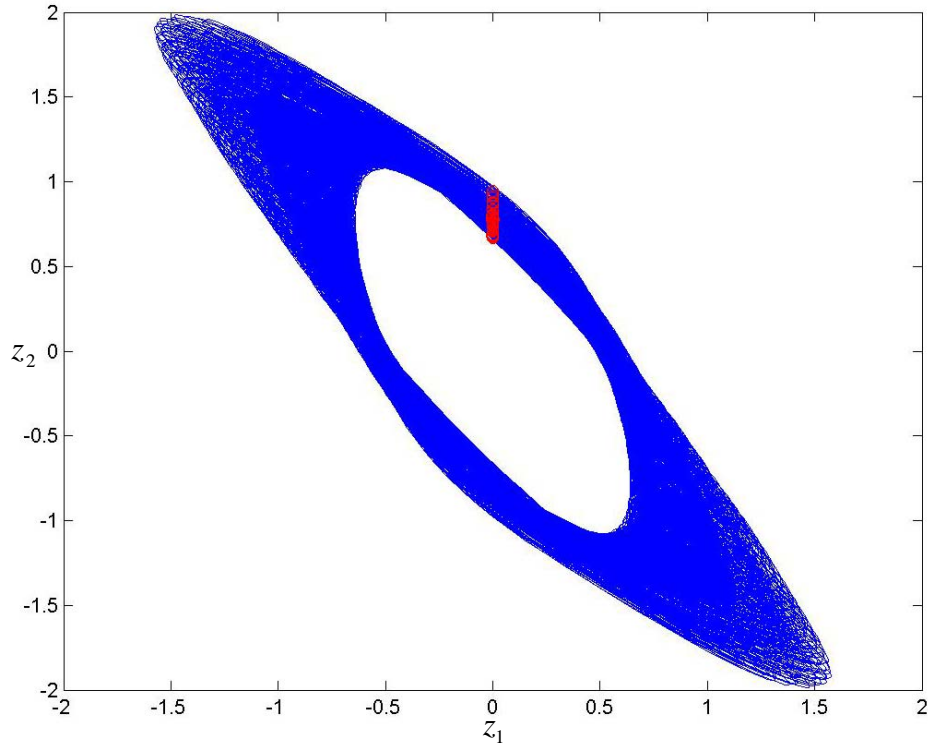
Fig.4.21. An IMG chaotic attractor when parameter is a chaos signal for *CASE VI*.
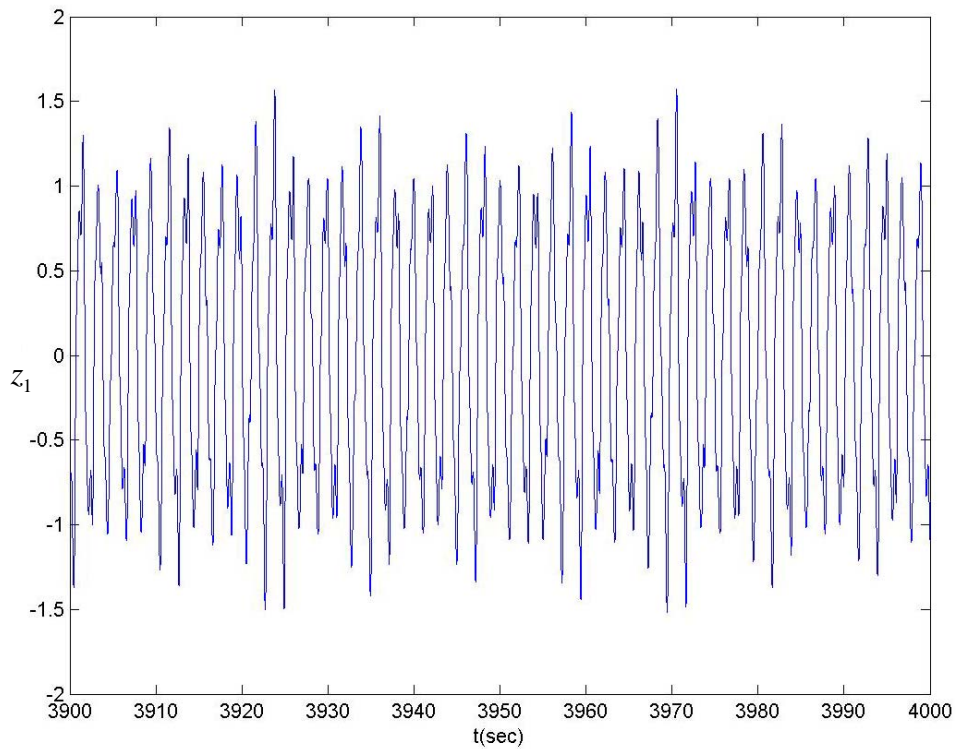
Fig.4.22. The time history of z_1 of an IMG system in chaotic behavior when parameter
is a chaos signal for *CASE VI*.

.
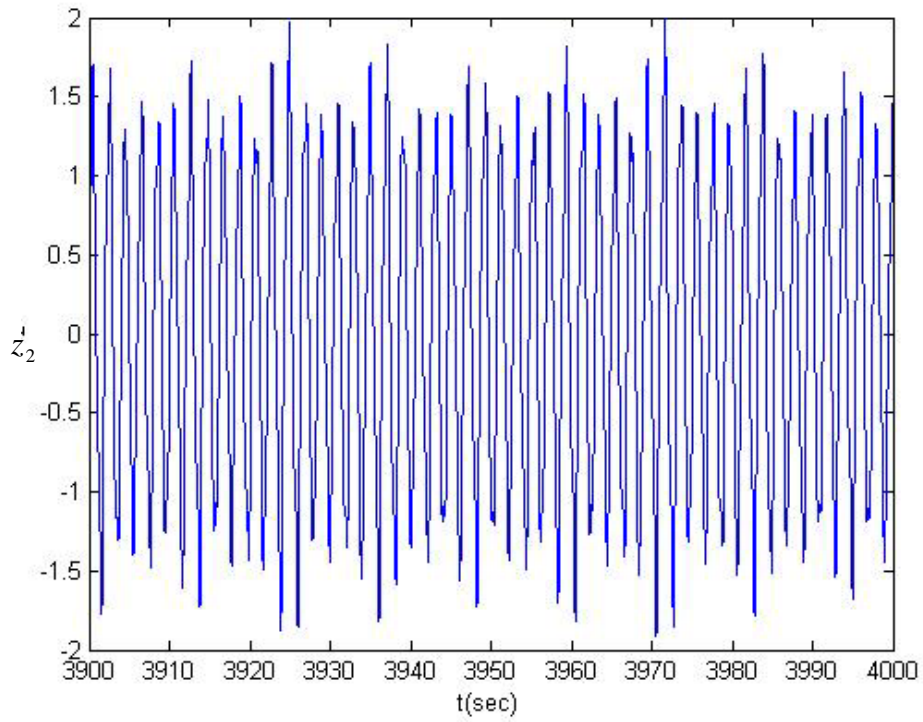
Fig.4.23. The time history of z_2 of an IMG system in chaotic behavior when parameter is a chaos signal for *CASE VI*.
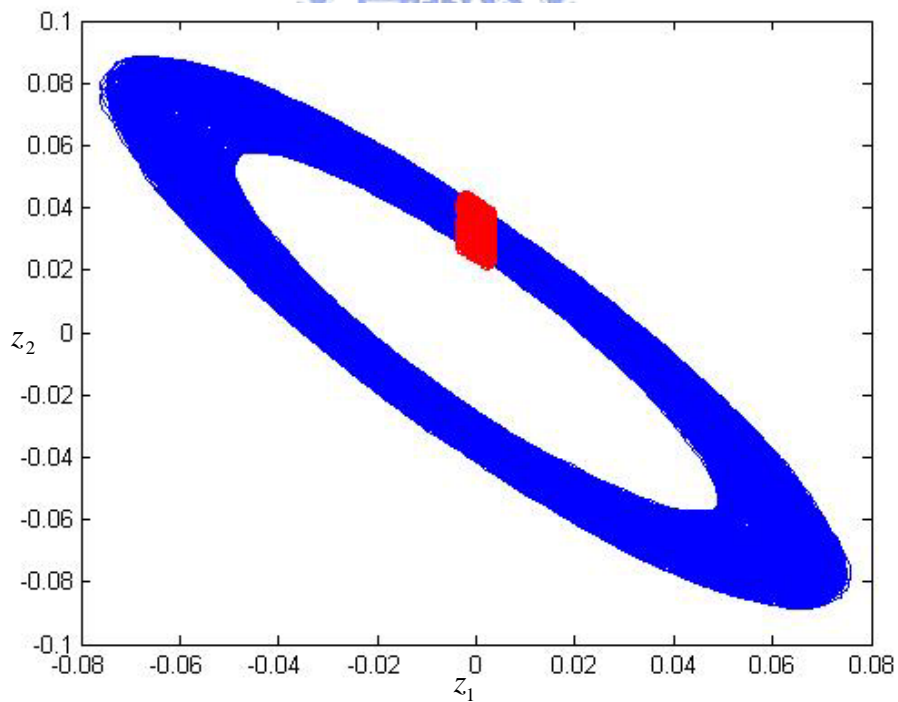
Fig.4.24. An IMG chaotic attractor when parameter is a chaos signal for *CASE VII*.
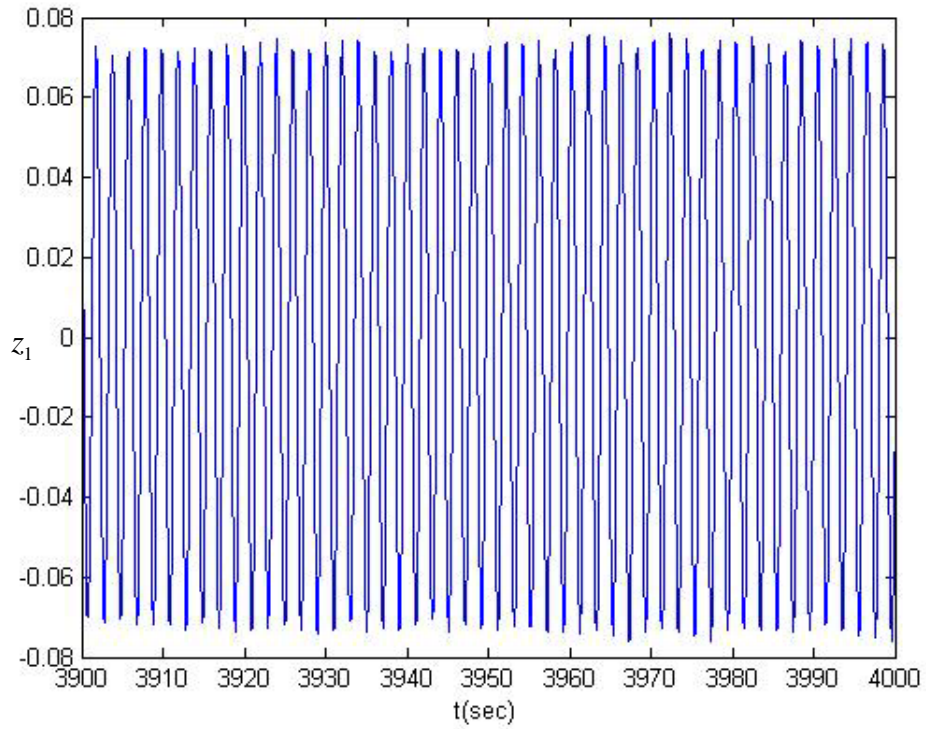
Fig.4.25. The time history of z_1 of an IMG system in chaotic behavior when parameter is a chaos signal for *CASE VII*.
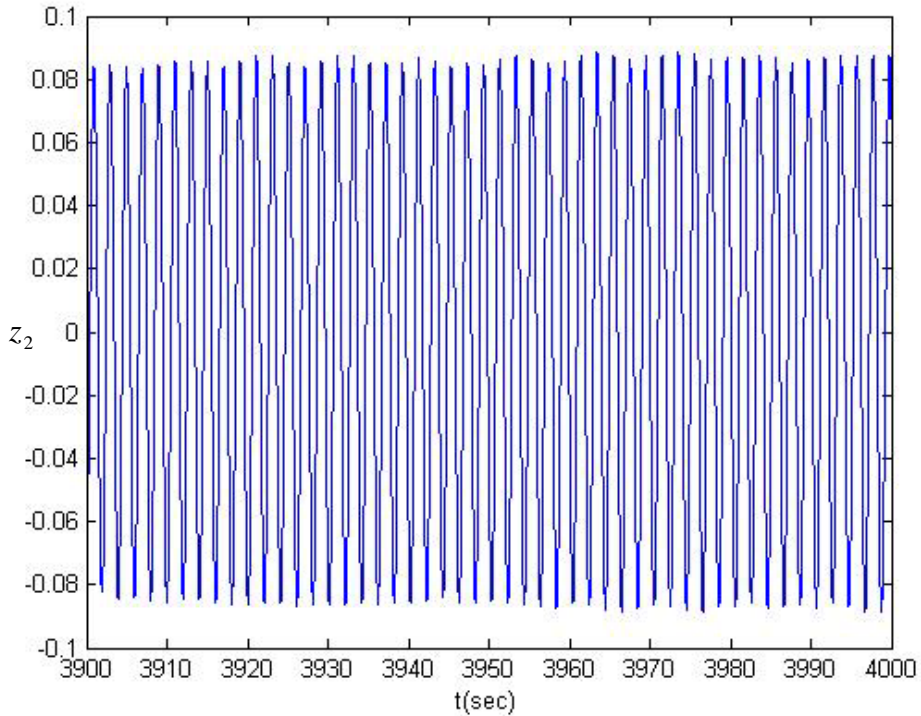
Fig.4.26. The time history of z_2 of an IMG system in chaotic behavior when parameter is a chaos signal for *CASE VII*.

33
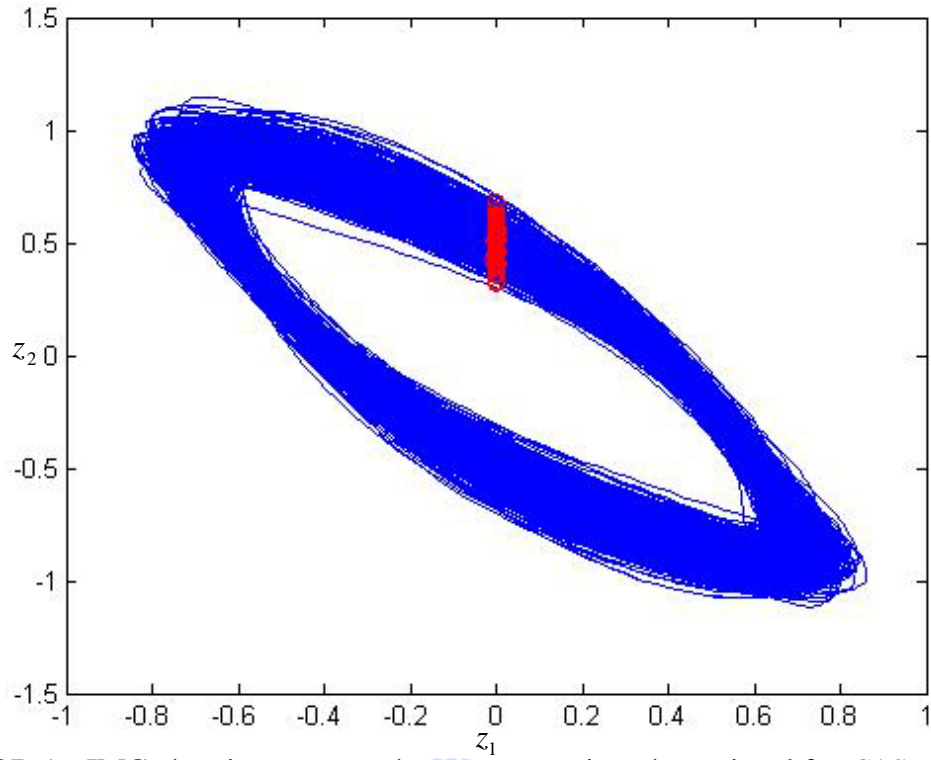
Fig.4.27. An IMG chaotic attractor when parameter is a chaos signal for *CASE VIII*.
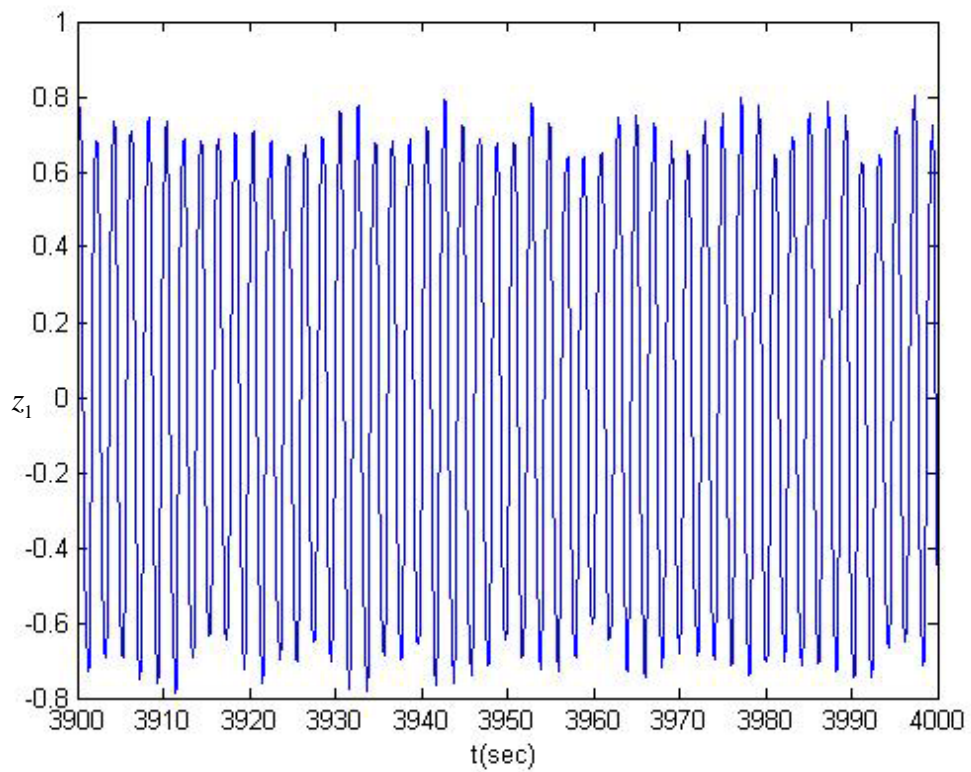
Fig.4.28. The time history of z_1 of an IMG system in chaotic behavior when parameter is a chaos signal for *CASE VIII*.
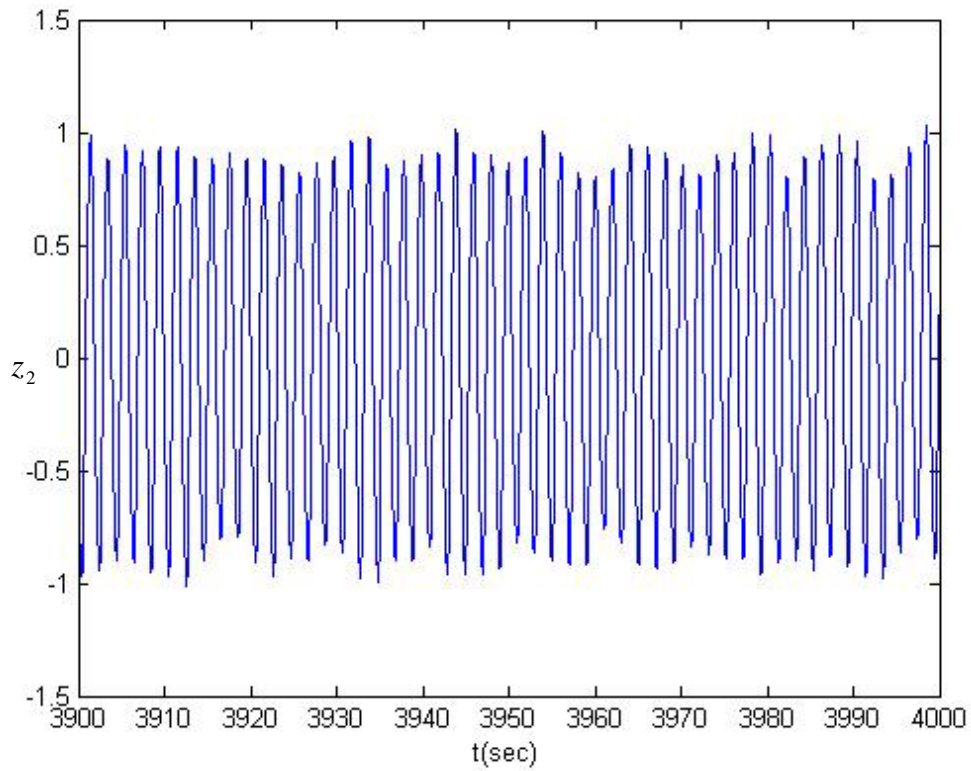
Fig.4.29. The time history of z_2 of an IMG system in chaotic behavior when parameter is a chaos signal for *CASE VIII*.
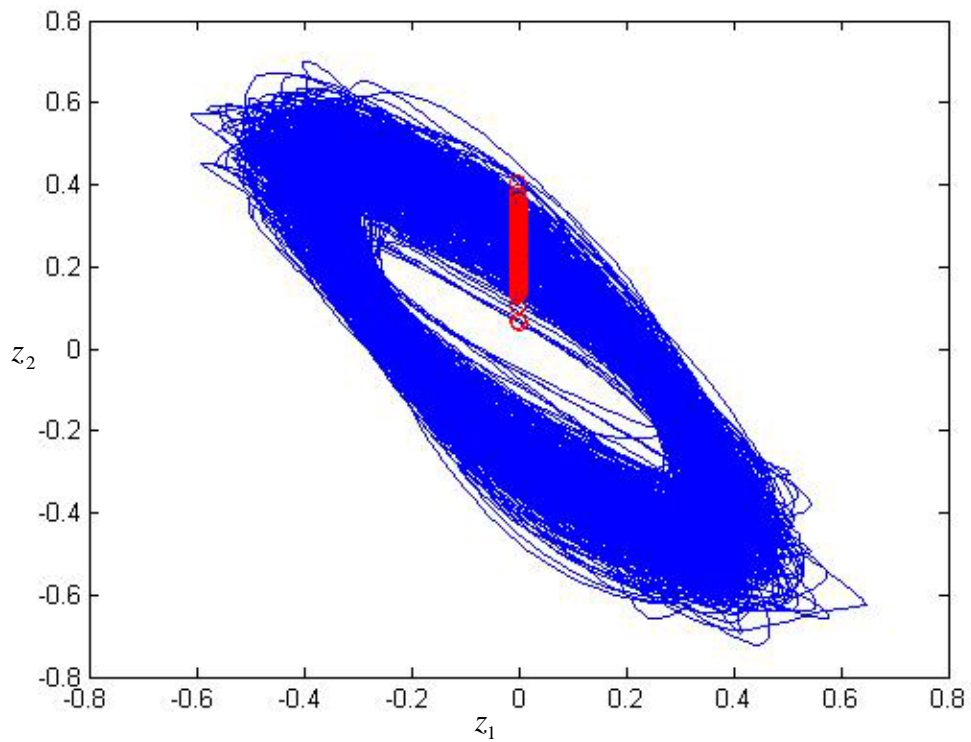
Fig.4.30. An IMG chaotic attractor when parameter is a chaos signal for *CASE IX*.
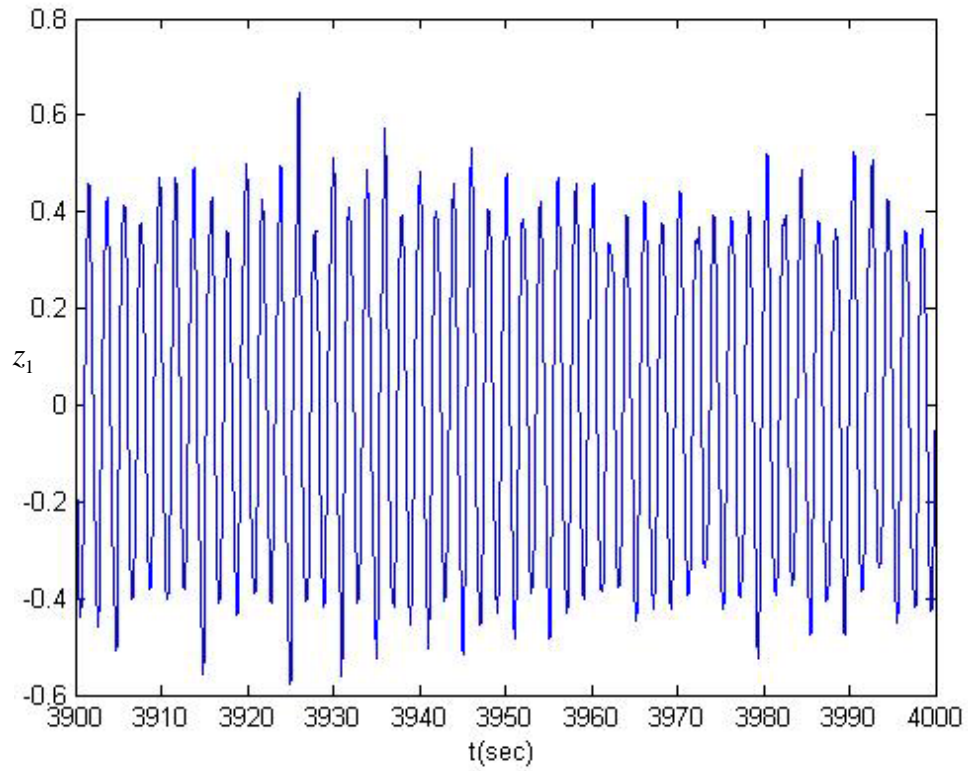
Fig.4.31. The time history of z_1 of an IMG system in chaotic behavior when parameter is a chaos signal *CASE IX*.
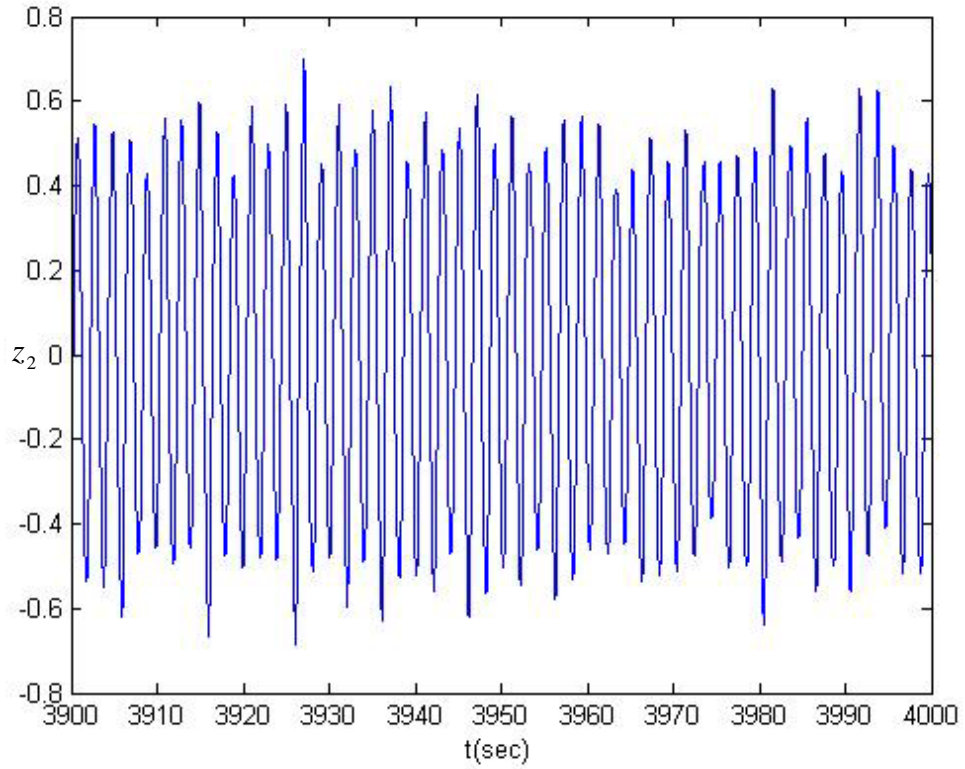
Fig.4.32. The time history of z_2 of an IMG system in chaotic behavior when parameter is a chaos signal *CASE IX*.

Chapter 5

Chaos of a New Ikeda-Lorenz System

5.1 Preliminaries

In this Chapter, given the equations of a new Ikeda-Lorenz system and verified the chaotic behavior by phase portraits and Lyapunov exponent.

5.2 Ikeda-Lorenz System

The Ikeda-Lorenz system is described as follows:

$$
\begin{aligned}
\dot{x}_1 &= -a_1 x_1 - b_1 \sin x_1 + \sigma(x_2 - x_1) \\
\dot{x}_2 &= -a_2 x_1 - b_2 \sin x_1 + r x_1 - x_1 x_3 - x_2 \\
\dot{x}_3 &= -a_3 x_1 - b_3 \sin x_1 + x_1 x_2 - c x_3
\end{aligned}
\tag{5.1}
$$

which is a combination of Ikeda system without time delay and Lorenz system. The parameters $a_1=0.1$, $b_1=1$, $\sigma=16$, $a_2=0.2$, $b_2=0.3$, $r=45.92$, $a_3=0.05$, $b_3=1.8$, $c=4$ are used. The chaotic attractor and Lyapunov exponents of the new Ikeda-Lorenz system are shown in Fig.5.1 and Fig.5.2.
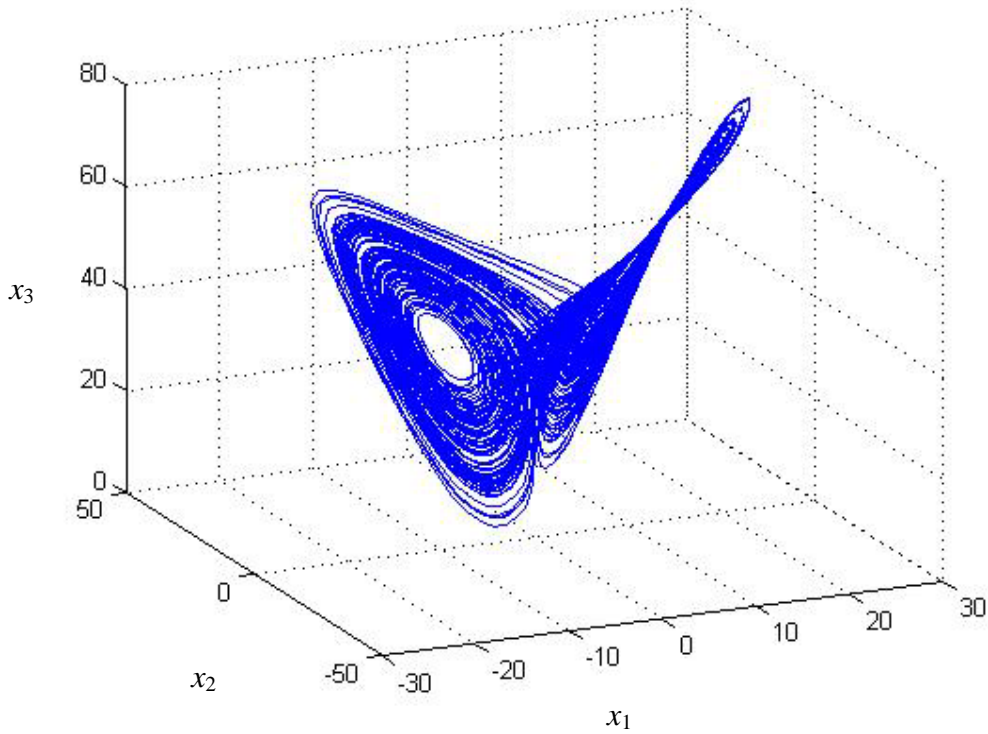
Fig.5.1. The chaotic attractor of a new Ikeda-Lorenz system with parameters a_1=0.1, b_1=1, σ =16, a_2=0.2, b_2=0.3, r=45.92, a_3=0.05, b_3=1.8, c=4 and initial conditions $x_1(0)$=1,$x_2(0)$=2,$x_3(0)$=3.
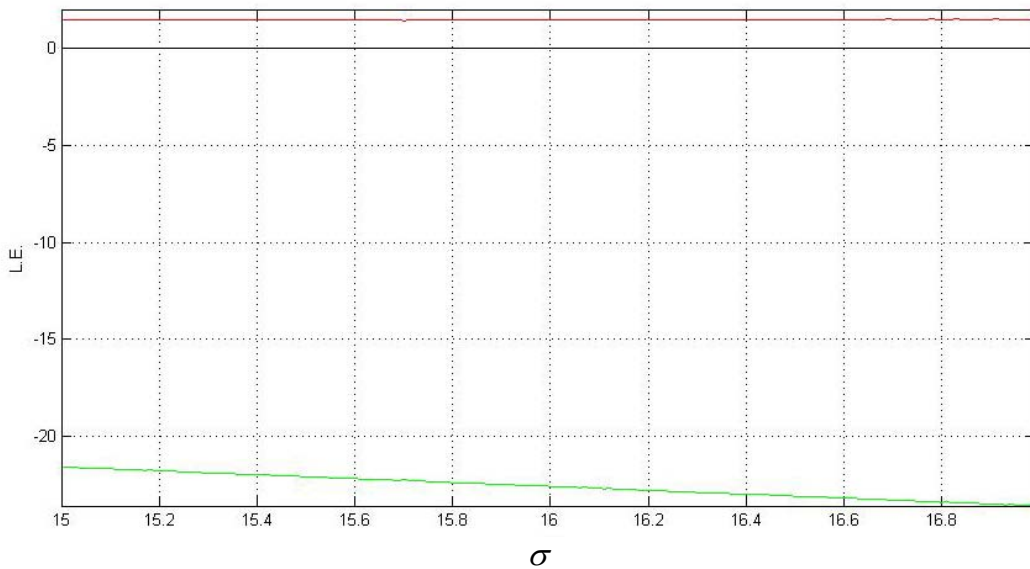
Fig.5.2. Lyapunov exponents of new Ikeda-Lorenz system with parameters a_1=0.1, b_1=1, σ =16, a_2=0.2, b_2=0.3, r=45.92, a_3=0.05, b_3=1.8, c=4 and initial conditions $x_1(0)$=1,$x_2(0)$=2,$x_3(0)$=3.

Chapter 6

Chaos Generalized Synchronization of New Ikeda-Lorenz Systems by GYC Partial Region Stability Theory

6.1 Preliminaries

The GYC partial region stability theory is proposed. By using the new strategy, the Lyapunov function is a simple linear homogeneous function of error states and the controllers are more simple and have less simulation error because they are in lower order than that of traditional controllers. Simulation results show that the new Ikeda-Lorenz system can be achieved chaos generalized synchronization by GYC partial region stability theory.

6.2 Chaos Generalized Synchronization Strategy

Consider the following unidirectional coupled chaotic systems

$$
\begin{aligned}
\dot{x} &= f(t, x) \\
\dot{y} &= h(t, y) + u
\end{aligned}
\tag{6.1}
$$

where $x = [x_1, x_2, ..., x_n]^T \in R^n$, $y = [y_1, y_2, \cdots, y_n]^T \in R^n$ denote two state vectors, f and h are nonlinear vector functions, and $u = [u_1, u_2, ... u_n]^T \in R^n$ is a control input vector.

The generalized synchronization can be accomplished when $t \to \infty$, the limit of the error vector $e = [e_1, e_2, ..., e_n]^T$ approaches zero:

$$\lim_{t \to \infty} e = 0 \tag{6.2}$$

where

$$e = G(x) - y \tag{6.3}$$

By using GYC partial region stability theory, the positive definite Lyapunov function is a homogeneous linear function of error states and the controllers can be designed in lower order than that of traditional controllers.

6.3 Simulation Results

Two new Ikeda-Lorenz systems with the unidirectional coupling are presented as follows:
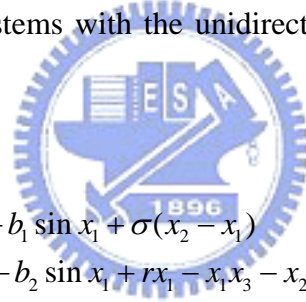
$$\begin{aligned}
\dot{x}_1 &= -a_1 x_1 - b_1 \sin x_1 + \sigma(x_2 - x_1) \\
\dot{x}_2 &= -a_2 x_1 - b_2 \sin x_1 + r x_1 - x_1 x_3 - x_2 \\
\dot{x}_3 &= -a_3 x_1 - b_3 \sin x_1 + x_1 x_2 - c x_3
\end{aligned}$$

$$\tag{6.4}$$

$$\begin{aligned}
\dot{y}_1 &= -a_1 y_1 - b_1 \sin y_1 + \sigma(y_2 - y_1) + u_1 \\
\dot{y}_2 &= -a_2 y_1 - b_2 \sin y_1 + r y_1 - y_1 y_3 - y_2 + u_2 \\
\dot{y}_3 &= -a_3 y_1 - b_3 \sin y_1 + y_1 y_2 - c y_3 + u_3
\end{aligned}$$

CASE I. The generalized synchronization error function is

$$e_i = x_i - y_i + 90, \quad (i=1,2,3) \tag{6.5}$$

Our goal is

$$y = x + 90 , \quad \text{i.e.} \lim_{t \to \infty} e = \lim_{t \to \infty} (x - y + 90) = 0 \tag{6.6}$$

The error dynamics becomes

$$
\begin{aligned}
\dot{e}_1 &= \dot{x}_1 - \dot{y}_1 = -a_1(x_1 - y_1) - b_1(\sin x_1 - \sin y_1) + \sigma[(x_2 - y_2) - (x_1 - y_1)] - u_1 \\
\dot{e}_2 &= \dot{x}_2 - \dot{y}_2 = -a_2(x_1 - y_1) - b_2(\sin x_1 - \sin y_1) + r(x_1 - y_1) - (x_1 x_3 - y_1 y_3) \\
&\quad - (x_2 - y_2) - u_2 \\
\dot{e}_3 &= \dot{x}_3 - \dot{y}_3 = -a_3(x_1 - y_1) - b_3(\sin x_1 - \sin y_1) + (x_1 x_2 - y_1 y_2) - c(x_3 - y_3) - u_3
\end{aligned}
\tag{6.7}
$$

Let initial states be $(x_1(0), x_2(0), x_3(0)) = (1, 2, 3)$, $(y_1(0), y_2(0), y_3(0)) = (3.5, 4, 1)$ and

system parameters a_1=0.1, b_1=1, σ=16, a_2=0.2, b_2=0.3, r=45.92, a_3=0.05, b_3=1.8 and

c=4, we find the error dynamics always exists in first quadrant as shown in Fig.6.1.

By GYC partial region asymptotical stability theorem, one can choose a Lyapunov

function in the form of a positive definite function in first quadrant:

$$V = e_1 + e_2 + e_3 + \frac{1}{2}(e_1^2 + e_2^2 + e_3^2) > 0 \tag{6.8}$$

Although V contains quadratic terms $\frac{1}{2}(e_1^2 + e_2^2 + e_3^2)$, the degree of terms of

following three controllers remain unchanged as that of $V = e_1 + e_2 + e_3$.

Its time derivative is

$$
\begin{aligned}
\dot{V} &= \dot{e}_1(1 + e_1) + \dot{e}_2(1 + e_2) + \dot{e}_3(1 + e_3) \\
&= (-a_1(x_1 - y_1) - b_1(\sin x_1 - \sin y_1) + \sigma[(x_2 - y_2) - (x_1 - y_1)] - u_1)(1 + e_1) \\
&\quad + (-a_2(x_1 - y_1) - b_2(\sin x_1 - \sin y_1) + r(x_1 - y_1) - (x_1 x_3 - y_1 y_3) - (x_2 - y_2) \\
&\quad - u_2)(1 + e_2) \\
&\quad + (-a_3(x_1 - y_1) - b_3(\sin x_1 - \sin y_1) + (x_1 x_2 - y_1 y_2) - c(x_3 - y_3) - u_3)(1 + e_3)
\end{aligned}
\tag{6.9}
$$

41

Choose

$$u_1 = -a_1(x_1 - y_1) - b_1(\sin x_1 - \sin y_1) + \sigma[(x_2 - y_2) - (x_1 - y_1)] + e_1$$
$$u_2 = -a_2(x_1 - y_1) - b_2(\sin x_1 - \sin y_1) + r(x_1 - y_1) - (x_1 x_3 - y_1 y_3) - (x_2 - y_2) + e_2 \qquad (6.10)$$
$$u_3 = -a_3(x_1 - y_1) - b_3(\sin x_1 - \sin y_1) + (x_1 x_2 - y_1 y_2) - c(x_3 - y_3) + e_3$$

We obtain

$$\dot{V} = -e_1(1 + e_1) - e_2(1 + e_2) - e_3(1 + e_3) < 0 \qquad (6.11)$$

which is a negative definite function in first quadrant. Three state errors versus time

and time histories of states are shown in Fig.6.2 and Fig.6.3.

CASE II. The generalized synchronization error function is

$$e_i = x_i - y_i + \sin^2 t \cos t + 80, \ (i=1,2,\ 3) \qquad (6.12)$$

Our goal is

$$y = x + \sin^2 t \cos t + 80, ,$$

$$(6.13)$$

i.e. $\lim\limits_{t\to\infty} e = \lim\limits_{t\to\infty}(x - y + \sin^2 t \cos t + 80) = 0, (i = 1, 2, 3)$

The error dynamics become

$$\dot{e}_1 = -a_1(x_1 - y_1) - b_1(\sin x_1 - \sin y_1) + \sigma[(x_2 - y_2) - (x_1 - y_1)] - u_1$$
$$+ \sin^2 t \cos t - \sin^3 t$$
$$\dot{e}_2 = -a_2(x_1 - y_1) - b_1(\sin x_1 - \sin y_1) + r(x_1 - y_1) - (x_1 x_3 - y_1 y_3)$$
$$- (x_2 - y_2) - u_2 + \sin^2 t \cos t - \sin^3 t \qquad (6.14)$$
$$\dot{e}_3 = -a_3(x_1 - y_1) - b_3(\sin x_1 - \sin y_1) + (x_1 x_2 - y_1 y_2) - c(x_3 - y_3) - u_3$$
$$+ \sin^2 t \cos t - \sin^3 t$$

Let initial states be $(x_1(0), x_2(0), x_3(0)) = (1, 2, 3)$, $(y_1(0), y_2(0), y_3(0)) = (3.5, 4, 1)$ and

system parameters a_1=0.1, b_1=1, σ=16, a_2=0.2, b_2=0.3, r=45.92, a_3=0.05, b_3=1.8 and

c=4, we find the error dynamics always exists in first quadrant as showen in Fig.6.4.

By GYC partial region asymptotical stability theorem, one can choose a Lyapunov

function in the form of a positive definite function in first quadrant:

$$V = e_1 + e_2 + e_3 + \frac{1}{2}(e_1^2 + e_2^2 + e_3^2) > 0 \qquad (6.15)$$
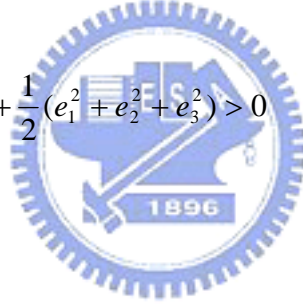
Its time derivative is

$$\dot{V} = \dot{e}_1(1 + e_1) + \dot{e}_2(1 + e_2) + \dot{e}_3(1 + e_3)$$
$$= (-a_1(x_1 - y_1) - b_1(\sin x_1 - \sin y_1) + \sigma[(x_2 - y_2) - (x_1 - y_1)] - u_1$$
$$+ \sin 2t \cos t - \sin t)(1 + e_1)$$
$$+ (-a_2(x_1 - y_1) - b_1(\sin x_1 - \sin y_1) + r(x_1 - y_1) - (x_1 x_3 - y_1 y_3) \qquad (6.16)$$
$$- (x_2 - y_2) - u_2 + \sin 2t \cos t - \sin t)(1 + e_2)$$
$$+ (-a_3(x_1 - y_1) - b_3(\sin x_1 - \sin y_1) + (x_1 x_2 - y_1 y_2) - c(x_3 - y_3) - u_3$$
$$+ \sin 2t \cos t - \sin t)(1 + e_3)$$

Choose

$$
\begin{aligned}
u_1 &= -a_1(x_1 - y_1) - b_1(\sin x_1 - \sin y_1) + \sigma[(x_2 - y_2) - (x_1 - y_1)] \\
&\quad + \sin 2t \cos t\text{-}\sin t + e_1 \\
u_2 &= -a_2(x_1 - y_1) - b_1(\sin x_1 - \sin y_1) + r(x_1 - y_1) - (x_1 x_3 - y_1 y_3) - (x_2 - y_2) \\
&\quad + \sin 2t \cos t\text{-}\sin t + e_2 \\
u_3 &= -a_3(x_1 - y_1) - b_3(\sin x_1 - \sin y_1) + (x_1 x_2 - y_1 y_2) - c(x_3 - y_3) \\
&\quad + \sin 2t \cos t\text{-}\sin t + e_3
\end{aligned} \tag{6.17}
$$

We obtain

$$
\dot{V} = -e_1(1 + e_1) - e_2(1 + e_2) - e_3(1 + e_3) < 0 \tag{6.18}
$$

which is a negative definite function. Three state errors versus time and time histories

of $x_i - y_i + 80$ are shown in Fig.6.5 and Fig.6.6.

CASE III. The generalized synchronization error function is

$$
e_i = \frac{1}{30} x_i^2 - y_i + 100 , \ (i=1,\ 2,\ 3) \tag{6.19}
$$

Our goal is

$$
y_i = \frac{1}{30} x_i^2 + 100 , \ (i=1,\ 2,\ 3)
$$

$$
\tag{6.20}
$$

i.e. $\lim_{t \to \infty} e_i = \lim_{t \to \infty} (\frac{1}{30} x_i^2 - y_i + 100) = 0, (i = 1,2,3)$

The error dynamics become

$$\dot{e}_1 = \frac{1}{15} x_1 \dot{x}_1 - \dot{y}_1 = \frac{1}{15} x_1 (-a_1 x_1 - b_1 \sin x_1 + \sigma(x_2 - x_1))$$
$$- (-a_1 y_1 - b_1 \sin y_1 + \sigma(y_2 - y_1)) - u_1$$

$$\dot{e}_2 = \frac{1}{15} x_2 \dot{x}_2 - \dot{y}_2 = \frac{1}{15} x_2 (-a_2 x_1 - b_2 \sin x_1 + r x_1 - x_1 x_3 - x_2)$$
$$- (-a_2 y_1 - b_2 \sin y_1 + r y_1 - y_1 y_3 - y_2) - u_2$$

$$\dot{e}_3 = \frac{1}{15} x_3 \dot{x}_3 - \dot{y}_3 = \frac{1}{15} x_3 (-a_3 x_1 - b_3 \sin x_1 + x_1 x_2 - c x_3)$$
$$- (-a_3 y_1 - b_3 \sin y_1 + y_1 y_2 - c y_3) - u_2$$

(6.21)

Let initial states be $(x_1(0), x_2(0), x_3(0)) = (1, 2, 3)$, $(y_1(0), y_2(0), y_3(0)) = (3.5, 4, 1)$ and system parameters a_1=0.1, b_1=1, σ=16, a_2=0.2, b_2=0.3, r=45.92, a_3=0.05, b_3=1.8 and c=4, we find the error dynamics always exists in first quadrant as shown in Fig.6.7. By GYC partial region asymptotical stability theorem, one can choose a Lyapunov function in the form of a positive definite function in first quadrant:

$$V = e_1 + e_2 + e_3 + \frac{1}{2}(e_1^2 + e_2^2 + e_3^2) > 0$$

(6.22)
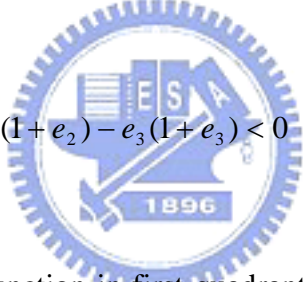
Its time derivative is

$$\dot{V} = [\frac{1}{15} x_1 (-a_1 x_1 - b_1 \sin x_1 + \sigma(x_2 - x_1)) - (-a_1 y_1 - b_1 \sin y_1 + \sigma(y_2 - y_1))$$
$$- u_1](1 + e_1)$$
$$+ [\frac{1}{15} x_2 (-a_2 x_1 - b_2 \sin x_1 + r x_1 - x_1 x_3 - x_2) - (-a_2 y_1 - b_2 \sin y_1 + r y_1$$
$$- y_1 y_3 - y_2) - u_2](1 + e_2)$$
$$+ [\frac{1}{15} x_3 (-a_3 x_1 - b_3 \sin x_1 + x_1 x_2 - c x_3) - (-a_3 y_1 - b_3 \sin y_1 + y_1 y_2 - c y_3)$$
$$- u_2](1 + e_3)$$

(6.23)

45

Choose

$$u_1 = \frac{1}{15} x_1(-a_1 x_1 - b_1 \sin x_1 + \sigma(x_2 - x_1)) - (-a_1 y_1 - b_1 \sin y_1 + \sigma(y_2 - y_1))$$
$$+ e_1$$

$$u_2 = \frac{1}{15} x_2(-a_2 x_1 - b_2 \sin x_1 + r x_1 - x_1 x_3 - x_2) - (-a_2 y_1 - b_2 \sin y_1 + r y_1$$
$$- y_1 y_3 - y_2) + e_2$$ (6.24)

$$u_3 = \frac{1}{15} x_3(-a_3 x_1 - b_3 \sin x_1 + x_1 x_2 - c x_3) - (-a_3 y_1 - b_3 \sin y_1 + y_1 y_2 - c y_3)$$
$$+ e_3$$

We obtain

$$\dot{V} = -e_1(1 + e_1) - e_2(1 + e_2) - e_3(1 + e_3) < 0$$ (6.25)

which is a negative definite function in first quadrant. Three state errors versus time

are shown in Fig.6.8.

CASE IV. The generalized synchronization error function is

$$e = x - y + z + K$$ (6.26)

where z is the chaotic state vector of Genesio system[48], $K=[100\ 100\ 100]^T$.

The goal system for synchronization is Genesio system and initial states is (1, 1, 1), system parameters $a_4=6$, $b_4=2.92$, $c_4=1.2$.

46

$$\dot{z}_1 = z_2$$
$$\dot{z}_2 = z_3 \qquad\qquad (6.27)$$
$$\dot{z}_3 = z_1^2 - a_4 z_1 - b_4 z_2 - c_4 z_3$$

We have

$$\lim_{t \to \infty} e = \lim_{t \to \infty} (x - y + z + K) = 0 \qquad\qquad (6.28)$$

The error dynamics becomes

$$
\begin{aligned}
\dot{e}_1 &= -a_1(x_1 - y_1) - b_1(\sin x_1 - \sin y_1) + \sigma[(x_2 - y_2) - (x_1 - y_1)] - u_1 \\
&\quad + z_2 \\
\dot{e}_2 &= -a_2(x_1 - y_1) - b_2(\sin x_1 - \sin y_1) + r(x_1 - y_1) - (x_1 x_3 - y_1 y_3) - (x_2 - y_2) - u_2 \\
&\quad + z_3 \\
\dot{e}_3 &= -a_3(x_1 - y_1) - b_3(\sin x_1 - \sin y_1) + (x_1 x_2 - y_1 y_2) - c(x_3 - y_3) - u_3 \\
&\quad + z_1^2 - a_4 z_1 - b_4 z_2 - c_4 z_3
\end{aligned}
\qquad (6.29)
$$

Let initial states be $(x_1(0), x_2(0), x_3(0)) = (1, 2, 3)$, $(y_1(0), y_2(0), y_3(0)) = (3.5, 4, 1)$ and system parameters a_1=0.1, b_1=1, σ =16, a_2=0.2, b_2=0.3, r=45.92, a_3=0.05, b_3=1.8 and c=4, we find the error dynamics always exists in first quadrant as shown in Fig.6.9. By GYC partial region asymptotical stability theorem, one can choose a Lyapunov function in the form of a positive definite function in first quadrant:

$$V = e_1 + e_2 + e_3 + \frac{1}{2}(e_1^2 + e_2^2 + e_3^2) > 0 \qquad\qquad (6.30)$$

Its time derivative is

$$
\begin{aligned}
\dot{V} = &(-a_1(x_1 - y_1) - b_1(\sin x_1 - \sin y_1) + \sigma[(x_2 - y_2) - (x_1 - y_1)] - u_1 \\
&+ z_2)(1 + e_1) \\
&+ (-a_2(x_1 - y_1) - b_1(\sin x_1 - \sin y_1) + r(x_1 - y_1) - (x_1 x_3 - y_1 y_3) \\
&- (x_2 - y_2) - u_2 + z_3)(1 + e_2) \\
&+ (-a_3(x_1 - y_1) - b_3(\sin x_1 - \sin y_1) + (x_1 x_2 - y_1 y_2) - c(x_3 - y_3) - u_3 \\
&+ z_1^2 - a_4 z_1 - b_4 z_2 - c_4 z_3)(1 + e_3)
\end{aligned}
\tag{6.31}
$$

Choose

$$
\begin{aligned}
u_1 = &-a_1(x_1 - y_1) - b_1(\sin x_1 - \sin y_1) + \sigma[(x_2 - y_2) - (x_1 - y_1)] \\
&+ z_2 + e_1 \\
u_2 = &-a_2(x_1 - y_1) - b_2(\sin x_1 - \sin y_1) + r(x_1 - y_1) - (x_1 x_3 - y_1 y_3) \\
&- (x_2 - y_2) + z_3 + e_2 \\
u_3 = &-a_3(x_1 - y_1) - b_3(\sin x_1 - \sin y_1) + (x_1 x_2 - y_1 y_2) - c(x_3 - y_3) \\
&+ z_1^2 - a_4 z_1 - b_4 z_2 - c_4 z_3 + e_3
\end{aligned}
\tag{6.32}
$$

We obtain

$$
\dot{V} = -e_1(1 + e_1) - e_2(1 + e_2) - e_3(1 + e_3) < 0
\tag{6.33}
$$

which is a negative definite function in first quadrant. Three state errors versus time

and time histories of $x_i - y_i + 100$, (i=1,2,3) are shown in Fig.6.10 and Fig.6.11.
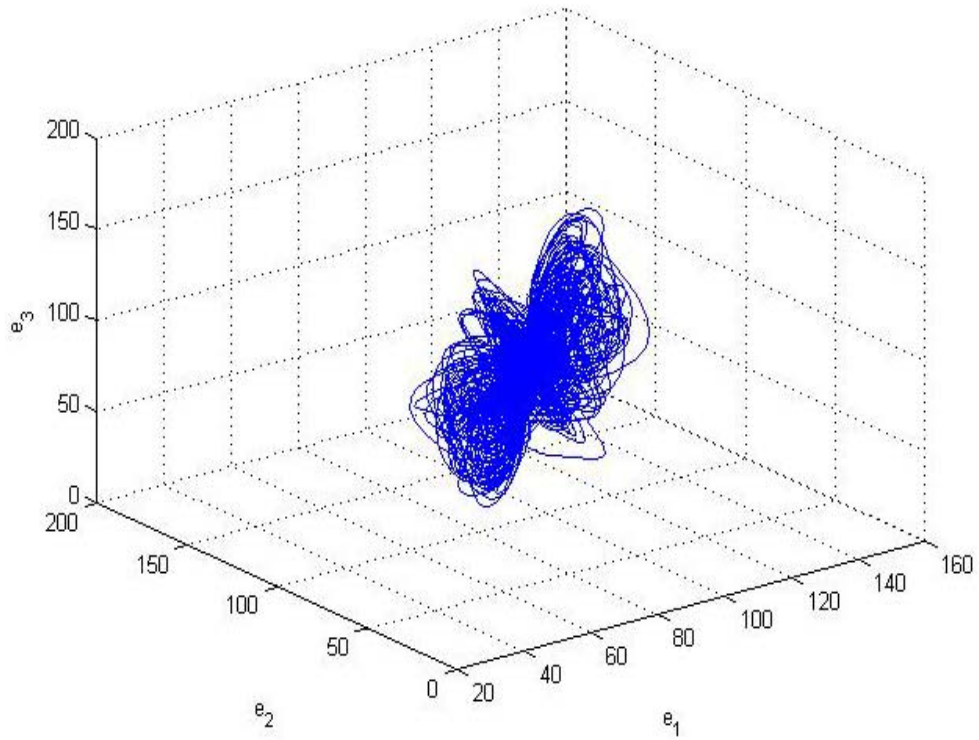
Fig. 6.1. Phase portrait of error dynamics for *CASE I*.
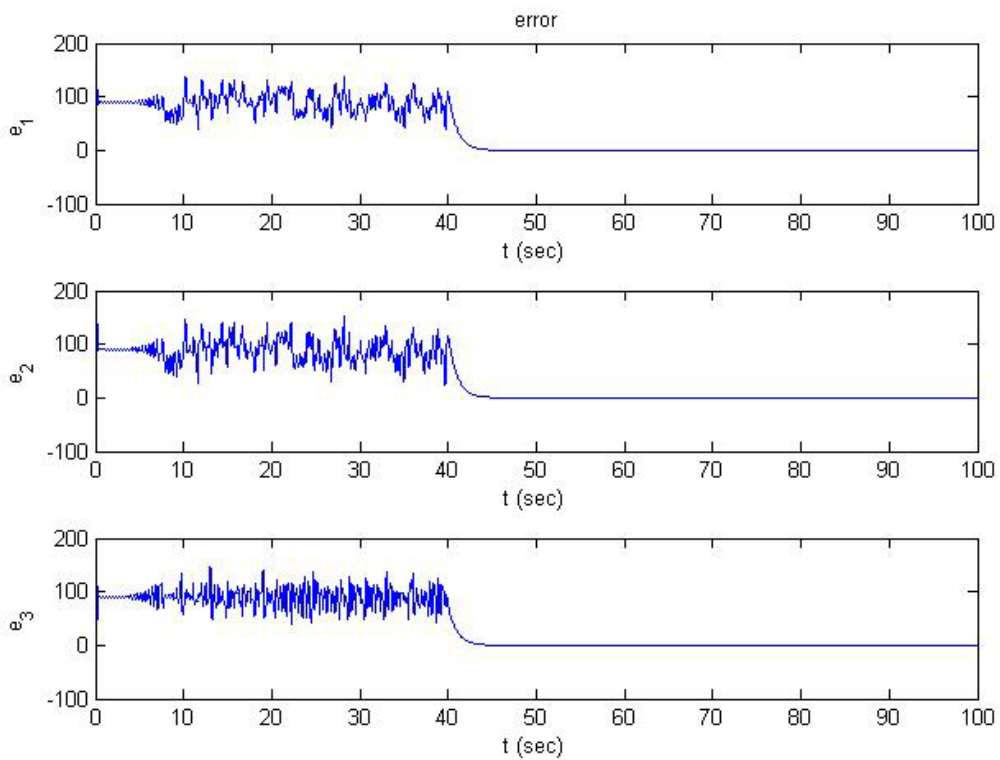
Fig. 6.2. Time histories of errors for *CASE I*.
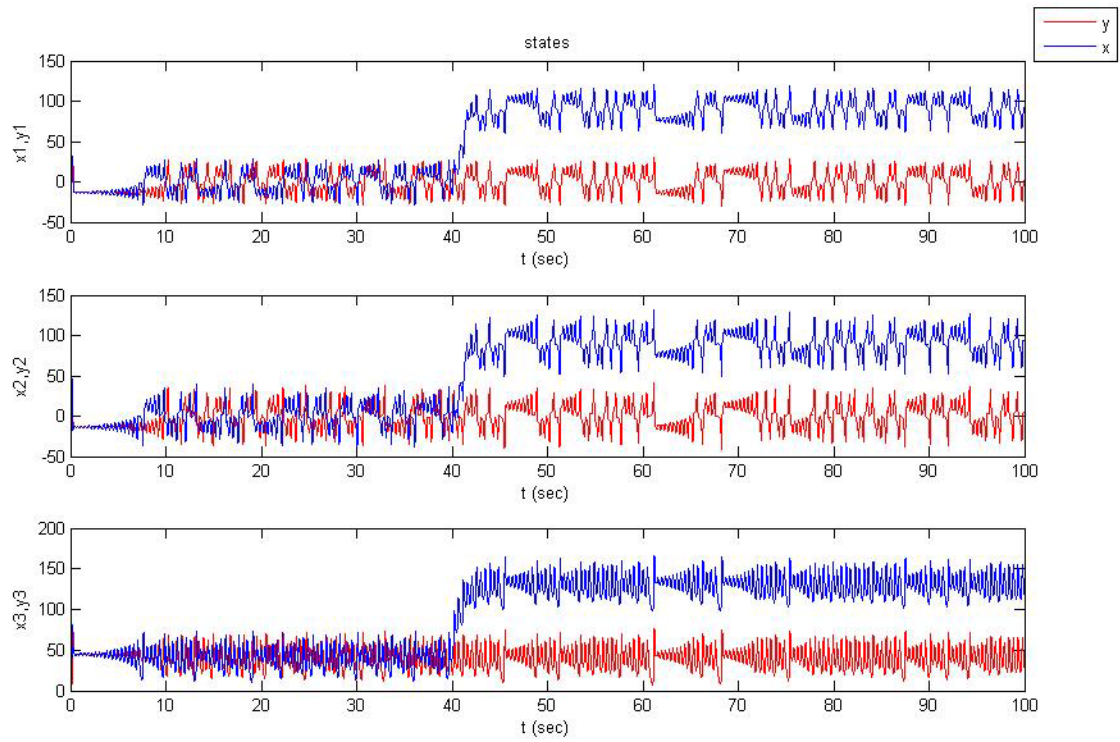
Fig.6.3. Time histories of x_1, x_2, x_3, y_1, y_2, y_3 for *CASE I*.
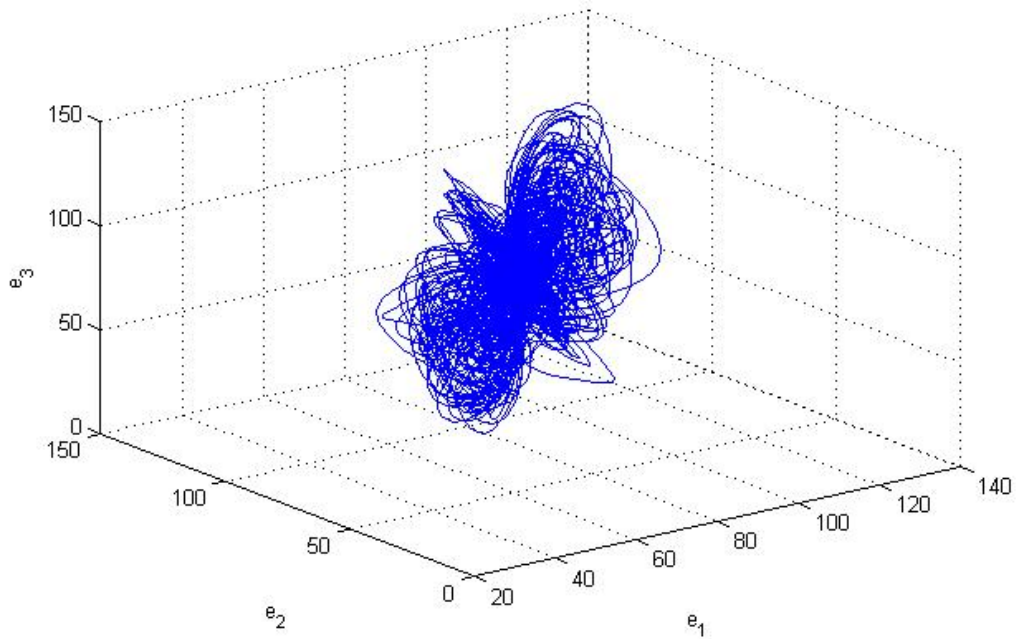
Fig.6.4. Phase portrait of error dynamics for *CASE II*.
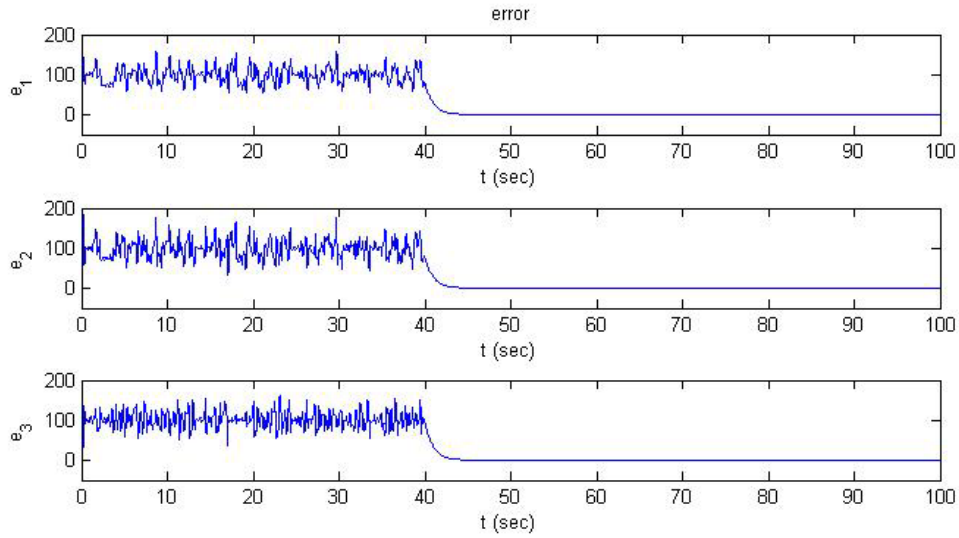
Fig.6.5. Time histories of errors for *CASE II*.
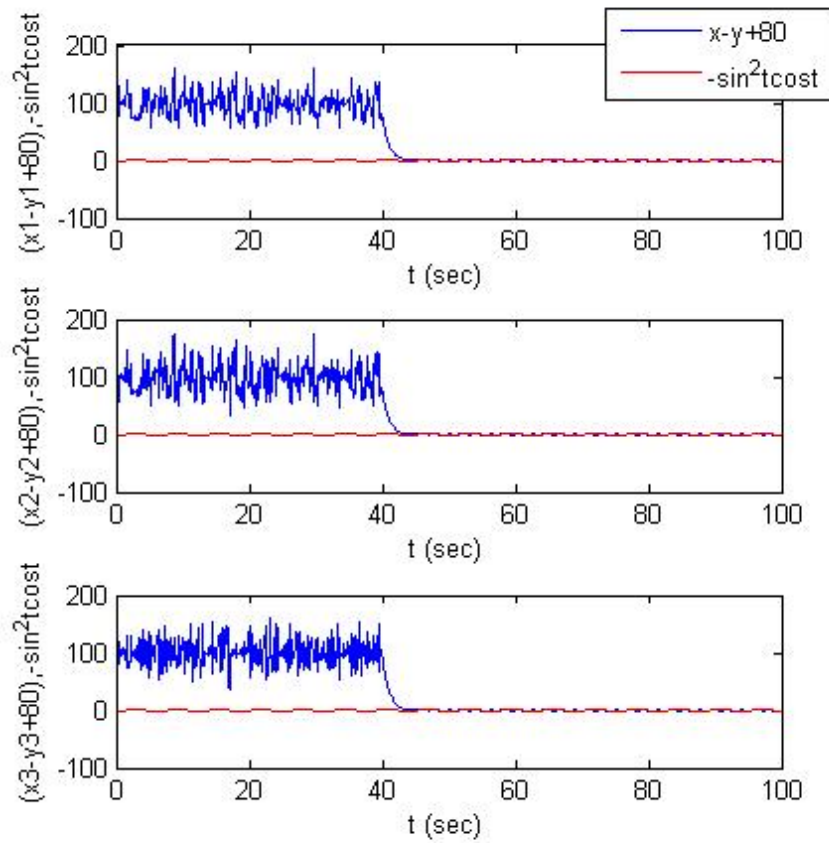
Fig.6.6. Time histories of $x_i - y_i + 80$ and $-\sin^2 t \cdot \cos t$ for *CASE II*.
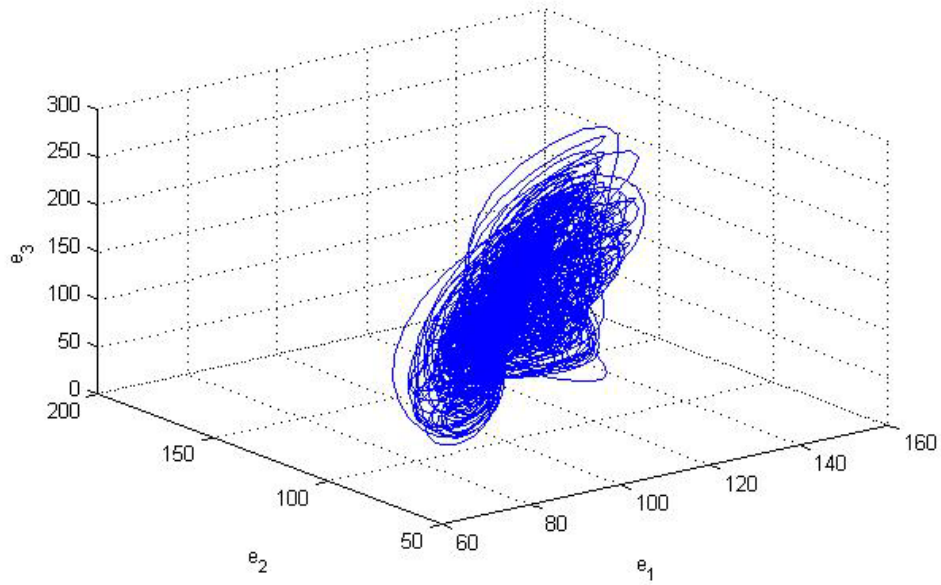
Fig.6.7. Phase portrait of error dynamics for *CASE III*.
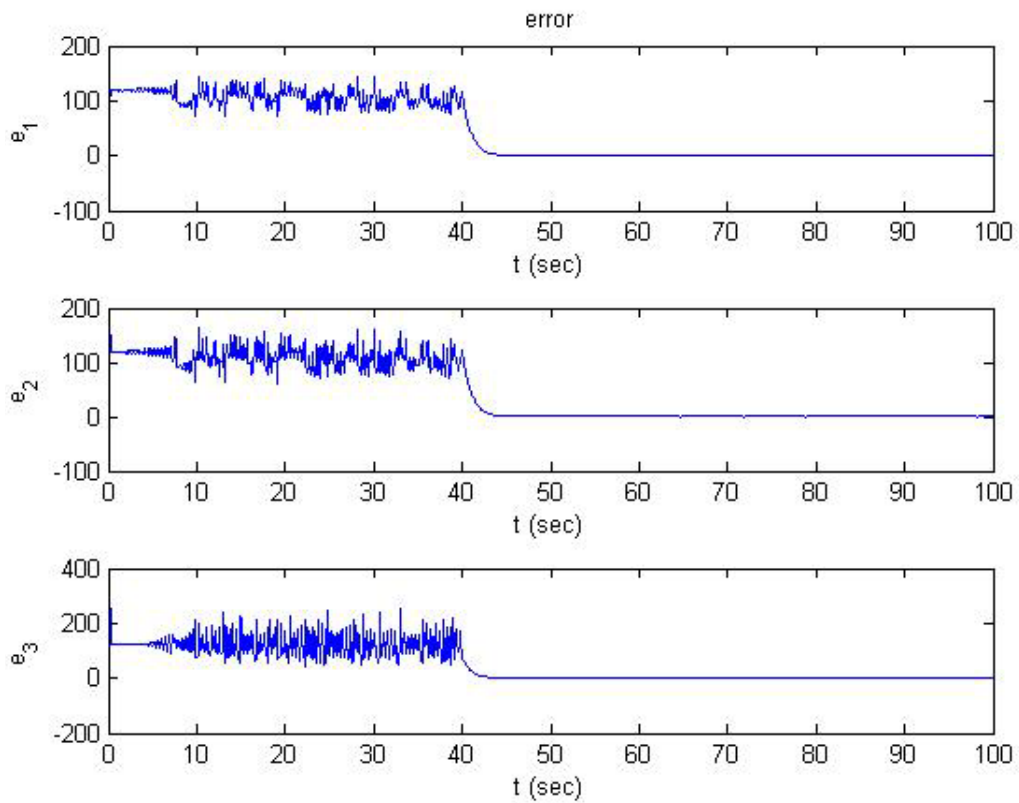
Fig.6.8. Time histories of errors for *CASE III*.
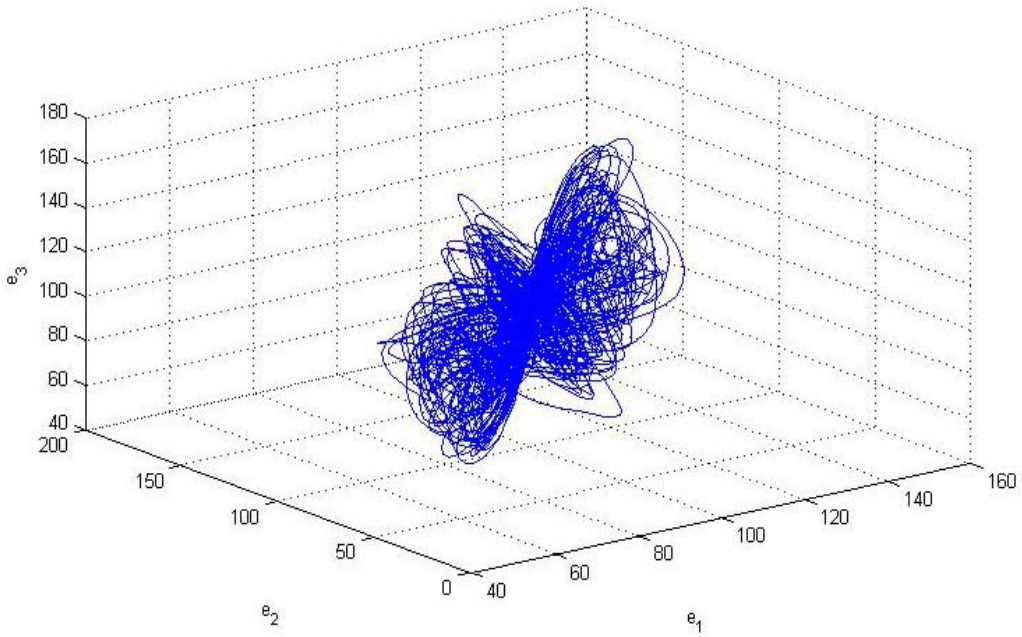
Fig.6.9. Phase portrait of error dymanics for *CASE IV*.
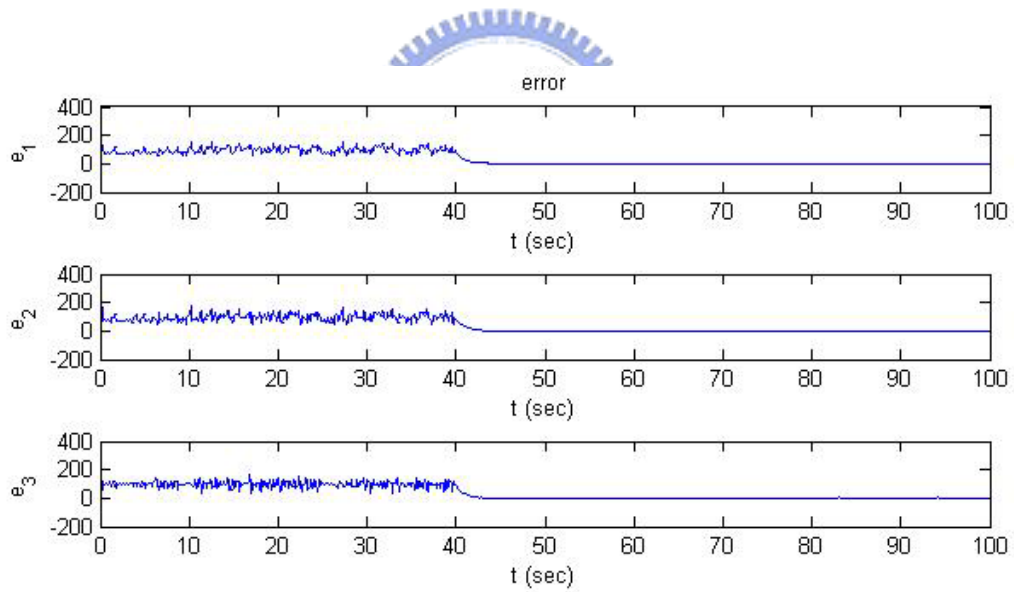
Fig.6.10. Time histories of errors for *CASE IV*.
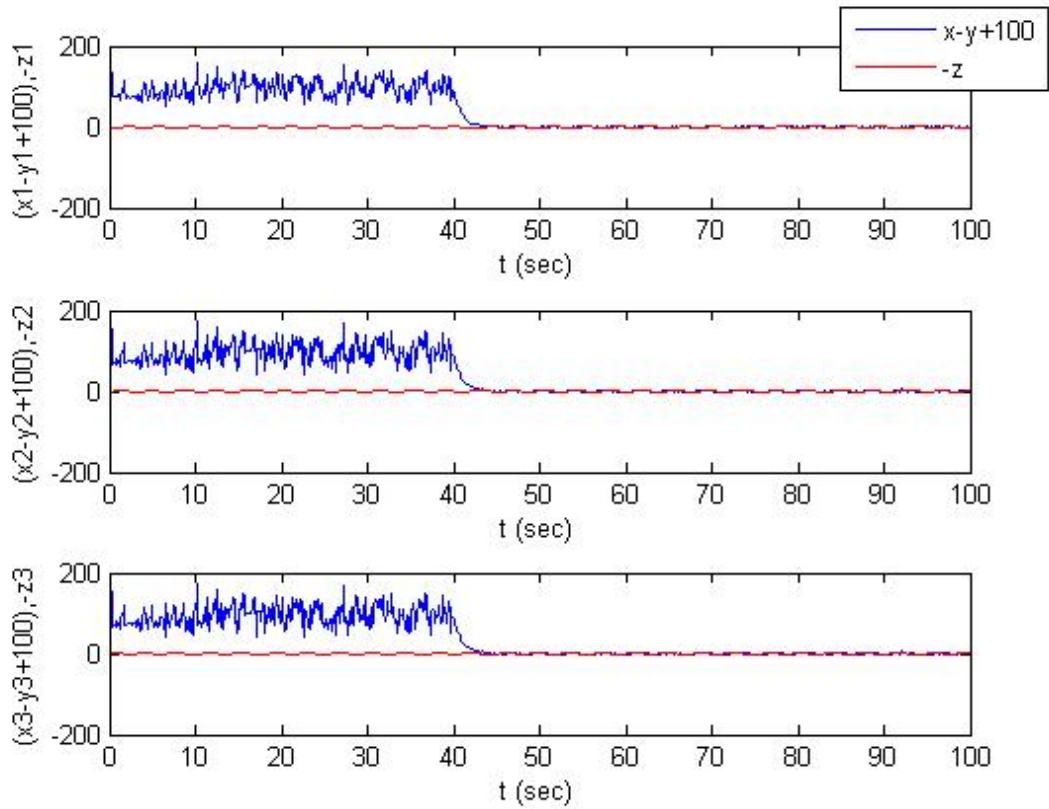
Fig.6.11. Time histories of $x - y + 100$ and $-z$ for *CASE IV*.

Chapter 7

Chaos Control of a New Ikeda-Lorenz System by

GYC Partial Region Stability Theory

7.1 Preliminaries

By using the GYC partial region stability theory in Appendix, the Lyapunov function is a simple linear homogeneous function of error states and the controllers are more simple and have less simulation error because they are in lower order than that of traditional controllers. Simulation results show that for a new Ikeda-Lorenz system can be achieved chaos control by GYC partial region stability theory.

7.2 Chaos Control Scheme

Consider the following chaotic systems
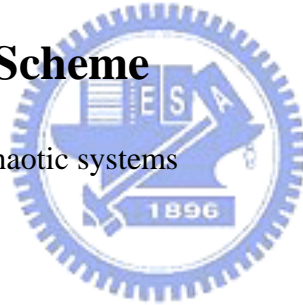
$$\dot{x} = f(t, x) \tag{7.1}$$

where $x = \left[x_1, x_2, \cdots, x_n \right]^T \in R^n$ is a the state vector, $f : R_+ \times R^n \to R^n$ is a vector function.

The goal system which can be either chaotic or regular, is

$$\dot{\mathbf{y}} = \mathbf{g}(t, \mathbf{y}) \tag{7.2}$$

where $\mathbf{y} = \left[y_1, y_2, \cdots, y_n \right]^T \in R^n$ is a state vector, $\mathbf{g} : R_+ \times R^n \to R^n$ is a vector function.

In order to make the chaos state x approaching the goal state y, define $e = x - y$ as the state error. The chaos control is accomplished in the sense that [41,49-55]:

$$\lim_{t \to \infty} e = \lim_{t \to \infty}(x - y) = 0 \tag{7.3}$$

By using GYC partial region stability theory, the positive definite Lyapunov function is a homogeneous linear function of error states and the controllers can be designed in lower order than that of traditional controllers.

7.3 Simulation Results

The following chaotic system is a new Ikeda-Lorenz system of which the old origin is translated to $(x_1, x_2, x_3) = (150,150,150)$ and the chaotic motion always happens in the first quadrant of coordinate system (x_1, x_2, x_3):

$$
\begin{aligned}
\dot{x}_1 &= -a_1(x_1 - 150) - b_1(\sin(x_1 - 150)) + \sigma((x_2 - 150) - (x_1 - 150)) \\
\dot{x}_2 &= -a_2(x_1 - 150) - b_2(\sin(x_1 - 150)) + r(x_1 - 150) - (x_1 - 150)(x_3 - 150) \\
&\quad - (x_2 - 150) \\
\dot{x}_3 &= -a_3(x_1 - 150) - b_3(\sin(x_1 - 150)) + (x_1 - 150)(x_2 - 150) - c(x_3 - 150)
\end{aligned}
\tag{7.4}
$$

This Ikeda-Lorenz system is presented as simulated examples where the initial conditions are $x_1(0) = 1$, $x_2(0) = 2$, $x_3(0) = 3$, $a_1 = 0.1$, $b_1 = 1$, $\sigma = 16$, $a_2 = 0.2$, $b_2 = 0.3$, $r = 45.92$, $a_3 = 0.05$, $b_3 = 1.8$, $c = 4$. The chaotic motion is shown in Fig.7.1.

In order to lead (x_1, x_2, x_3) to the goal, we add control terms u_1, u_2 and u_3 to each equation of Eq. (7.4), respectively.

$$
\begin{aligned}
\dot{x}_1 &= -a_1(x_1 - 150) - b_1(\sin(x_1 - 150)) + \sigma((x_2 - 150) - (x_1 - 150)) + u_1 \\
\dot{x}_2 &= -a_2(x_1 - 150) - b_2(\sin(x_1 - 150)) + r(x_1 - 150) - (x_1 - 150)(x_3 - 150) \\
&\quad - (x_2 - 150) + u_2 \\
\dot{x}_3 &= -a_3(x_1 - 150) - b_3(\sin(x_1 - 150)) + (x_1 - 150)(x_2 - 150) - c(x_3 - 150) + u_3
\end{aligned}
\tag{7.5}
$$

CASE I. Control the chaotic motion to zero.

In this case we will control the chaotic motion of the Ikeda-Lorenz system (7.4) to zero. The goal is $y = 0$. The state error is $e = x - y = x$ and error dynamics becomes

$$
\begin{aligned}
\dot{e}_1 &= \dot{x}_1 = -a_1(x_1 - 150) - b_1(\sin(x_1 - 150)) + \sigma((x_2 - 150) - (x_1 - 150)) + u_1 \\
\dot{e}_2 &= \dot{x}_2 = -a_2(x_1 - 150) - b_2(\sin(x_1 - 150)) + r(x_1 - 150) - (x_1 - 150)(x_3 - 150) \\
&\quad - (x_2 - 150) + u_2 \\
\dot{e}_3 &= \dot{x}_3 = -a_3(x_1 - 150) - b_3(\sin(x_1 - 150)) + (x_1 - 150)(x_2 - 150) - c(x_3 - 150) + u_3
\end{aligned}
\tag{7.6}
$$

In Fig.7.1, we see that the error dynamics always exists in first quadrant. By GYC partial region asymptotical stability theorem, one can choose a Lyapunov function in the form of a positive definite function in first quadrant:

$$
V = e_1 + e_2 + e_3 + \frac{1}{2}(e_1^2 + e_2^2 + e_3^2) > 0
\tag{7.7}
$$
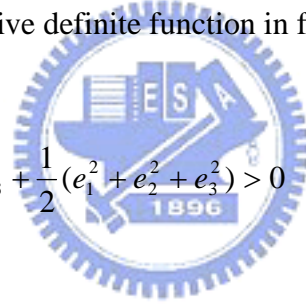
Although V contains quadratic terms $\frac{1}{2}(e_1^2 + e_2^2 + e_3^2)$, the degree of terms of following three controllers remain unchanged as that of $V = e_1 + e_2 + e_3$. Its time derivative is

$$
\begin{aligned}
\dot{V} &= \dot{e}_1(1 + e_1) + \dot{e}_2(1 + e_2) + \dot{e}_3(1 + e_3) \\
&= (-a_1(e_1 - 150) - b_1(\sin(e_1 150)) + \sigma[(e_2 - 150) - (e_1 - 150)] + u_1)(1 + e_1) \\
&\quad + (-a_2(e_1 - 150) - b_2(\sin(e_1 - 150)) + r(e_1 - 150) - (e_1 - 150)(e_3 - 150) \\
&\quad - (e_2 - 150) - u_2)(1 + e_2) \\
&\quad + (-a_3(e_1 - 150) - b_3(\sin(e_1 - 150)) + (e_1 - 150)(e_2 - 150) - c(e_3 - 150) \\
&\quad - u_3)(1 + e_3)
\end{aligned}
\tag{7.8}
$$

Choose

$$u_1 = -[-a_1(e_1 - 150) - b_1(\sin(e_1 - 150)) + \sigma((e_2 - 150) - (e_1 - 150))] - e_1$$
$$u_2 = -[-a_2(e_1 - 150) - b_2(\sin(e_1 - 150)) + r(e_1 - 150) - (e_1 - 150)(e_3 - 150)$$
$$\quad - (e_2 - 150)] - e_2$$
$$u_3 = -[-a_3(e_1 - 150) - b_3(\sin(e_1 - 150)) + (e_1 - 150)(e_2 - 150) - c(e_3 - 150)] - e_3$$

(7.9)

We obtain

$$\dot{V} = -e_1(1 + e_1) - e_2(1 + e_2) - e_3(1 + e_3) < 0 \tag{7.10}$$

which is a negative definite function in first quadrant. Simulation results are shown in Fig.7.2. the motion trajectories approach the origin after 40sec.

CASE II. Control the chaotic motion to a periodic function.

In this case we will control the chaotic motion of the Ikeda-Lorenz system (7.4) to a periodic function of time. The goal is $y = F\sin^2 \omega t$. The equation

$$e = x - F\sin^2 \omega t \tag{7.11}$$

$$\lim_{t \to \infty} e_i = \lim_{t \to \infty}(x - F_i\sin^2 \omega_i t), \ i=1,2,3. \tag{7.12}$$
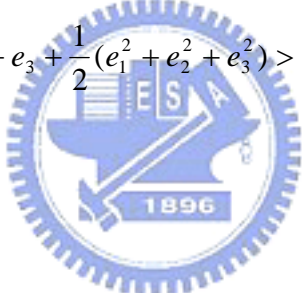
and $\dot{e}_i = \dot{x}_i - F_i\omega_i\sin 2\omega_i t$, (i=1,2,3), and $F_1 = F_2 = F_3 = 10$, $\omega_1 = 0.5$, $\omega_2 = 2$,

$\omega_3 = 0.2$.

The error dynamics is

$$\dot{e}_1 = \dot{x}_1 - F\omega_1 \sin 2\omega_1 t = -a_1(x_1 - 150) - b_1(\sin(x_1 - 150)) + \sigma(x_2 - 150)$$
$$- (x_1 - 150) - F\omega_1 \sin 2\omega_1 t + u_1$$
$$\dot{e}_2 = \dot{x}_2 - F\omega_2 \sin 2\omega_2 t = -a_2(x_1 - 150) - b_2(\sin(x_1 - 150)) + r(x_1 - 150) \qquad (7.13)$$
$$- (x_1 - 150)(x_3 - 150) - (x_2 - 150) - F\omega_2 \sin 2\omega_2 t + u_2$$
$$\dot{e}_3 = \dot{x}_3 - F\omega_3 \sin 2\omega_3 t = -a_3(x_1 - 150) - b_3(\sin(x_1 - 150)) + (x_1 - 150)(x_2 - 150)$$
$$- c(x_3 - 150) - F\omega_3 \sin 2\omega_3 t + u_3$$

Let initial states be $(x_1(0), x_2(0), x_3(0)) = (1, 2, 3)$, $(y_1(0), y_2(0), y_3(0)) = (3.5, 4, 1)$ and system parameters $a_1=0.1$, $b_1=1$, $\sigma=16$, $a_2=0.2$, $b_2=0.3$, $r=45.92$, $a_3=0.05$, $b_3=1.8$ and $c=4$, we find that the error dynamics always exists in first quadrant as showen in Fig.7.3. By GYC partial region asymptotical stability theorem, one can choose a Lyapunov function in the form of a positive definite function in first quadrant:

$$V = e_1 + e_2 + e_3 + \frac{1}{2}(e_1^2 + e_2^2 + e_3^2) > 0 \qquad (7.14)$$

Its time derivative is

$$\dot{V} = \dot{e}_1(1 + e_1) + \dot{e}_2(1 + e_2) + \dot{e}_3(1 + e_3)$$
$$= [-a_1(x_1 - 150) - b_1(\sin(x_1 - 150)) + \sigma((x_2 - 150) - (x_1 - 150))$$
$$- F \cdot \omega_1 \cdot \sin 2\omega_1 t + u_1](1 + e_1)$$
$$+ [-a_2(x_1 - 150) - b_2(\sin(x_1 - 150)) + r(x_1 - 150) - (x_1 - 150)(x_3 - 150) \qquad (7.15)$$
$$- (x_2 - 150) - F \cdot \omega_2 \cdot \sin 2\omega_2 t + u_2](1 + e_2)$$
$$+ [-a_3(x_1 - 150) - b_3(\sin(x_1 - 150)) + (x_1 - 150)(x_2 - 150) - c(x_3 - 150)$$
$$- F \cdot \omega_3 \cdot \sin 2\omega_3 t + u_3](1 + e_3)$$

Choose

$$
\begin{aligned}
u_1 =& -[-a_1(x_1 - 150) - b_1(\sin(x_1 - 150)) + \sigma((x_2 - 150) - (x_1 - 150)) \\
& - F\omega_1 \sin 2\omega_1 t] - e_1 \\
u_2 =& -[-a_2(x_1 - 150) - b_2(\sin(x_1 - 150)) + r(x_1 - 150) - (x_1 - 150)(x_3 - 150) \\
& - (x_2 - 150) - F\omega_2 \sin 2\omega_2 t] - e_2 \\
u_3 =& -[-a_3(x_1 - 150) - b_3(\sin(x_1 - 150)) + (x_1 - 150)(x_2 - 150) - c(x_3 - 150) \\
& - F\omega_3 \sin 2\omega_3 t] - e_3
\end{aligned}
\tag{7.16}
$$

We obtain

$$
\dot{V} = -e_1(1 + e_1) - e_2(1 + e_2) - e_3(1 + e_3) < 0 \tag{7.17}
$$

which is a negative definite function. The numerical results are shown in Fig.7.4 and Fig.7.5. After 40 sec, the errors approach zero and the motion trajectories approach to the periodic functions.
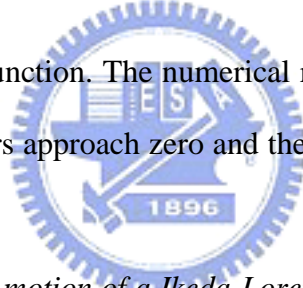
CASE III. *Control the chaotic motion of a Ikeda-Lorenz system to chaotic motion of a Genesio system*[48].

In this case we will control chaotic motion of Ikeda-Lorenz system (7.4) to that of a Genesio system. The goal system is Genesio system:

$$
\begin{aligned}
\dot{z}_1 &= z_2 \\
\dot{z}_2 &= z_3 \\
\dot{z}_3 &= z_1^2 - a_4 z_1 - b_4 z_2 - c_4 z_3
\end{aligned}
\tag{7.18}
$$

The error equation is $e = x - z$, Our aim is $\lim\limits_{t \to \infty} e = 0$. The error dynamics become

The error dynamics become

$$\dot{e}_1 = \dot{x}_1 - \dot{z}_1 = -a_1(x_1 - 150) - b_1(\sin(x_1 - 150)) + \sigma((x_2 - 150)$$
$$- (x_1 - 150)) - z_2 + u_1$$
$$\dot{e}_2 = \dot{x}_2 - \dot{z}_2 = -a_2(x_1 - 150) - b_2(\sin(x_1 - 150)) + r(x_1 - 150)$$
$$- (x_1 - 150)(x_3 - 150) - (x_2 - 150) - z_3 + u_2 \qquad (7.19)$$
$$\dot{e}_3 = \dot{x}_3 - \dot{z}_3 = -a_3(x_1 - 150) - b_3(\sin(x_1 - 150)) + (x_1 - 150)(x_2 - 150)$$
$$- c(x_3 - 150) - (z_1^2 - a_4 z_1 - b_4 z_2 - c_4 z_3) + u_3$$

Let initial states be $(x_1(0), x_2(0), x_3(0)) = (1, 2, 3)$, $(y_1(0), y_2(0), y_3(0)) = (3.5, 4, 1)$ and system parameters a_1=0.1, b_1=1, σ=16, a_2=0.2, b_2=0.3, r=45.92, a_3=0.05, b_3=1.8 and c=4, we find that the error dynamics always exists in first quadrant as shown in Fig.7.6.

By GYC partial region asymptotical stability theorem, one can choose a Lyapunov function in the form of a positive definite function in first quadrant:

$$V = e_1 + e_2 + e_3 + \frac{1}{2}(e_1^2 + e_2^2 + e_3^2) > 0 \qquad (7.20)$$

Its time derivative is

$$\dot{V} = \dot{e}_1(1 + e_1) + \dot{e}_2(1 + e_2) + \dot{e}_3(1 + e_3)$$
$$= [-a_1(x_1 - 150) - b_1(\sin(x_1 - 150)) + \sigma((x_2 - 150) - (x_1 - 150))$$
$$- z_2 + u_1](1 + e_1)$$
$$+ [-a_2(x_1 - 150) - b_2(\sin(x_1 - 150)) + r(x_1 - 150) - (x_1 - 150)(x_3 - 150) \qquad (7.21)$$
$$- (x_2 - 150) - z_3 + u_2](1 + e_2)$$
$$+ [-a_3(x_1 - 150) - b_3(\sin(x_1 - 150)) + (x_1 - 150)(x_2 - 150) - c(x_3 - 150)$$
$$- (z_1^2 - a_4 z_1 - b_4 z_2 - c_4 z_3) + u_3](1 + e_3)$$

Choose

$$
\begin{aligned}
u_1 = &-[-a_1(x_1 - 150) - b_1(\sin(x_1 - 150)) + \sigma((x_2 - 150) - (x_1 - 150)) \\
&- z_2] - e_1 \\
u_2 = &-[-a_2(x_1 - 150) - b_2(\sin(x_1 - 150)) + r(x_1 - 150) - (x_1 - 150)(x_3 - 150) \\
&- (x_2 - 150) - z_3] - e_2 \\
u_3 = &-[-a_3(x_1 - 150) - b_3(\sin(x_1 - 150)) + (x_1 - 150)(x_2 - 150) - c(x_3 - 150) \\
&- (z_1^2 - a_4 z_1 - b_4 z_2 - c_4 z_3)] - e_3
\end{aligned}
\tag{7.22}
$$

We obtain

$$
\dot{V} = -e_1(1 + e_1) - e_2(1 + e_2) - e_3(1 + e_3) < 0
\tag{7.23}
$$

which is a negative definite function. The numerical results are shown in Fig.7.7 and Fig.7.8. After 40 sec, the errors approach zero and the chaotic trajectories of Ikeda-Lorenz system approach to that of the Genesio system.
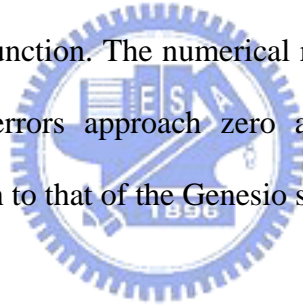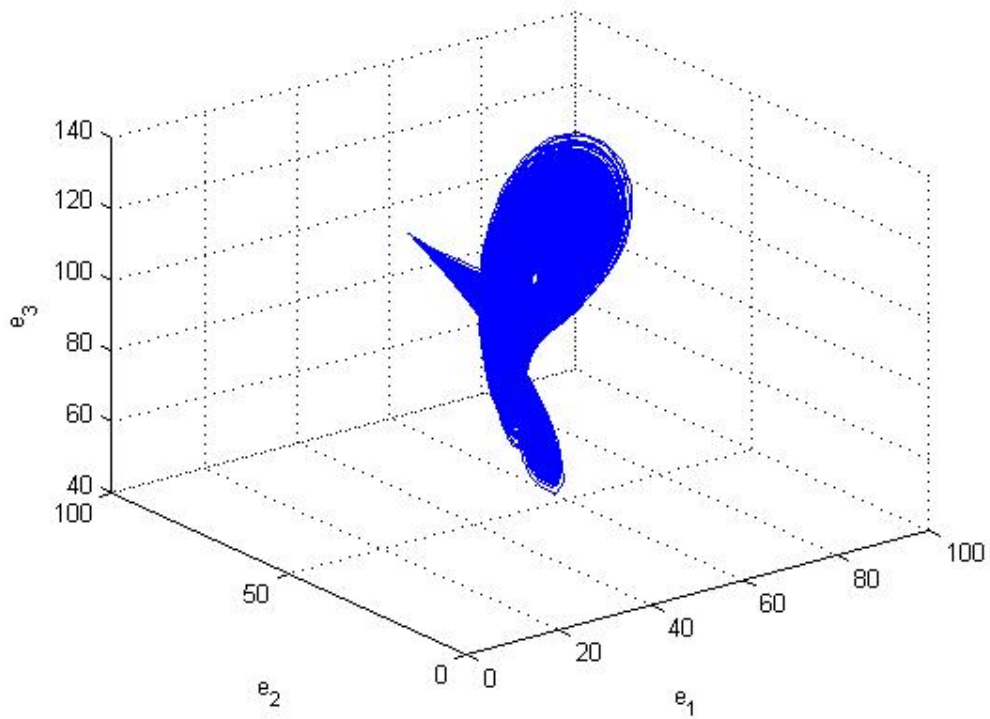
Fig. 7.1. Phase portrait of error dynamics for *CASE I*.
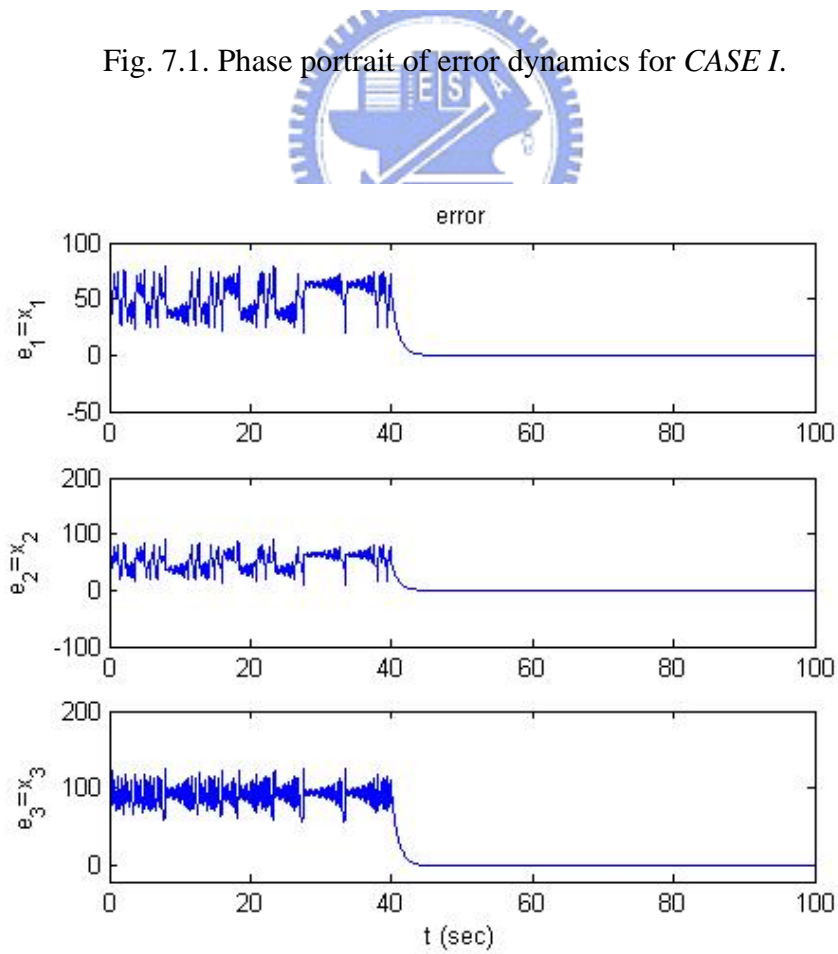
Fig. 7.2. Time histories of errors for *CASE I*.
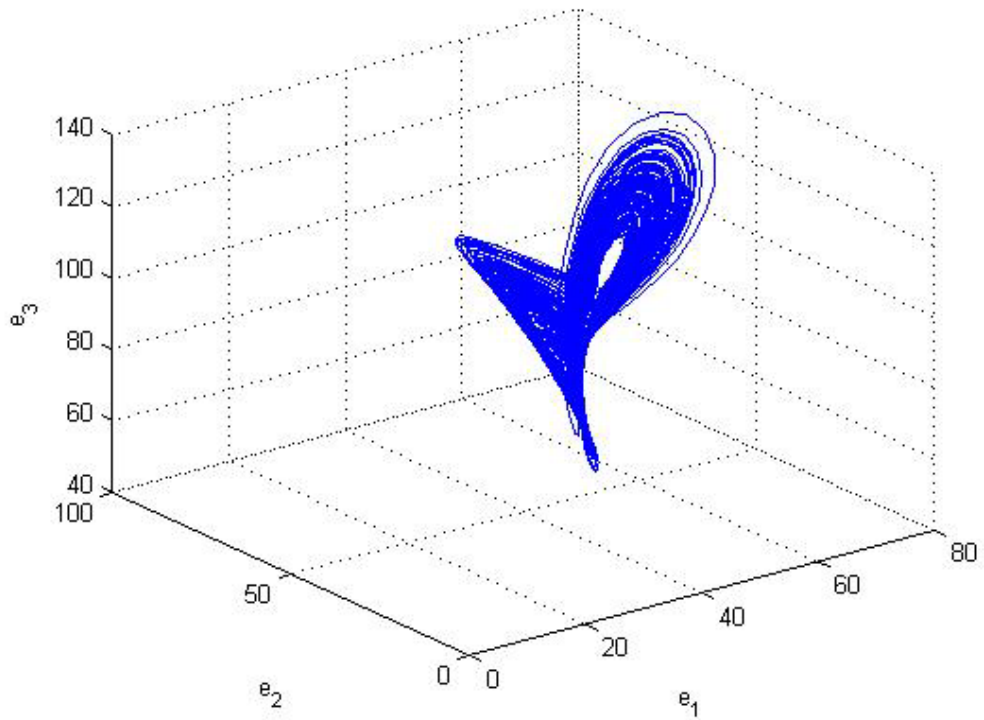
Fig.7.3. Phase portrait of error dynamics for *CASE II*.
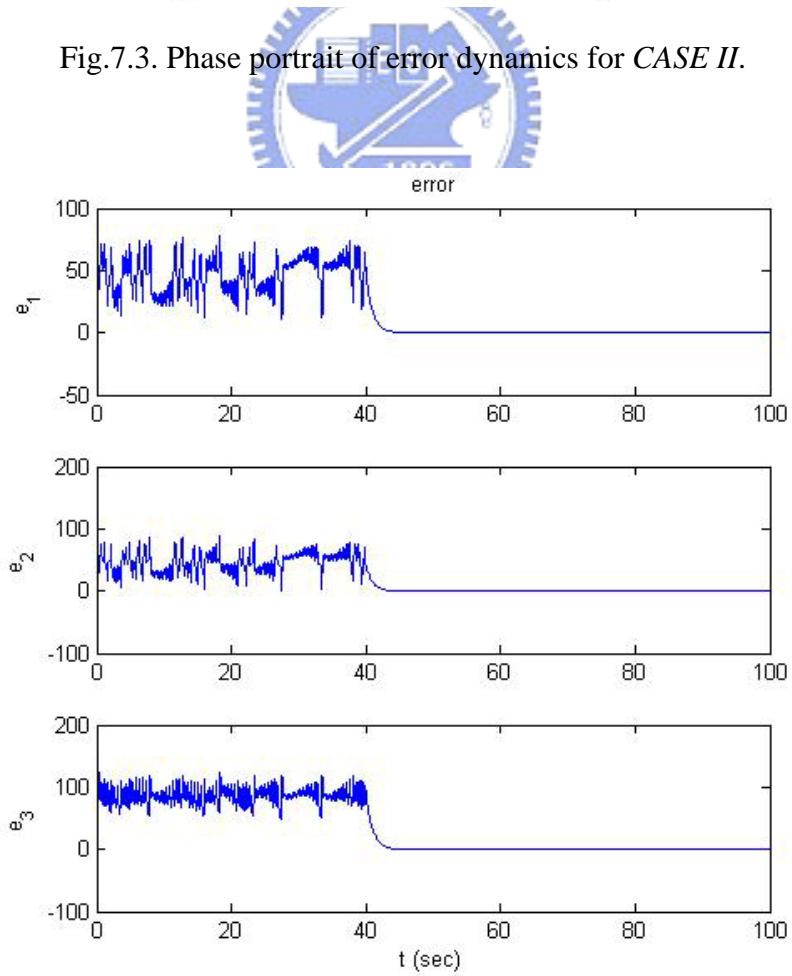
Fig.7.4..Time histories of errors for *CASE II*.
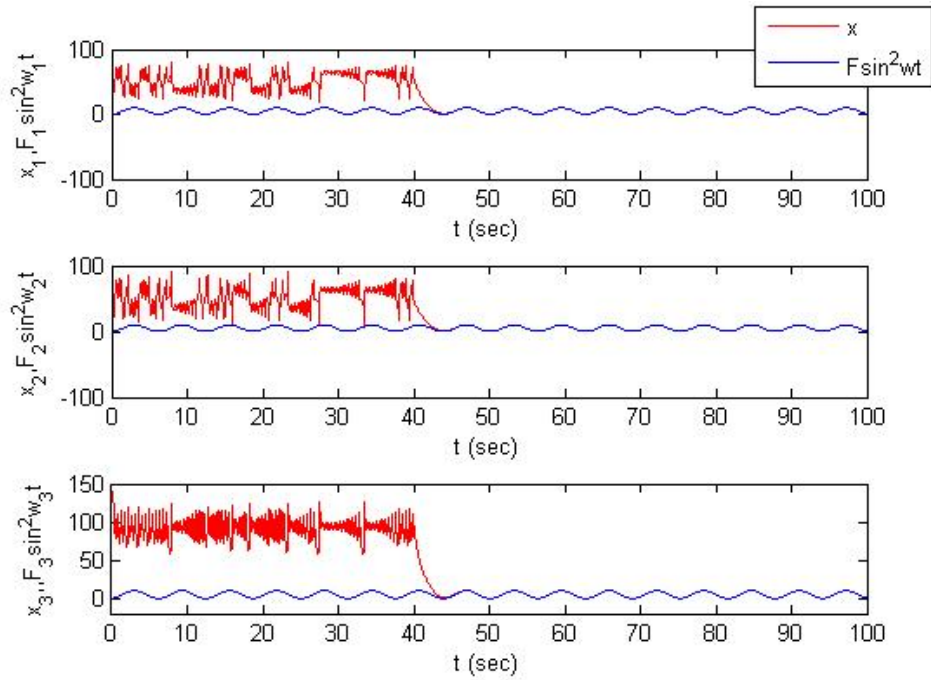
Fig.7.5. Time histories of errors for *CASE II*.
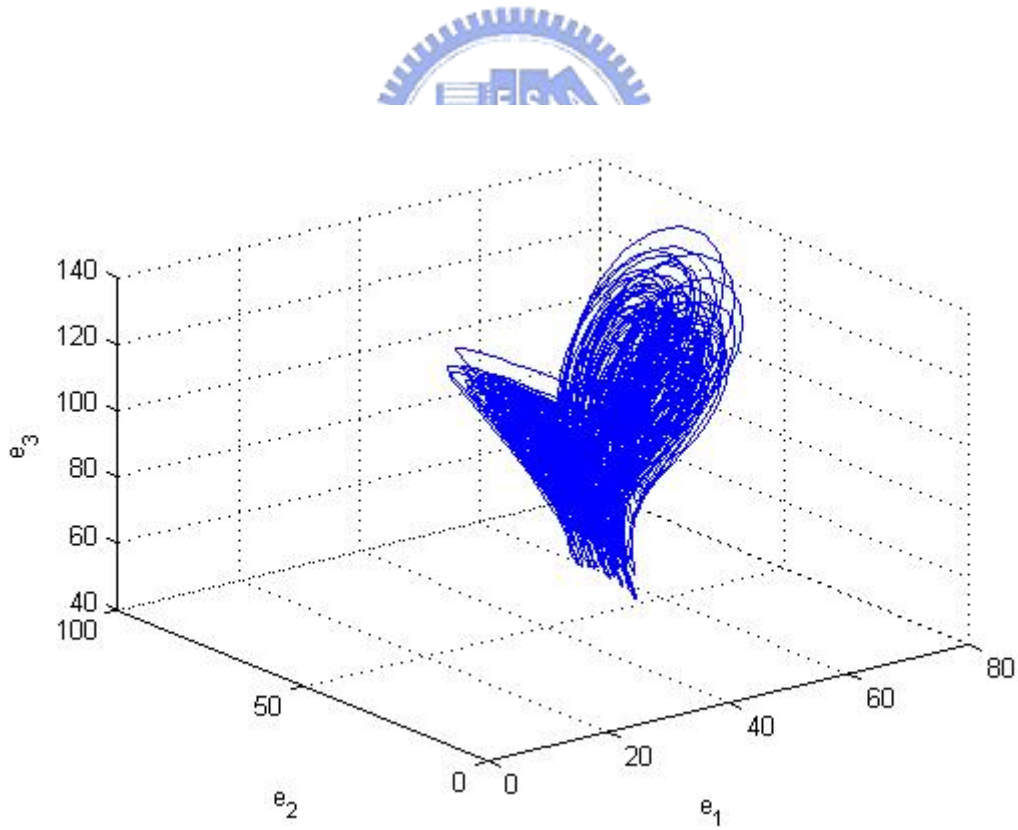
Fig.7.6. Phase portrait of error dynamics for *CASE III*.

65
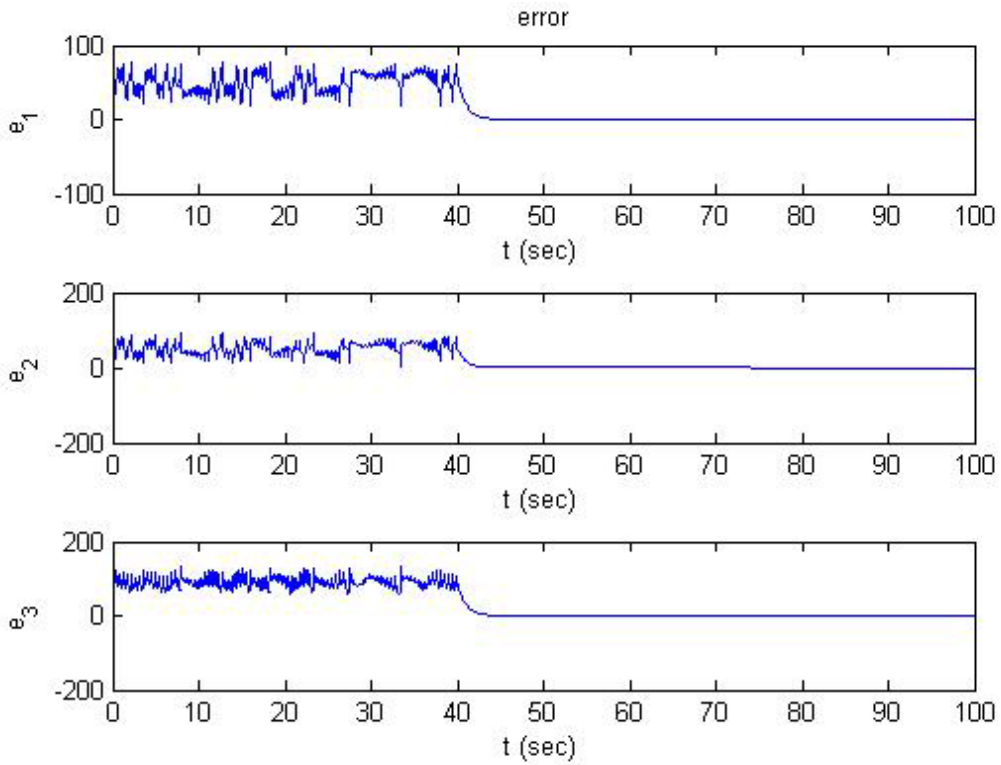
Fig.7.7. Time histories of errors for *CASE III*.
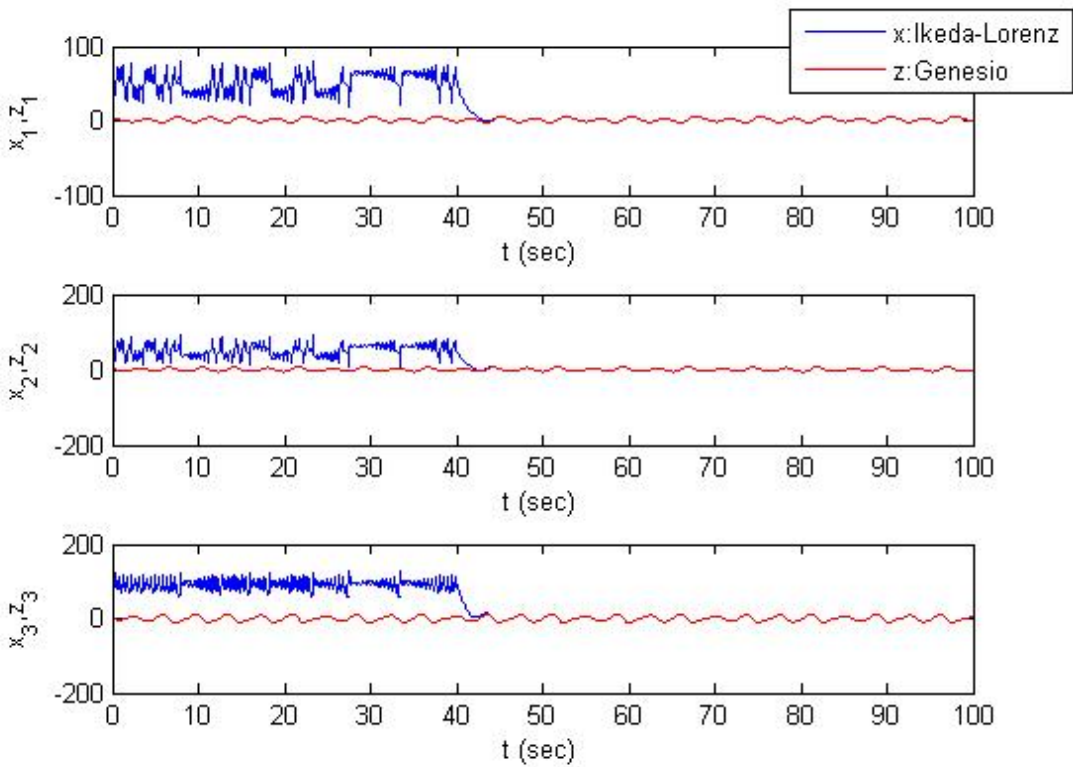
Fig.7.8. Time histories of errors for *CASE III*.

Chapter 8

Estimation of Parameters of a New Ikeda-Mackey-Glass System through Chaos Synchronization with Random Disturbance

8.1 Preliminaries

Estimation of parameters of a new IMG system by using a least square approach is achieved. When the corresponding parameters converge to same values, two time delay Ikeda-Mackey-Glass systems are synchronized.

8.2 Chaos Synchronization Scheme

Differential equations of a general delay system are described as follows [56]:

$$\dot{x} = f(x(t), x(t-\tau), \beta) \tag{8.1}$$

where $x \in R^n$ is the state vector, $\beta \in R^m$ is the parameter vector which is to be estimated.

Let

$$\dot{y} = g(y(t), y(t-\tau), \hat{\beta}) \tag{8.2}$$

be coupled to Eq.(8.1), where $y \in R^n$ is the state vector, $\hat{\beta} \in R^m$ is the parameter vector. The state vector y is asymptotically synchronized with x when $\hat{\beta}$ approaches

β.

The general representation of the feedback coupling is

$$\dot{y} = g(y(t), y(t-\tau), \hat{\beta}) - BG^T[y-x] \qquad (8.3)$$

where B is a constant vector and G is the gain vector. Next we construct a mechanism that drives the measured synchronization error y-x to zero so that $(y, \hat{\beta}) \rightarrow (x, \beta)$ as $t \rightarrow \infty$. For that we consider the following minimization problem to construct a system of differential equation governing the evolution of the model system parameter $\hat{\beta}$,

$$F(\hat{\beta}) \rightarrow \min\{[y-x]^2\} \qquad (8.4)$$

The parameter vector $\hat{\beta}$ is to be suitably tuned so that the system (8.3) asymptotically synchronizes with the system (8.1) through the choice of function given by Eq.(8.4). By the minimization problem, a system of differential equations governing the evolution of $\hat{\beta}$ is constructed:

$$\dot{\hat{\beta}}_j = -\frac{\partial F}{\partial \hat{\beta}_j} = -2(y_i - x_i)\frac{\partial y_i}{\partial \hat{\beta}_j} \quad, j=1,...,m \qquad (8.5)$$

The variational derivatives $\dfrac{\partial y_i}{\partial \hat{\beta}_j}$ for $i=1,...,n$ and $j=1,...,m$ are to be known for solving this system of equations. These derivatives are given by

$$\frac{d}{dt}\left(\frac{\partial y_i}{\partial \hat{\beta}_j}\right) = \sum_{k=1}^{n} \frac{\partial g_i}{\partial y_k}\frac{\partial y_k}{\partial \hat{\beta}_j} + \frac{\partial g_i}{\partial \hat{\beta}_j} - BG^T \frac{\partial y_k}{\partial \hat{\beta}_j} \quad \text{for i=1,...,n and j=1,...,m} \qquad (8.6)$$

In Eq.(8.5), a vector of parameters ε is added, which is needed for controlling the stability of the overall system and rate of synchronization:

$$\dot{\hat{\beta}}_j = -\varepsilon_j \frac{\partial F}{\partial \hat{\beta}_j} = -2\varepsilon_j(y_i - x_i)\frac{\partial y_i}{\partial \hat{\beta}_j}, \, j=1,...m \qquad (8.7)$$

Finally we have to solve Eqs.(8.1), (8.3), (8.6), (8.7) altogether.

So an extended system consisting of ($n+m+nm$) equations is to be solved in order to estimate m parameters and simultaneous synchronization of the n-dimensional system.

8.3 Parameters Estimation of a New Ikeda-Mackey -Glass System without Disturbance

In this Section, a new Ikeda-Mackey-Glass system is used for the chaos synchronization scheme to estimate parameters,

$$\dot{x}_1(t) = -25x_1(t) - 24.8\sin x_1(t-\tau_1) + 14.1x_2(t-\tau_2)$$

$$\dot{x}_2(t) = -4.7x_2(t) + 1.2348\frac{x_2(t-\tau_1)}{1+\{x_2(t-\tau_1)\}^{10}} + 8x_1(t-\tau_2)$$

$\qquad\qquad\qquad\qquad\qquad\qquad\qquad\qquad\qquad\qquad (8.8)$

According to Chapter 2, we know that for a new Ikeda-Mackey-Glass system, chaotic motion can be obtained when $\tau_1=5$, $\tau_2=1$.

Using chaos synchronization scheme in Section 8.2, the equations are described as follows:

$$\dot{x}_1(t) = -25x_1(t) - 24.8\sin x_1(t-\tau_1) + 14.1x_2(t-\tau_2) \tag{8.9}$$

$$\dot{x}_2(t) = -4.7x_2(t) + 1.2348\frac{x_2(t-\tau_1)}{1+\{x_2(t-\tau_1)\}^{10}} + 8x_1(t-\tau_2) \tag{8.10}$$

$$\dot{y}_1(t) = -25y_1(t) - \hat{\beta}_1\sin y_1(t-\tau_1) + 14.1y_2(t-\tau_2) - G_1[y_1(t) - x_1(t)] \tag{8.11}$$

$$\dot{y}_2(t) = -\hat{\beta}_2 y_2(t) + 1.2348\frac{y_2(t-\tau_1)}{1+y_2(t-\tau_1)^{10}} + 8y_1(t-\tau_2) - G_2[y_2(t) - x_2(t)] \tag{8.12}$$

$$\dot{\hat{\beta}}_1(t) = -2\varepsilon_1[y_1(t) - x_1(t)]\frac{\partial y_1}{\partial \hat{\beta}_1} \tag{8.13}$$

$$\dot{\hat{\beta}}_2(t) = -2\varepsilon_2[y_2(t) - x_2(t)]\frac{\partial y_2}{\partial \hat{\beta}_2} \tag{8.14}$$

$$\frac{d}{dt}[\frac{\partial y_1}{\partial \hat{\beta}_1}] = [-25 - \frac{\hat{\beta}_1(t)\cos y_1(t-\tau_1)\dot{y}_1(t-\tau_1)}{\dot{y}_1(t)}]\frac{\partial y_1}{\partial \hat{\beta}_1} - 2\sin y_1(t-\tau_1)$$
$$-G_1\frac{\partial y_1}{\partial \hat{\beta}_1} + \frac{14.1\dot{y}_2(t-\tau_2)}{\dot{y}_2(t)}\frac{\partial y_2}{\partial \hat{\beta}_1} - G_1\frac{\partial y_2}{\partial \hat{\beta}_1} \tag{8.15}$$

$$\frac{d}{dt}[\frac{\partial y_2}{\partial \hat{\beta}_2}] = 8\frac{\dot{y}_1(t-\tau_2)}{\dot{y}_1(t)}\frac{\partial y_1}{\partial \hat{\beta}_2} - 2y_2(t) - G_2\frac{\partial y_1}{\partial \hat{\beta}_2} +$$
$$[-\hat{\beta}_2 + \frac{1.2348\dot{y}_2(t-\tau_1)\{1-9y_2(t-\tau_1)^{10}\}}{\dot{y}_2(t)\{1+y_2(t-\tau_1)^{10}\}^2}]\frac{\partial y_2}{\partial \hat{\beta}_2} - G_2\frac{\partial y_2}{\partial \hat{\beta}_2} \tag{8.16}$$

$$\frac{d}{dt}[\frac{\partial y_1}{\partial \hat{\beta}_2}] = [-25 - \frac{\hat{\beta}_1(t)\cos y_1(t-\tau_1)\dot{y}_1(t-\tau_1)}{\dot{y}_1(t)}]\frac{\partial y_1}{\partial \hat{\beta}_2} - G_1\frac{\partial y_1}{\partial \hat{\beta}_2}$$
$$+ \frac{14.1\dot{y}_2(t-\tau_2)}{\dot{y}_2(t)}\frac{\partial y_2}{\partial \hat{\beta}_2} - G_1\frac{\partial y_2}{\partial \hat{\beta}_2}$$

(8.17)

$$\frac{d}{dt}[\frac{\partial y_2}{\partial \hat{\beta}_1}] = 8\frac{\dot{y}_1(t-\tau_2)}{\dot{y}_1(t)}\frac{\partial y_1}{\partial \hat{\beta}_1} - G_2\frac{\partial y_1}{\partial \hat{\beta}_1} +$$
$$[-\hat{\beta}_2 + \frac{1.2348\dot{y}_2(t-\tau_1)\{1-9y_2(t-\tau_1)^{10}\}}{\dot{y}_2(t)\{1+y_2(t-\tau_1)^{10}\}^2}]\frac{\partial y_2}{\partial \hat{\beta}_2} + G_2\frac{\partial y_2}{\partial \hat{\beta}_1}$$

(8.18)

where

$$\dot{y}_1(t-\tau_1) = -25y_1(t-\tau_1) - \hat{\beta}_1\sin y_1(t-2\tau_1) + 14.1y_2(t-(\tau_1+\tau_2))$$
$$-G_1[y_1(t-\tau_1) - x_1(t-\tau_1)]$$

(8.19)

$$\dot{y}_2(t-\tau_1) = -\hat{\beta}_2 y_2(t-\tau_1) + 1.2348\frac{y_2(t-2\tau_1)}{1+y_2(t-2\tau_1)^{10}} + 8y_1(t-(\tau_1+\tau_2))$$
$$-G_2[y_2(t-\tau_1) - x_2(t-\tau_1)]$$

(8.20)

We tried to estimate the parameters $\hat{\beta}_1$ and $\hat{\beta}_2$ of the system. The results show that the parameter $\hat{\beta}_1$ and $\hat{\beta}_2$ converges to their actual values when the master and response systems are synchronized. The simulation results are shown in Fig.8.1, Fig.8.2, Fig.8.3 and Fig.8.4.

8.4. Parameters Estimation of a New Ikeda-Mackey -Glass System with Random Disturbance

Parameters estimation of a new Ikeda-Mackey-Glass system is studied when there exists random disturbance.

CASE I: Disturbance φ exists in the state y₁, where φ is the the Rayleigh noise:

$$\varphi(t) = \frac{t}{\sigma}\exp(-\frac{t^2}{2\sigma^2})$$

where σ^2 is known as the fading envelope of the Rayleigh distribution.

The equations are described as follows:

$$\dot{x}_1(t) = -25x_1(t) - 24.8\sin x_1(t-\tau_1) + 14.1x_2(t-\tau_2) \tag{8.21}$$

$$\dot{x}_2(t) = -4.7x_2(t) + 1.2348\frac{x_2(t-\tau_1)}{1+\{x_2(t-\tau_1)\}^{10}} + 8x_1(t-\tau_2) \tag{8.22}$$

$$\dot{y}_1(t) = -25y_1(t) - \hat{\beta}_1\sin y_1(t-\tau_1) + 14.1y_2(t-\tau_2)$$
$$- G_1[y_1(t) - x_1(t) - \varphi] \tag{8.23}$$

$$\dot{y}_2(t) = -\hat{\beta}_2 y_2(t) + 1.2348\frac{y_2(t-\tau_1)}{1+y_2(t-\tau_1)^{10}} + 8y_1(t-\tau_2) - G_2[y_2(t) - x_2(t)] \tag{8.24}$$

$$\dot{\hat{\beta}}_1(t) = -2\varepsilon_1[y_1(t) - x_1(t) - \varphi]\frac{\partial y_1}{\partial\hat{\beta}_1} \tag{8.25}$$

$$\dot{\hat{\beta}}_2(t) = -2\varepsilon_2[y_2(t) - x_2(t)]\frac{\partial y_2}{\partial\hat{\beta}_2} \tag{8.26}$$

$$\frac{d}{dt}[\frac{\partial y_1}{\partial\hat{\beta}_1}] = [-25 - \frac{\hat{\beta}_1(t)\cos y_1(t-\tau_1)\dot{y}_1(t-\tau_1)}{\dot{y}_1(t)}]\frac{\partial y_1}{\partial\hat{\beta}_1} - 2\sin y_1(t-\tau_1)$$
$$-G_1\frac{\partial y_1}{\partial\hat{\beta}_1} + \frac{14.1\dot{y}_2(t-\tau_2)}{\dot{y}_2(t)}\frac{\partial y_2}{\partial\hat{\beta}_1} - G_1\frac{\partial y_2}{\partial\hat{\beta}_1} \tag{8.27}$$

$$\frac{d}{dt}[\frac{\partial y_2}{\partial \hat{\beta}_2}] = 8\frac{\dot{y}_1(t-\tau_2)}{\dot{y}_1(t)}\frac{\partial y_1}{\partial \hat{\beta}_2} - 2y_2(t) - G_2\frac{\partial y_1}{\partial \hat{\beta}_2} +$$
$$[-\hat{\beta}_2 + \frac{1.2348\dot{y}_2(t-\tau_1)\{1-9y_2(t-\tau_1)^{10}\}}{\dot{y}_2(t)\{1+y_2(t-\tau_1)^{10}\}^2}]\frac{\partial y_2}{\partial \hat{\beta}_2} - G_2\frac{\partial y_2}{\partial \hat{\beta}_2} \qquad (8.28)$$

$$\frac{d}{dt}[\frac{\partial y_1}{\partial \hat{\beta}_2}] = [-25 - \frac{\hat{\beta}_1(t)\cos y_1(t-\tau_1)\dot{y}_1(t-\tau_1)}{\dot{y}_1(t)}]\frac{\partial y_1}{\partial \hat{\beta}_2} - G_1\frac{\partial y_1}{\partial \hat{\beta}_2}$$
$$+ \frac{14.1\dot{y}_2(t-\tau_2)}{\dot{y}_2(t)}\frac{\partial y_2}{\partial \hat{\beta}_2} - G_1\frac{\partial y_2}{\partial \hat{\beta}_2} \qquad (8.29)$$

$$\frac{d}{dt}[\frac{\partial y_2}{\partial \hat{\beta}_1}] = 8\frac{\dot{y}_1(t-\tau_2)}{\dot{y}_1(t)}\frac{\partial y_1}{\partial \hat{\beta}_1} - G_2\frac{\partial y_1}{\partial \hat{\beta}_1} +$$
$$[-\hat{\beta}_2 + \frac{1.2348\dot{y}_2(t-\tau_1)\{1-9y_2(t-\tau_1)^{10}\}}{\dot{y}_2(t)\{1+y_2(t-\tau_1)^{10}\}^2}]\frac{\partial y_2}{\partial \hat{\beta}_2} + G_2\frac{\partial y_2}{\partial \hat{\beta}_1} \qquad (8.30)$$

where

$$\dot{y}_1(t-\tau_1) = -25y_1(t-\tau_1) - \hat{\beta}_1\sin y_1(t-2\tau_1) + 14.1y_2(t-(\tau_1+\tau_2))$$
$$- G_1[y_1(t-\tau_1) - x_1(t-\tau_1) - \varphi] \qquad (8.31)$$

$$\dot{y}_2(t-\tau_1) = -\hat{\beta}_2 y_2(t-\tau_1) + 1.2348\frac{y_2(t-2\tau_1)}{1+y_2(t-2\tau_1)^{10}} + 8y_1(t-(\tau_1+\tau_2))$$
$$- G_2[y_2(t-\tau_1) - x_2(t-\tau_1)] \qquad (8.32)$$

Simulate the twelve equations (8.21-8.32), parameters $\hat{\beta}_1$ and $\hat{\beta}_2$ can converge to their actual values ($\hat{\beta}_1 = \beta_1, \hat{\beta}_2 = \beta_2$) when master system ($x_1, x_2$) are synchronized with the response system (y_1, y_2). The simulation results are shown in Fig.8.5,Fig.8.6,Fig.8.7 and Fig.8.8.

CASE II: Disturbance φ *exists in the state y₂, where* φ *is the the Rayleigh noise.*

The equations are described as follows:

$$\dot{x}_1(t) = -25x_1(t) - 24.8\sin x_1(t-\tau_1) + 14.1x_2(t-\tau_2) \tag{8.33}$$

$$\dot{x}_2(t) = -4.7x_2(t) + 1.2348\frac{x_2(t-\tau_1)}{1+\{x_2(t-\tau_1)\}^{10}} + 8x_1(t-\tau_2) \tag{8.34}$$

$$\dot{y}_1(t) = -25y_1(t) - \hat{\beta}_1\sin y_1(t-\tau_1) + 14.1y_2(t-\tau_2) \\ - G_1[y_1(t) - x_1(t)] \tag{8.35}$$

$$\dot{y}_2(t) = -\hat{\beta}_2 y_2(t) + 1.2348\frac{y_2(t-\tau_1)}{1+y_2(t-\tau_1)^{10}} + 8y_1(t-\tau_2) \\ - G_2[y_2(t) - x_2(t) - \varphi] \tag{8.36}$$

$$\dot{\hat{\beta}}_1(t) = -2\varepsilon_1[y_1(t) - x_1(t)]\frac{\partial y_1}{\partial \hat{\beta}_1} \tag{8.37}$$

$$\dot{\hat{\beta}}_2(t) = -2\varepsilon_2[y_2(t) - x_2(t) - \varphi]\frac{\partial y_2}{\partial \hat{\beta}_2} \tag{8.38}$$

$$\frac{d}{dt}[\frac{\partial y_1}{\partial \hat{\beta}_1}] = [-25 - \frac{\hat{\beta}_1(t)\cos y_1(t-\tau_1)\dot{y}_1(t-\tau_1)}{\dot{y}_1(t)}]\frac{\partial y_1}{\partial \hat{\beta}_1} - 2\sin y_1(t-\tau_1) \\ -G_1\frac{\partial y_1}{\partial \hat{\beta}_1} + \frac{14.1\dot{y}_2(t-\tau_2)}{\dot{y}_2(t)}\frac{\partial y_2}{\partial \hat{\beta}_1} - G_1\frac{\partial y_2}{\partial \hat{\beta}_1} \tag{8.39}$$

$$\frac{d}{dt}[\frac{\partial y_2}{\partial \hat{\beta}_2}] = 8\frac{\dot{y}_1(t-\tau_2)}{\dot{y}_1(t)}\frac{\partial y_1}{\partial \hat{\beta}_2} - 2y_2(t) - G_2\frac{\partial y_1}{\partial \hat{\beta}_2} +$$
$$[-\hat{\beta}_2 + \frac{1.2348\dot{y}_2(t-\tau_1)\{1-9y_2(t-\tau_1)^{10}\}}{\dot{y}_2(t)\{1+y_2(t-\tau_1)^{10}\}^2}]\frac{\partial y_2}{\partial \hat{\beta}_2} - G_2\frac{\partial y_2}{\partial \hat{\beta}_2}$$

(8.40)

$$\frac{d}{dt}[\frac{\partial y_1}{\partial \hat{\beta}_2}] = [-25 - \frac{\hat{\beta}_1(t)\cos y_1(t-\tau_1)\dot{y}_1(t-\tau_1)}{\dot{y}_1(t)}]\frac{\partial y_1}{\partial \hat{\beta}_2} - G_1\frac{\partial y_1}{\partial \hat{\beta}_2}$$
$$+ \frac{14.1\dot{y}_2(t-\tau_2)}{\dot{y}_2(t)}\frac{\partial y_2}{\partial \hat{\beta}_2} - G_1\frac{\partial y_2}{\partial \hat{\beta}_2}$$

(8.41)

$$\frac{d}{dt}[\frac{\partial y_2}{\partial \hat{\beta}_1}] = 8\frac{\dot{y}_1(t-\tau_2)}{\dot{y}_1(t)}\frac{\partial y_1}{\partial \hat{\beta}_1} - G_2\frac{\partial y_1}{\partial \hat{\beta}_1} +$$
$$[-\hat{\beta}_2 + \frac{1.2348\dot{y}_2(t-\tau_1)\{1-9y_2(t-\tau_1)^{10}\}}{\dot{y}_2(t)\{1+y_2(t-\tau_1)^{10}\}^2}]\frac{\partial y_2}{\partial \hat{\beta}_2} + G_2\frac{\partial y_2}{\partial \hat{\beta}_1}$$

(8.42)

where

$$\dot{y}_1(t-\tau_1) = -25y_1(t-\tau_1) - \hat{\beta}_1\sin y_1(t-2\tau_1) + 14.1y_2(t-(\tau_1+\tau_2))$$
$$- G_1[y_1(t-\tau_1) - x_1(t-\tau_1)]$$

(8.43)

$$\dot{y}_2(t-\tau_1) = -\hat{\beta}_2 y_2(t-\tau_1) + 1.2348\frac{y_2(t-2\tau_1)}{1+y_2(t-2\tau_1)^{10}} + 8y_1(t-(\tau_1+\tau_2))$$
$$- G_2[y_2(t-\tau_1) - x_2(t-\tau_1) - \varphi]$$

(8.44)

Simulate the twelve equations (8.33-8.44), parameters $\hat{\beta}_1$ and $\hat{\beta}_2$ can converge to their actual values ($\hat{\beta}_1 = \beta_1, \hat{\beta}_2 = \beta_2$) when master system ($x_1, x_2$) are synchronized with the response system (y_1, y_2). The simulation results are shown in Fig.8.9, Fig.8.10, Fig.8.11 and Fig.8.12.

75

CASE III: Disturbance φ exists in the state y_1 and y_2, where φ is the Rayleigh

   noise.

The equations are described as follows:

$$\dot{x}_1(t) = -25x_1(t) - 24.8\sin x_1(t-\tau_1) + 14.1x_2(t-\tau_2) \tag{8.45}$$

$$\dot{x}_2(t) = -4.7x_2(t) + 1.2348\frac{x_2(t-\tau_1)}{1+\{x_2(t-\tau_1)\}^{10}} + 8x_1(t-\tau_2) \tag{8.46}$$

$$\dot{y}_1(t) = -25y_1(t) - \hat{\beta}_1\sin y_1(t-\tau_1) + 14.1y_2(t-\tau_2) \\ - G_1[y_1(t) - x_1(t) - \varphi] \tag{8.47}$$

$$\dot{y}_2(t) = -\hat{\beta}_2 y_2(t) + 1.2348\frac{y_2(t-\tau_1)}{1+y_2(t-\tau_1)^{10}} + 8y_1(t-\tau_2) \\ - G_2[y_2(t) - x_2(t) - \varphi] \tag{8.48}$$

$$\dot{\hat{\beta}}_1(t) = -2\varepsilon_1[y_1(t) - x_1(t) - \varphi]\frac{\partial y_1}{\partial \hat{\beta}_1} \tag{8.49}$$

$$\dot{\hat{\beta}}_2(t) = -2\varepsilon_2[y_2(t) - x_2(t) - \varphi]\frac{\partial y_2}{\partial \hat{\beta}_2} \tag{8.50}$$

$$\frac{d}{dt}[\frac{\partial y_1}{\partial \hat{\beta}_1}] = [-25 - \frac{\hat{\beta}_1(t)\cos y_1(t-\tau_1)\dot{y}_1(t-\tau_1)}{\dot{y}_1(t)}]\frac{\partial y_1}{\partial \hat{\beta}_1} - 2\sin y_1(t-\tau_1) \\ -G_1\frac{\partial y_1}{\partial \hat{\beta}_1} + \frac{14.1\dot{y}_2(t-\tau_2)}{\dot{y}_2(t)}\frac{\partial y_2}{\partial \hat{\beta}_1} - G_1\frac{\partial y_2}{\partial \hat{\beta}_1} \tag{8.51}$$

$$\frac{d}{dt}[\frac{\partial y_2}{\partial \hat{\beta}_2}] = 8\frac{\dot{y}_1(t-\tau_2)}{\dot{y}_1(t)}\frac{\partial y_1}{\partial \hat{\beta}_2} - 2y_2(t) - G_2\frac{\partial y_1}{\partial \hat{\beta}_2} +$$
$$[-\hat{\beta}_2 + \frac{1.2348\dot{y}_2(t-\tau_1)\{1-9y_2(t-\tau_1)^{10}\}}{\dot{y}_2(t)\{1+y_2(t-\tau_1)^{10}\}^2}]\frac{\partial y_2}{\partial \hat{\beta}_2} - G_2\frac{\partial y_2}{\partial \hat{\beta}_2}$$

(8.52)

$$\frac{d}{dt}[\frac{\partial y_1}{\partial \hat{\beta}_2}] = [-25 - \frac{\hat{\beta}_1(t)\cos y_1(t-\tau_1)\dot{y}_1(t-\tau_1)}{\dot{y}_1(t)}]\frac{\partial y_1}{\partial \hat{\beta}_2} - G_1\frac{\partial y_1}{\partial \hat{\beta}_2}$$
$$+ \frac{14.1\dot{y}_2(t-\tau_2)}{\dot{y}_2(t)}\frac{\partial y_2}{\partial \hat{\beta}_2} - G_1\frac{\partial y_2}{\partial \hat{\beta}_2}$$

(8.53)

$$\frac{d}{dt}[\frac{\partial y_2}{\partial \hat{\beta}_1}] = 8\frac{\dot{y}_1(t-\tau_2)}{\dot{y}_1(t)}\frac{\partial y_1}{\partial \hat{\beta}_1} - G_2\frac{\partial y_1}{\partial \hat{\beta}_1} +$$
$$[-\hat{\beta}_2 + \frac{1.2348\dot{y}_2(t-\tau_1)\{1-9y_2(t-\tau_1)^{10}\}}{\dot{y}_2(t)\{1+y_2(t-\tau_1)^{10}\}^2}]\frac{\partial y_2}{\partial \hat{\beta}_2} + G_2\frac{\partial y_2}{\partial \hat{\beta}_1}$$

(8.54)

where

$$\dot{y}_1(t-\tau_1) = -25y_1(t-\tau_1) - \hat{\beta}_1 \sin y_1(t-2\tau_1) + 14.1y_2(t-(\tau_1+\tau_2))$$
$$- G_1[y_1(t-\tau_1) - x_1(t-\tau_1) - \varphi]$$

(8.55)

$$\dot{y}_2(t-\tau_1) = -\hat{\beta}_2 y_2(t-\tau_1) + 1.2348\frac{y_2(t-2\tau_1)}{1+y_2(t-2\tau_1)^{10}} + 8y_1(t-(\tau_1+\tau_2))$$
$$- G_2[y_2(t-\tau_1) - x_2(t-\tau_1) - \varphi]$$

(8.56)

Simulate the twelve equations (8.45-8.56), parameters $\hat{\beta}_1$ and $\hat{\beta}_2$ can converge to their actual values ($\hat{\beta}_1 = \beta_1, \hat{\beta}_2 = \beta_2$) when master system ($x_1, x_2$) are synchronized with the response system (y_1, y_2). The simulation results are shown in Fig.8.13, Fig.8.14, Fig.8.15 and Fig.8.16.
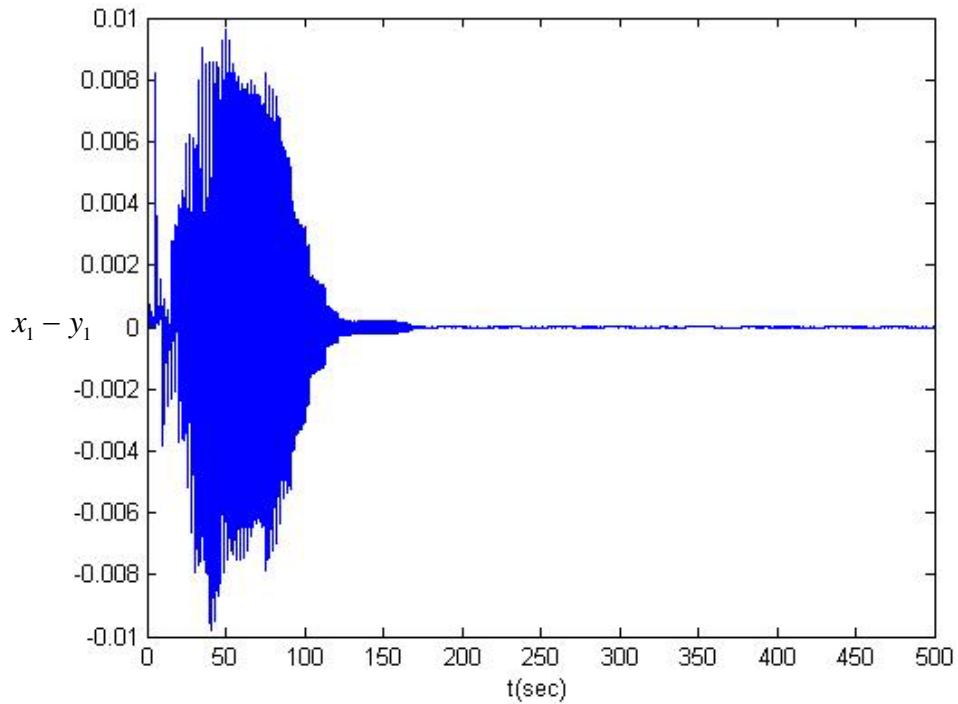
Fig.8.1. Error of master system state x_1 and response system y_1

without disturbance.
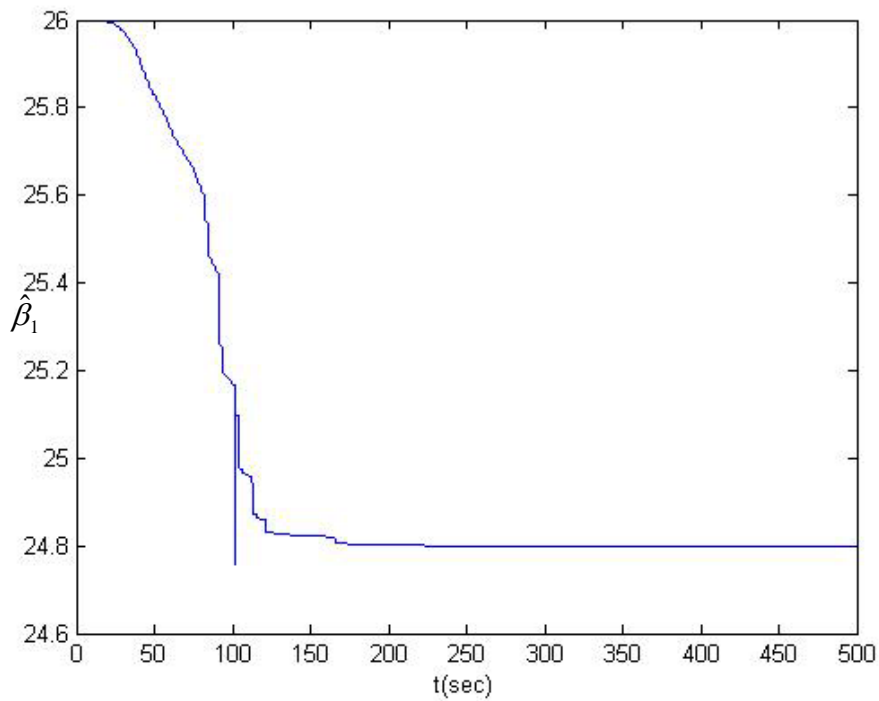
Fig.8.2. Convergence of the estimated parameter $\hat{\beta}_1$ to its actual value

without disturbance in this system.
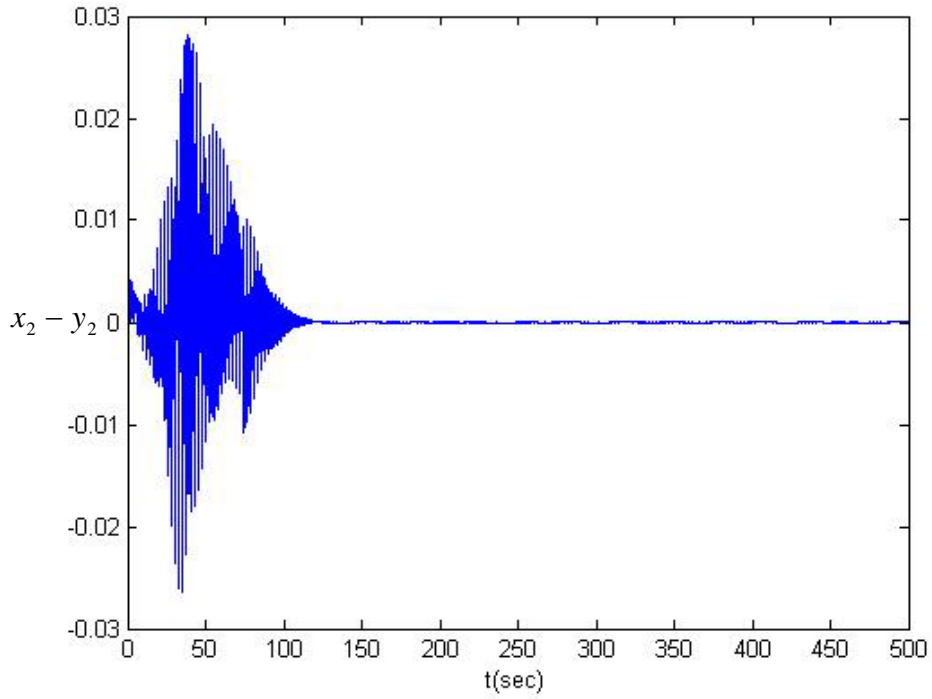
Fig.8.3. Error of master system state x_2 and response system y_2

without disturbance.
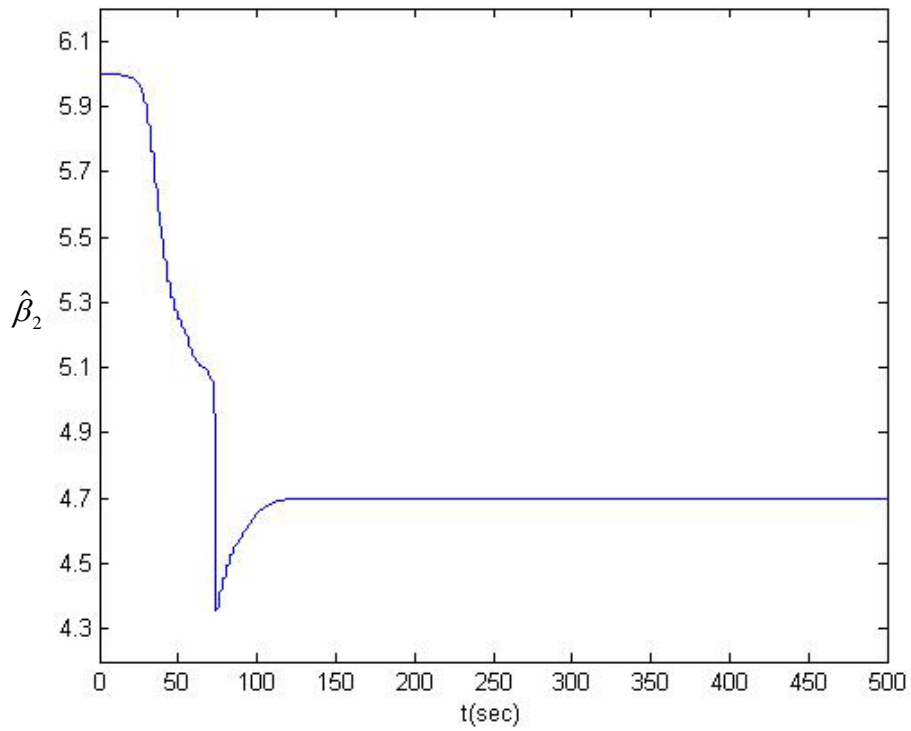
Fig.8.4. Convergence of the estimated parameter $\hat{\beta}_2$ to its actual value

without disturbance in this system.
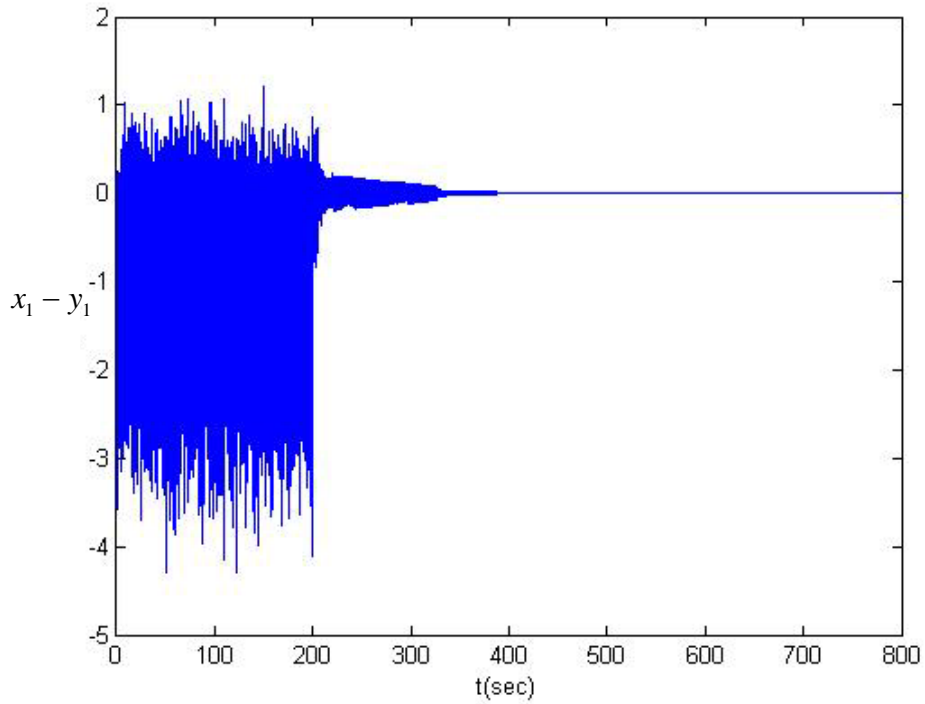
Fig.8.5. Error of master system state x_1 and response system y_1

with disturbance for *CASE I*.
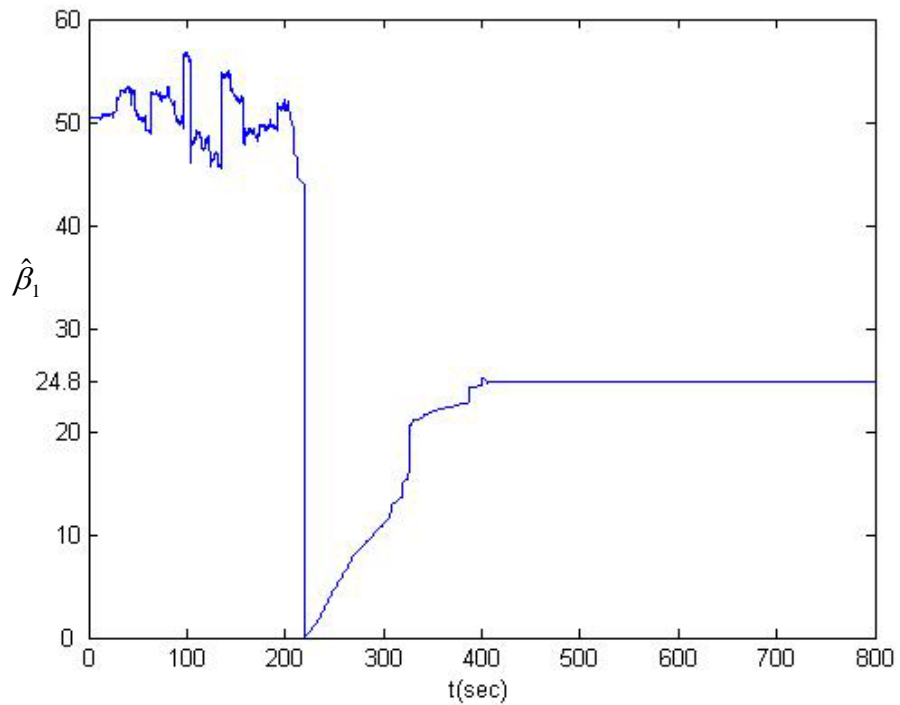
Fig.8.6. Convergence of the estimated parameter $\hat{\beta}_1$ to its actual value

with disturbance in the system for *CASE I*.
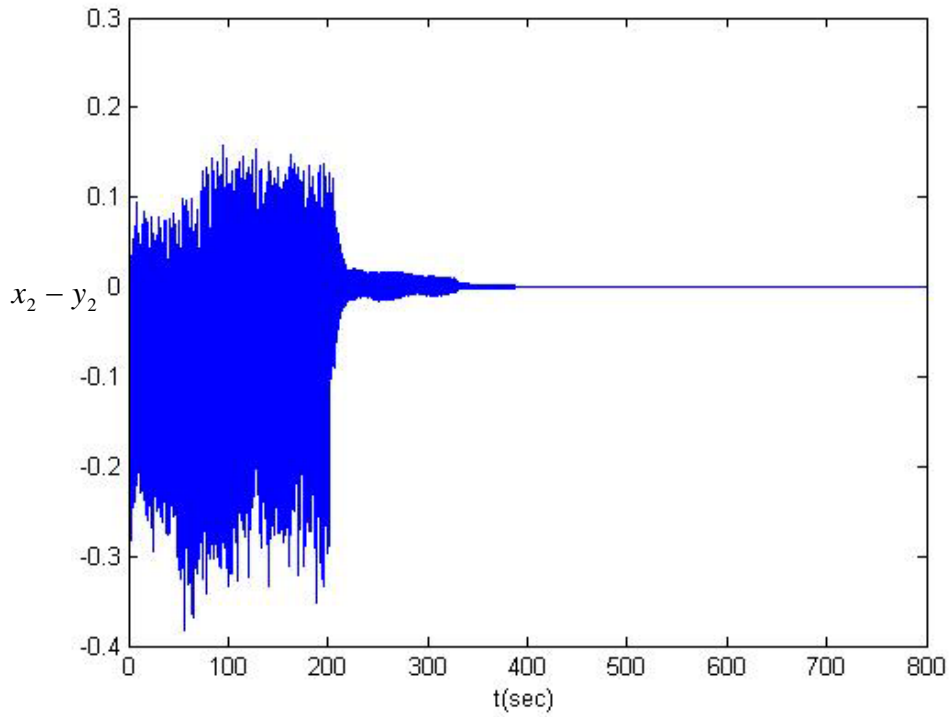
Fig.8.7. Error of master system state x_2 and response system y_2

with disturbance for *CASE I.*
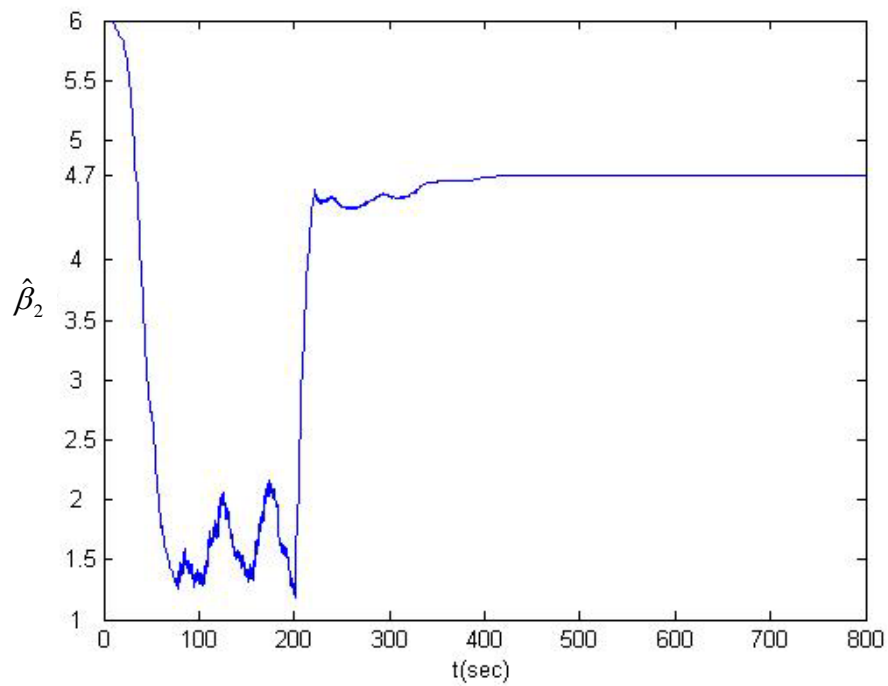
Fig.8.8. Convergence of the estimated parameter $\hat{\beta}_2$ to its actual value

with disturbance in the system for *CASE I.*
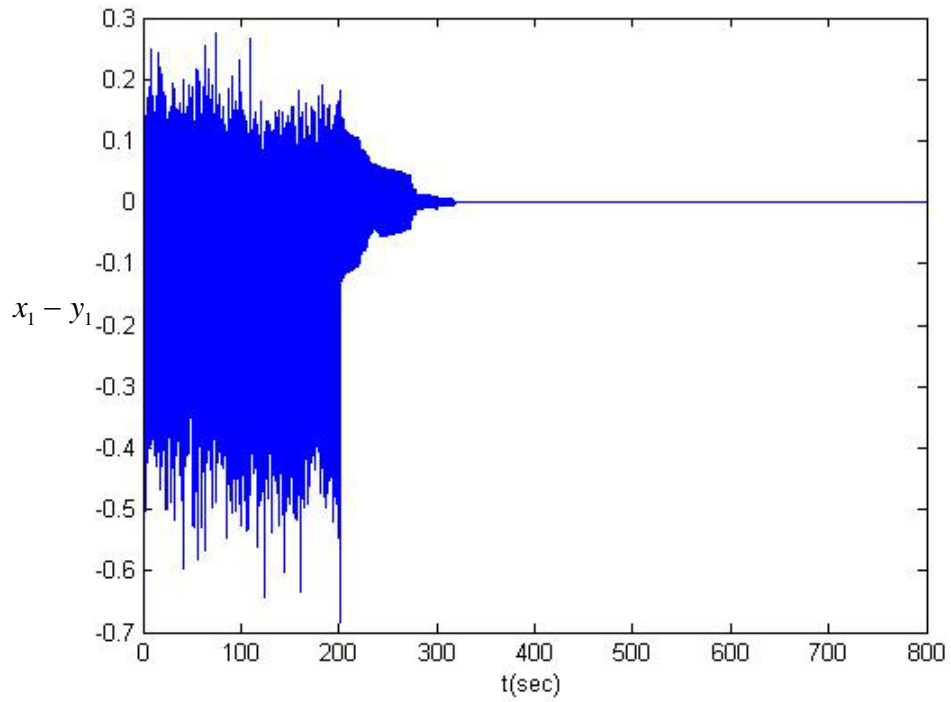
Fig.8.9. Error of master system state x_1 and response system y_1

with disturbance for *CASE II*.
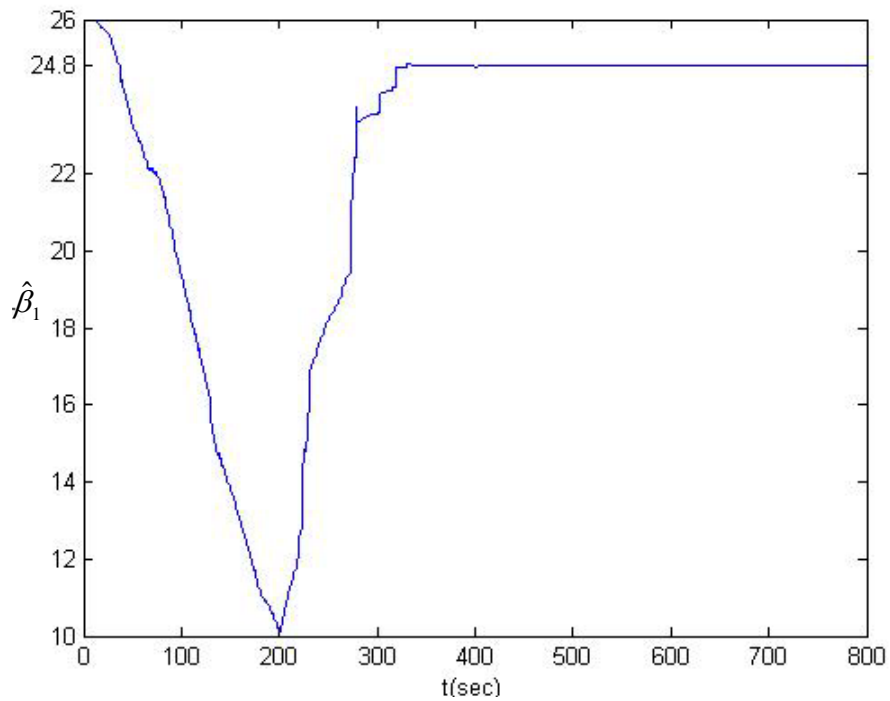
Fig.8.10. Convergence of the estimated parameter $\hat{\beta}_1$ to its actual value

with disturbance in the system for *CASE II*.
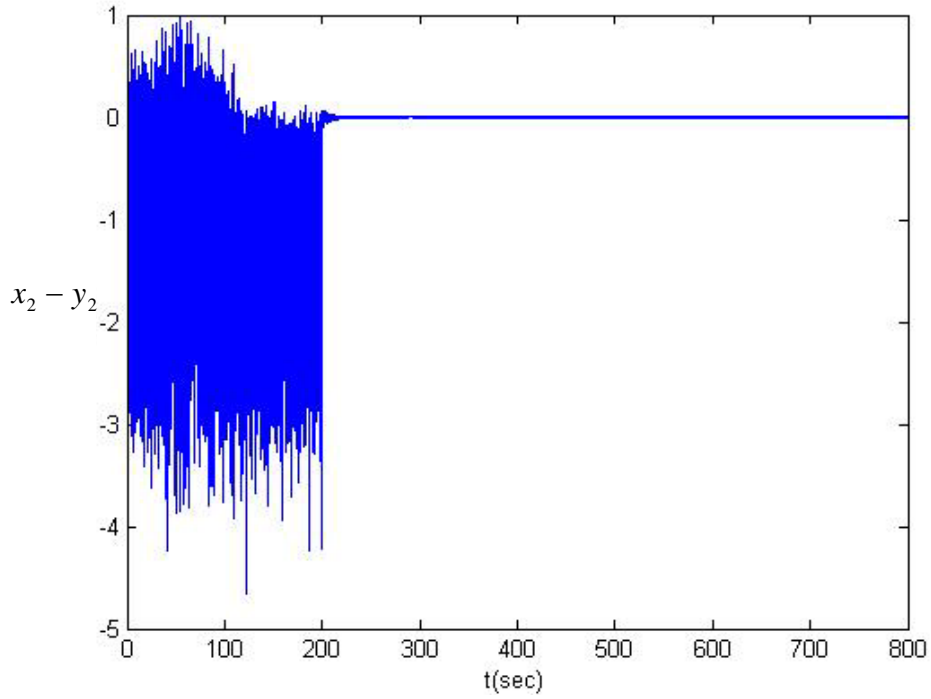
Fig.8.11. Error of master system state x_2 and response system y_2

with disturbance for *CASE II.*
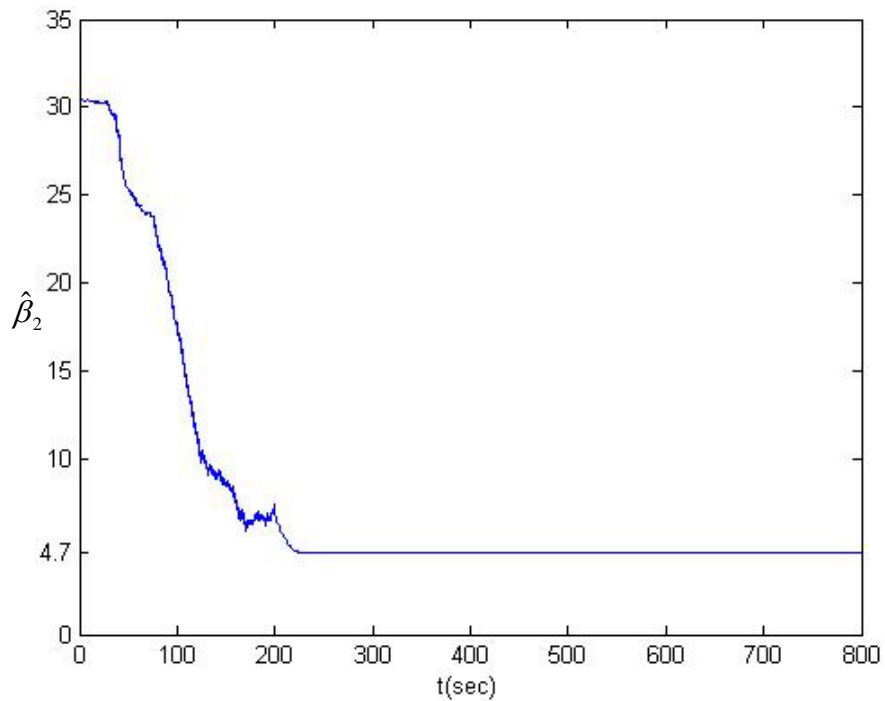
Fig.8.12. Convergence of the estimated parameter $\hat{\beta}_2$ to its actual value

with disturbance in the system for *CASE II.*
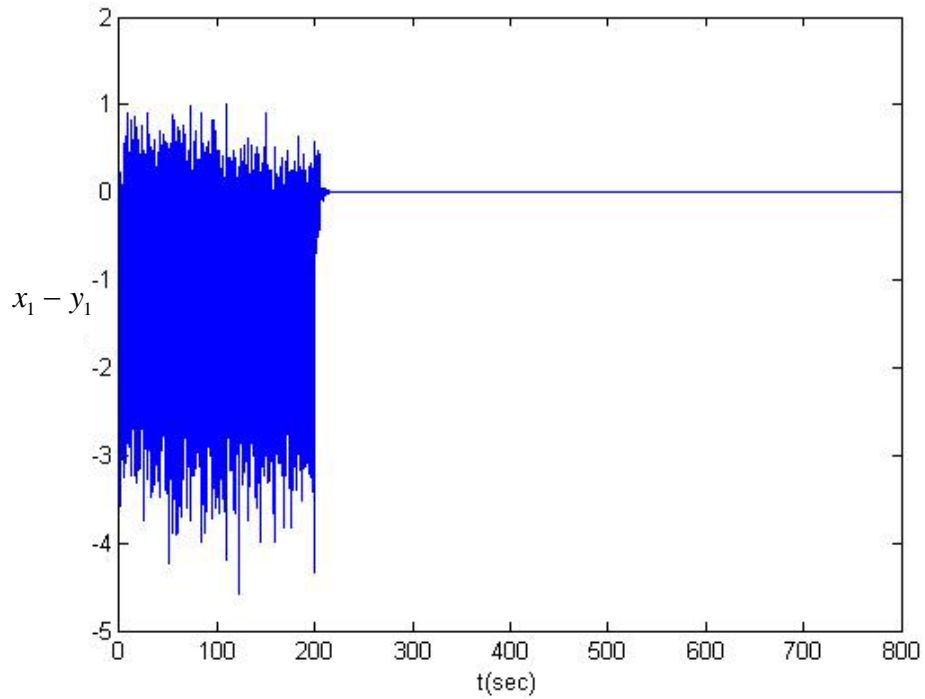
Fig.8.13. Error of master system state x_1 and response system y_1

with disturbance for *CASE III*.
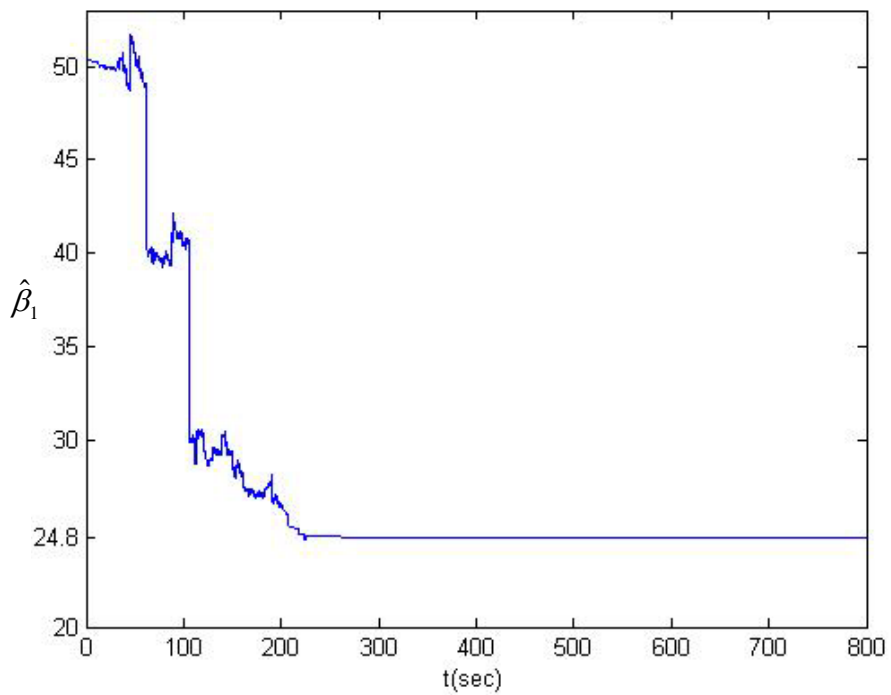
Fig.8.14. Convergence of the estimated parameter $\hat{\beta}_1$ to its actual value

with disturbance in the system for *CASE III*.
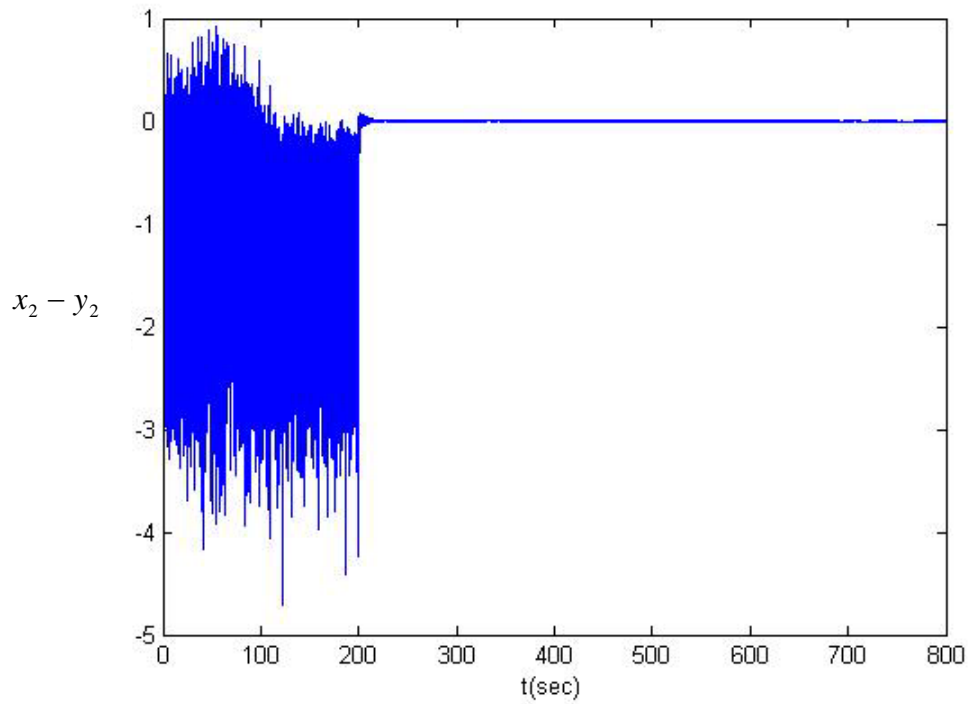
Fig.8.15. Error of master system state x_2 and response system y_2

with disturbance for *CASE III*.
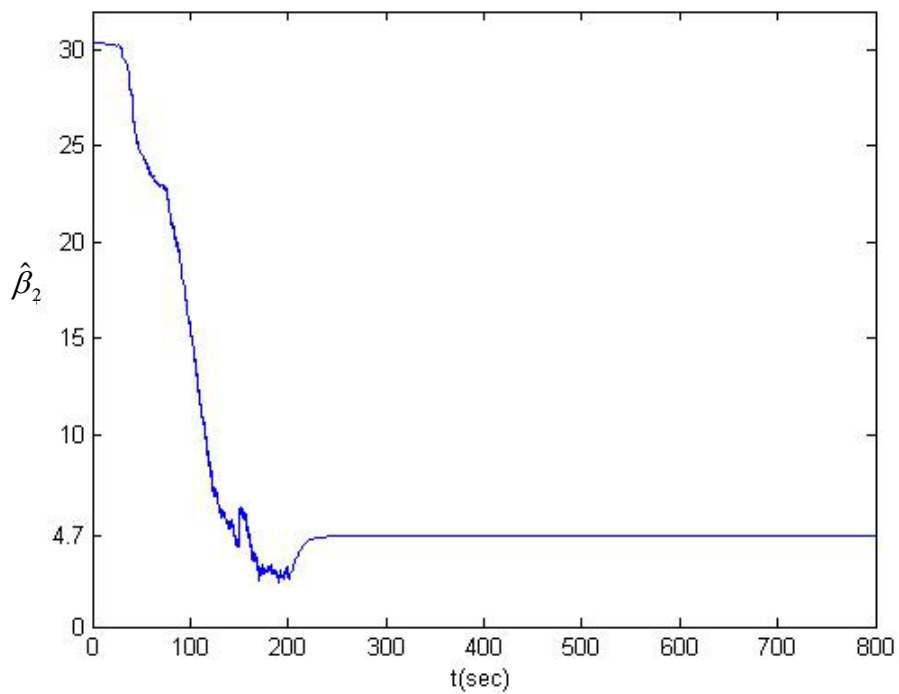
Fig.8.16. Convergence of the estimated parameter $\hat{\beta}_2$ to its actual value

with disturbance in the system for *CASE III*.

Chapter 9

Conclusions

In this thesis, a new Ikeda-Mackey-Glass (IMG) and a new Ikeda-Lorenz (IL) system are studied. In Chapter 2, we show that the chaotic motion of a new IMG system by phase portraits and bifurcation diagrams.

In Chapter 3, chaos synchronization of a new IMG system is studied. To achieve chaos synchronization by tuning delay time τ_2. Chaos synchronization of the two identical chaotic IMG systems can be obtained with slightly different initial conditions when the delay time τ_2 is not zero. Simulation results show that for this chaotic system generalized lag-synchronized, anti-synchronized and generalized-synchronized without any control can be obtained.

In Chapter 4, another chaotization method is presented by using different types of chaos signals as parameters. A new IMG system is a time delayed system. By using the chaotization method, this new IMG system chaotic behaviors can be obtained.

In Chapter 5, we study a new Ikeda-Lorenz system that is a non-time delayed system and presents the chaotic motion by phase portraits and Lyapunov exponent.

In Chapter 6 and in Chapter 7, a new GYC partial region stability strategy is proposed. By using the GYC partial region stability theory to achieve chaos generalized synchronization and chaos control. The new Ikeda-Lorenz system and Genesio system are used as simulation examples which effectively confirm the synchronization scheme and chaos control scheme.

In Chapter 8, estimated parameters of a new Ikeda-Mackey-Glass system through synchronization can be obtained with the following results:

1. Estimated parameter $\hat{\beta}_1$ and $\hat{\beta}_2$ through synchronization can converge to their actual values rapidly when the Ikeda-Mackey-Glass system has no disturbance.

2. When a new Ikeda-Mackey-Glass system has Rayleigh noise disturbance, two transient error states and two transient parameter errors are larger than that of the system without disturbance. However parameters $\hat{\beta}_1$ and $\hat{\beta}_2$ through synchronization still converge to their actual values successfully.

Appendix

GYC Partial Region Stability Theory [40,41]

Consider the differential equations of disturbed motion of a nonautonomous system in the normal form

$$\frac{dx_s}{dt} = X_s(t, x_1, \cdots, x_n), \qquad (s = 1, \cdots, n) \tag{A1}$$

where the function X_s is defined on the intersection of the partial region Ω (shown in Fig.A1) and

$$\sum_s x_s^2 \leq H \tag{A2}$$

and $t > t_0$, where t_0 and H are certain positive constants. X_s which vanishes when the variables x_s are all zero, is a real valued function of t, $x_1, \cdots, x_n$. It is assumed that X_s is smooth enough to ensure the existence, uniqueness of the solution of the initial value problem. When X_s does not contain t explicitly, the system is autonomous.

Obviously, $x_s = 0$ $(s = 1, \cdots n)$ is a solution of Eq.(A1). We are interested to the asymptotical stability of this zero solution on partial region Ω (including the boundary) of the neighborhood of the origin which in general may consist of several subregions (Fig.A1).

Definition 1:

For any given number $\varepsilon > 0$, if there exists a $\delta > 0$, such that on the closed given partial region Ω when

$$\sum_s x_{s0}^2 \leq \delta, \quad (s = 1, \cdots, n) \tag{A3}$$

for all $t \geq t_0$, the inequality

$$\sum_s x_s^2 < \varepsilon, \qquad (s = 1, \cdots, n) \tag{A4}$$

is satisfied for the solutions of Eq.(A1) on Ω, then the disturbed motion $x_s = 0$ $(s = 1, \cdots n)$ is stable on the partial region Ω.

Definition 2:

If the undisturbed motion is stable on the partial region Ω, and there exists a $\delta^{'} > 0$, so that on the given partial region Ω when

$$\sum_s x_{s0}^2 \leq \delta^{'}, \quad (s = 1, \cdots, n) \tag{A5}$$

The equality

$$\lim_{t \to \infty} \left(\sum_s x_s^2 \right) = 0 \tag{A6}$$

is satisfied for the solutions of Eq.(A1) on Ω, then the undisturbed motion $x_s = 0$ $(s = 1, \cdots n)$ is asymptotically stable on the partial region Ω.

The intersection of Ω and region defined by Eq.(A5) is called the region of attraction.

Definition of Functions $V(t, x_1, \cdots, x_n)$:

Let us consider the functions $V(t, x_1, \cdots, x_n)$ given on the intersection Ω_1 of the partial region Ω and the region

$$\sum_s x_s^2 \leq h, \quad (s = 1, \cdots, n) \tag{A7}$$

for $t \geq t_0 > 0$, where t_0 and h are positive constants. We suppose that the functions are single-valued and have continuous partial derivatives and become zero when $x_1 = \cdots = x_n = 0$.

Definition 3:

If there exists $t_0 > 0$ and a sufficiently small $h > 0$, so that on partial region Ω_1 and $t \geq t_0$, $V \geq 0$ (or ≤ 0), then V is a positive (or negative) semidefinite, in general semidefinite, function on the Ω_1 and $t \geq t_0$.

Definition 4:

If there exists a positive (negative) definitive function $W(x_1 \ldots x_n)$ on Ω_1, so that on the partial region Ω_1 and $t \geq t_0$

$$V - W \geq 0 \ (or -V - W \geq 0),\tag{A8}$$

then $V(t, x_1, \ldots, x_n)$ is a positive definite function on the partial region Ω_1 and $t \geq t_0$.

Definition 5:

If $V(t, x_1, \ldots, x_n)$ is neither definite nor semidefinite on Ω_1 and $t \geq t_0$, then $V(t, x_1, \ldots, x_n)$ is an indefinite function on partial region Ω_1 and $t \geq t_0$. That is, for any small $h > 0$ and any large $t_0 > 0$, $V(t, x_1, \ldots, x_n)$ can take either positive or negative value on the partial region Ω_1 and $t \geq t_0$.

Definition 6: Bounded function V

If there exist $t_0 > 0$, $h > 0$, so that on the partial region Ω_1, we have

$$|V(t, x_1, \ldots, x_n)| < L\tag{A9}$$

where L is a positive constant, then V is said to be bounded on Ω_1.

Definition 7: Function with infinitesimal upper bound

If V is bounded, and for any $\lambda > 0$, there exists $\mu > 0$, so that on Ω_1 when $\sum_s x_s^2 \leq \mu$, and $t \geq t_0$, we have

$$|V(t, x_1, \ldots, x_n)| \leq \lambda\tag{A10}$$

then V admits an infinitesimal upper bound on Ω_1.

Theorem 1

If there can be found for the differential equations of the disturbed motion a definite function $V(t, x_1, \ldots, x_n)$ on the partial region, and for which the derivative with respect to time based on these equations as given by the following :

$$\frac{dV}{dt} = \frac{\partial V}{\partial t} + \sum_{s=1}^{n} \frac{\partial V}{\partial x_s} X_s \qquad (A11)$$

is a semidefinite function on the partial region whose sense is opposite to that of V, or if it becomes zero identically, then the undisturbed motion is stable on the partial region.

Proof:

Let us assume for the sake of definiteness that V is a positive definite function. Consequently, there exists a sufficiently large number t_0 and a sufficiently small number $h < H$, such that on the intersection Ω_1 of partial region Ω and

$$\sum_s x_s^2 \leq h, \quad (s = 1, \ldots, n) \qquad (A12)$$

and $t \geq t_0$, the following inequality is satisfied

$$V(t, x_1, \ldots, x_n) \geq W(x_1, \ldots, x_n), \qquad (A13)$$

where W is a certain positive definite function which does not depend on t. Besides that, Eq. (A7) may assume only negative or zero value in this region.

Let ε be an arbitrarily small positive number. We shall suppose that in any case $\varepsilon < h$. Let us consider the aggregation of all possible values of the quantities $x_1, \ldots, x_n$, which are on the intersection ω_2 of Ω_1 and

$$\sum_s x_s^2 = \varepsilon, \qquad (A14)$$

and let us designate by $l > 0$ the precise lower limit of the function W under this condition. by virtue of Eq. (A5), we shall have

$$V(t, x_1, \ldots, x_n) \geq l \quad \text{for} \quad (x_1, \ldots, x_n) \quad \text{on} \quad \omega_2. \qquad (A15)$$

We shall now consider the quantities x_s as functions of time which satisfy the differential equations of disturbed motion. We shall assume that the initial values x_{s0} of these functions for $t = t_0$ lie on the intersection Ω_2 of Ω_1 and the region

$$\sum_s x_s^2 \leq \delta, \qquad (A16)$$

91

where δ is so small that

$$V(t_0, x_{10}, \ldots, x_{n0}) < l \tag{A17}$$

By virtue of the fact that $V(t_0, 0, \ldots, 0) = 0$, such a selection of the number δ is obviously possible. We shall suppose that in any case the number δ is smaller than ε. Then the inequality

$$\sum_s x_s^2 < \varepsilon, \tag{A18}$$

being satisfied at the initial instant will be satisfied, in the very least, for a sufficiently small $t - t_0$, since the functions $x_s(t)$ very continuously with time. We shall show that these inequalities will be satisfied for all values $t > t_0$. Indeed, if these inequalities were not satisfied at some time, there would have to exist such an instant $t=T$ for which this inequality would become an equality. In other words, we would have

$$\sum_s x_s^2(T) = \varepsilon, \tag{A19}$$

and consequently, on the basis of Eq. (A11)

$$V(T, x_1(T), \ldots, x_n(T)) \geq l \tag{A20}$$

On the other hand, since $\varepsilon < h$, the inequality Eq.(A4) is satisfied in the entire interval of time [t₀, T], and consequently, in this entire time interval $\dfrac{dV}{dt} \leq 0$. This yields

$$V(T, x_1(T), \ldots, x_n(T)) \leq V(t_0, x_{10}, \ldots, x_{n0}), \tag{A21}$$

which contradicts Eq.(A18) on the basis of Eq.(A17). Thus, the inequality Eq.(A1) must be satisfied for all values of $t > t_0$, hence follows that the motion is stable.

Finally, we must point out that from the view-point of mathenatics, the stability on partial region in general does not be related logically to the stability on whole region. If an undisturbed solution is stable on a partial region, it may be either stable or unstable on the whole region and vice versa. From the viewpoint of dynamics, we

wre not interesting to the solution starting from Ω_2 and going out of Ω.

Theorem 2

If in satisfying the conditions of theorem 1, the derivative $\frac{dV}{dt}$ is a definite function on the partial region with opposite sign to that of V and the function V itself permits an infinitesimal upper limit, then the undisturbed motion is asymptotically stable on the partial region.

Proof:

Let us suppose that V is a positive definite function on the partial region and that consequently, $\frac{dV}{dt}$ is negative definite. Thus on the intersection Ω_1 of Ω and the region defined by Eq.(A7) and $t \geq t_0$ there will be satisfied not only the inequality Eq.(A8), but the following inequality as will:

$$\frac{dV}{dt} \leq -W_1(x_1, \ldots x_n),$$ (A22)

where W_1 is a positive definite function on the partial region independent of t.

Let us consider the quantities x_s as functions of time which satisfy the differential equations of disturbed motion assuming that the initial values $x_{s0} = x_s(t_0)$ of these quantities satisfy the inequalities Eq.(A16). Since the undisturbed motion is stable in any case, the magnitude δ may be selected so small that for all values of $t \geq t_0$ the quantities x_s remain within Ω_1. Then, on the basis of Eq.(A22) the derivative of function $V(t, x_1(t), \ldots, x_n(t))$ will be negative at all times and, consequently, this function will approach a certain limit, as *t* increases without limit, remaining larger than this limit at all times. We shall show that this limit is equal to some positive quantity different from zero. Then for all values of $t \geq t_0$ the following inequality will be satisfied:

$$V(t, x_1(t), \ldots, x_n(t)) > \alpha$$ (A23)

93

where $\alpha > 0$.

Since V permits an infinitesimal upper limit, it follows from this inequality that

$$\sum_s x_s^2(t) \geq \lambda, \quad (s = 1, \ldots, n), \tag{A24}$$

where λ is a certain sufficiently small positive number. Indeed, if such a number λ did not exist, that is , if the quantity $\sum_s x_s(t)$ were smaller than any preassigned number no matter how small, then the magnitude $V(t, x_1(t), \ldots, x_n(t))$, as follows from the definition of an infinitesimal upper limit, would also be arbitrarily small, which contradicts(A23).

If for all values of $t \geq t_0$ the inequality Eq. (A24) is satisfied, then Eq. (A22) shows that the following inequality will be satisfied at all times:

$$\frac{dV}{dt} \leq -l_1, \tag{A25}$$

where l_1 is positive number different from zero which constitutes the precise lower limit of the function $W_1(t, x_1(t), \ldots, x_n(t))$ under condition (Eq. (A24)). Consequently, for all values of $t \geq t_0$ we shall have:

$$V(t, x_1(t), \ldots, x_n(t)) = V(t_0, x_{10}, \ldots, x_{n0}) + \int_{t_0}^t \frac{dV}{dt} dt \leq V(t_0, x_{10}, \ldots, x_{n0}) - l_1(t - t_0),$$
$$\tag{A26}$$

which is, obviously, in contradiction with Eq.(A23). The contradiction thus obtained shows that the function $V(t, x_1(t), \ldots, x_n(t))$ approached zero as t increase without limit. Consequently, the same will be true for the function $W(x_1(t), \ldots, x_n(t))$ as well, from which it follows directly that

$$\lim_{t \to \infty} x_s(t) = 0, \quad (s = 1, \ldots, n), \tag{A27}$$

which proves the theorem.
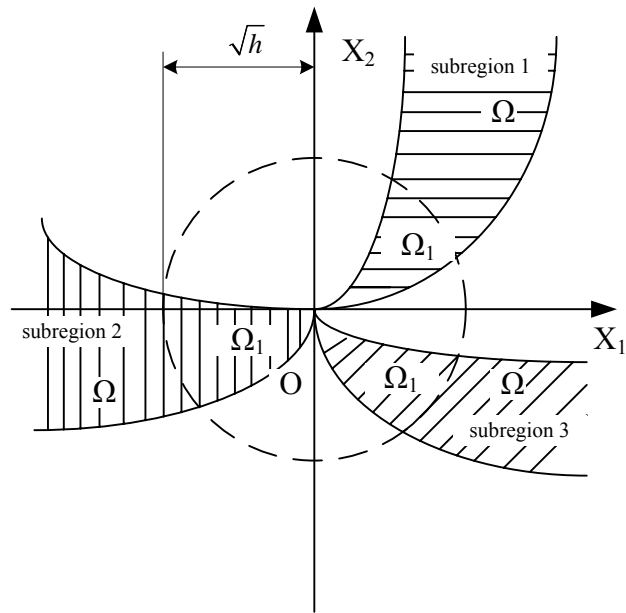
Fig.A1. Partial regions Ω and Ω_1

References

[1].E.N.Lorenz, "Deterministic Non-periodic Flows". J. Atmos. Sci., 20, pp.130–141, 1963.

[2].J.K.Hale, S.M.V.Lunel, *Introduction to Functional Differential Equations. New york: Springer*, 1993.

[3].K.Pyragas, **"**Synchronization of Coupled Time-delay Analytical Estimations Systems"**,** Phys. Rev. E., 58, pp.3067-3071, 1998.

[4].E.M.Shahverdiev, S. Vaprakasam, K.A.Shore,"Parameter Mismatches and Perfect Anticipating Synchronization in Bidirectionally Coupled External Cavity Laser Diodes"**,** Phys. Rev. E., 66, 017206, 2002.

[5].H.U.Voss, "Anticipating Chaotic Synchronization"**,** Phys. Rev. E., 61, pp.5115-5119, 2000.

[6].C.Masoller, D.H.Zanette, "Anticipated Synchronization in Coupled Chaotic Maps with Delays", Physica. A., 300, pp.359-366, 2001.

[7].S.K.Yang, C.L.Chen, H.T. Yau, "Control of Chaos in Lorenz System", Chaos, Solitons and Fractals., 13, pp.767-780, 2002.

[8].L.M.Pecora, T.L.Carroll, **"**Synchronization in Chaotic Systems**"**, Phys.Rev.Lett., 64, pp.821-824, 1990.

[9].S.Boccaletti, "The Synchronization of Chaotic Systems", Phys. Rep., 366, pp. 1-101, 2002.

[10].A.Kittel, J.Parisi, K.Pyragas, "Generalized Synchronization of Chaos in Electronic Circuit Experiments", Physica.D., 112, pp.459-471,1998.

[11].M.Rosenblum, A. Pikovsky, J.Kurths, **"**Phase Synchronization of Chaotic Oscillators"**,** Phys.Rev. Lett., 76, pp.1804-1807, 1996.

[12].A. Pikovsky, M.Rosenblum, J. Kurths, "Synchronization in a Population of

Globally Coupled Chaotic Oscillators", Europhys.Lett., 34, pp.165-170, 1996.

[13].A.S.Pikovsky, M.G.Rosenblum, G.V.Osipov, J. Kurths, "Phase Synchronization of Chaotic Oscillators by External Driving", Physica.D.,104, pp.219–238,1997.

[14].A.Barsella, C.Lepers, "Chaotic Lag Synchronization and Pulse-induced Transient Chaos in Lasers Coupled by Saturable Absorber", Opt. Commun., 205, pp. 397–403, 2002.

[15].S.Sivaprakasam, E.M.Shahverdiev, P.S.Spencer, K.A.Shore, "Experimental Demonstration of Anticipating Synchronization in Chaotic Semiconductor Lasers with Optical Feedback", Phys. Rev. Lett., 87, 154101, 2001.

[16].J.Y.Chen, K.W.Wong, L.M.Cheng, J.W.Shuai, "A Secure Communication Scheme Based on the Phase Synchronization of Chaotic Systems", Chaos., 13, pp.508-514, 2003.

[17].G.Grassi, S.Mascolo, "Nonlinear Observer Design to Synchronize Hyperchaotic Systems via a Scalar Signal", IEEE Trans. CAS., 44, pp.1143–1147, 1997.

[18].C.Li, X.Liao, R.Zhang, "Impulsive Synchronization of Nonlinear Coupled Chaotic Systems", Phys. Lett. A., 328,pp. 47–50, 2004.

[19].T. Yang, *Impulsive Control Theory*, Springer-Verlag, Berlin, 2001.

[20].T. Yang, O.C. Leon, "Impulsive Stability for Control and Synchronization of Chaotic Systems": Theory and Application to Secure Communication, IEEE Trans. CAS-1.,44, pp.976–988, 1997.

[21].C.Li, X.Liao, R.Zhang, "A Unified Approach for Impulsive Lag Synchronization of Chaotic Systems with Time Delay", Chaos, Solitons and Fractals., 23, pp. 1177–1184, 2005.

[22].E.Ott., C.Grebogi., J.A.Yorke., "Controlling Chaos" Phys.Rev.Lett., 64, pp.1196-1199, 1990.

[23].T.Shinbrot., E.Ott., C.Grebogi., J.A.Yorke., "Using Small Perturbations to

Control Chaos" Nature, 363, pp.411-417, 1993.

[24].G.Hu, Z.Qu, K.He , "Feedback Control of Chaos in Spatiotemporal Systems".Int. J.of Bif. and Chaos, 5, pp.901-936, 1995.

[25].W.L.Ditto, S.N.Rauseo, M.L.Spano, "Experimental Control of Chaos". Phys. Rev.Lett., 65, pp.3211-3214,1990.

[26].V.Petrov, V.Gaspar, J.Masere, K.Showalter, " Controlling Chaos in the Belousov-Zhabotinsky Reaction".Nature., 361, pp.240-243, 1993.

[27].L.O.Chua, L.Kocarev, K.Eckert, M. Itoh, " Experimental Chaos Synchronization in Chua's Circuit".Int. J. Bif.and Chaos., 2, pp.705-708, 1992.

[28].R.Roy, T.W.Murphy, T.D.Maier, A.Gills, E.R.Hunt, " Dynamical Control of a Chaotic Laser: Experimental Stabilization of a Globally Coupled System". Phys.Rev. Lett., 68, pp.1259-1262, 1992.

[29].S.Hayes, C.Grebogi, E.Ott, A.Mark, "Experimental Control of Chaos for Communication". Phys.Rev.Lett., 73, pp.1781-1784, 1994.

[30].A.Garfinkel, M.L.Spano, W.L.Ditto, J.N.Weiss, "Controlling Cardiac Chaos". Science. ,257, pp. 1230-1235,1992.

[31].C.C. Fuh, P.C. Tung, "Controlling Chaos Using Differential Geometric Method". Phys.Rev.Lett., 75, pp.2952-2955, 1995.

[32].G.Chen, X.Dong, "On Feedback Control of Chaotic Continuous Time Systems". IEEE.Trans.Circ.Syst., 40, pp.591-601, 1993.

[33].M.T.Yassen, "Chaos Control of Chen Chaotic Dynamical System". Chaos, Solitons and Fractals., 15, pp.271-283, 2003.

[34].M.T. Yassen, "Controlling Chaos and Synchronization for New Chaotic System Using Linear Feedback". Chaos, Solitons and Fractals., 26, pp.913-920, 2005.

[35].H.N.Agiza, "Controlling Chaos for the Dynamical System of Coupled Dynamos". Chaos, Solitons and Fractals., 12, pp.341-347, 2002.

[36].E.N. Sanchez, J.P.Perez, M. Martinez, G. Chen, "Chaos Stabilization: An Inverse Optimal Control Approach". Latin.Am.Appl.Res: Int. J., 32, pp.111-114, 2002.

[37].M.T.Yassen, "Adaptive Control and Synchronization of a Modified Chua's Circuit System". Appl.Math.Comp., 135, pp. 113-128, 2001.

[38].T.L.Liao, S.H. Lin, "Adaptive Control and Synchronization of Lorenz Systems". J. Franklin. Inst., 336, pp.925-937, 1999.

[39].J.Lu, S.Zhang, "Controlling Chen's Chaotic Attractor Using Backstepping Design Based on Parameters Identification". Phys. Lett. A., 286, pp148-152, 2001.

[40].Z.M.Ge, C.W.Yao, H.K.Chen, "Stability on Partial Region in Dynamics", Journal of Chinese Society of Mechanical Engineer.,115, pp.140-151, 1994.

[41].Z.M.Ge, H.K.Chen, "Three Asymptotical Stability Theorems on Partial Region with Applications", Japanse Journal of Applied Physics., 37, pp.2762-2773, 1998 .

[42].M.Casdagli, "Nonlinear Prediction of Chaotic Time Series", Physica.D.,35, pp.335-356, 1989.

[43].E.Baake, M.Baake, H.G.Bock, K.M.Briggs, "Fitting Ordinary Differential Equations to Chaotic Data", Physical.Review.A., 45, pp.5524–5529, 1992.

[44].B.P.Bezruchko, D.A.Smirnov, "Constructing Nonautonomous Differential Equations from Experimental Time Series", Physical.Review.E., 63, 016207 , 2000.

[45].L.Li, H.Peng, X.Wang, Y.Yang, "Comment on Two Papers of Chaotic Synchronization", Physics.Letters.A., 333, pp.269–270, 2004.

[46].D.Yu, A.Wu, ''Comment on Estimating Model Parameters from Time Series by Autosynchronization'', Physical.Review.Letters., 94, 219401, 2005.

[47].D.Huang, "Adaptive-feedback Control Algorithm", Physical.Review.E., 73,

066204, 2006.

[48].R.Genesio, A.Tesi, "A Harmonic Balance Methods for the Analysis of Chaotic Dynamics in Nonlinear Systems". Automatica., 28, pp.531–48, 1992.

[49].Z.M.Ge, C.H.Yang, H.H.Chen, S.C. Lee, "Non-linear Dynamics and Chaos Control of a Physical Pendulum with Vibrating and Rotation Support" , Journal of Sound and Vibration, 242, pp.247-264, 2001.

[50].Z.M.Ge, J.K.Yu, "Pragmatical Asymptotical Stability Theoremon Partial Region and for Partial Variable with Applications to Gyroscopic Systems", The Chinses Journal of Mechanics, 16, pp.179-187, 2000.

[51].Z.M.Ge, C.M.Chang, "Chaos Synchronization and Parameters Identification of Single Time Scale Brushless DC Motors", Chaos, Solitons and Fractals., 20, pp. 883-903, 2004.

[52].F. Liu, Y. Ren, X. Shan, Z.Qiu, "A Linear Feedback Synchronization Theorem for a Class of Chaotic Systems", Chaos, Solitons and Fractals, 13, pp.723-730, 2002.

[53].Z.M. Ge, C.H.Yang, "Generalized Synchronization of Quantum-CNN Chaotic Oscillator with Different Order Systems", Chaos, Solitons and Fractals, 35, pp.980-990, 2008.

[54].A.Krawiecki., A. Sukiennicki., "Generalizations of the Concept of Marginal Synchronization of Chaos", Chaos, Solitons and Fractals, 11, pp.1445–1458, 2000.

[55].Z.M.Ge, C.H.Yang, "Synchronization of Complex Chaotic Systems in Series Expansion Form", Chaos, Solitons and Fractals., 34, pp.1649-1658, 2007.

[56].B.Rakshit, A.R.Chowdhury, P.Saha, "Parameter Estimation of a Delay Dynamical System Using Synchronization in Presence of Noise", Chaos, Solitons and Fractals., 32, pp.1278-1284, 2007.